ISSN Print : 0377 - 2969
ISSN Online : 2306 - 1448
Vol. 51(2), June 2014

PROCEEDINGS
OF THE PAKISTAN ACADEMY OF SCIENCES

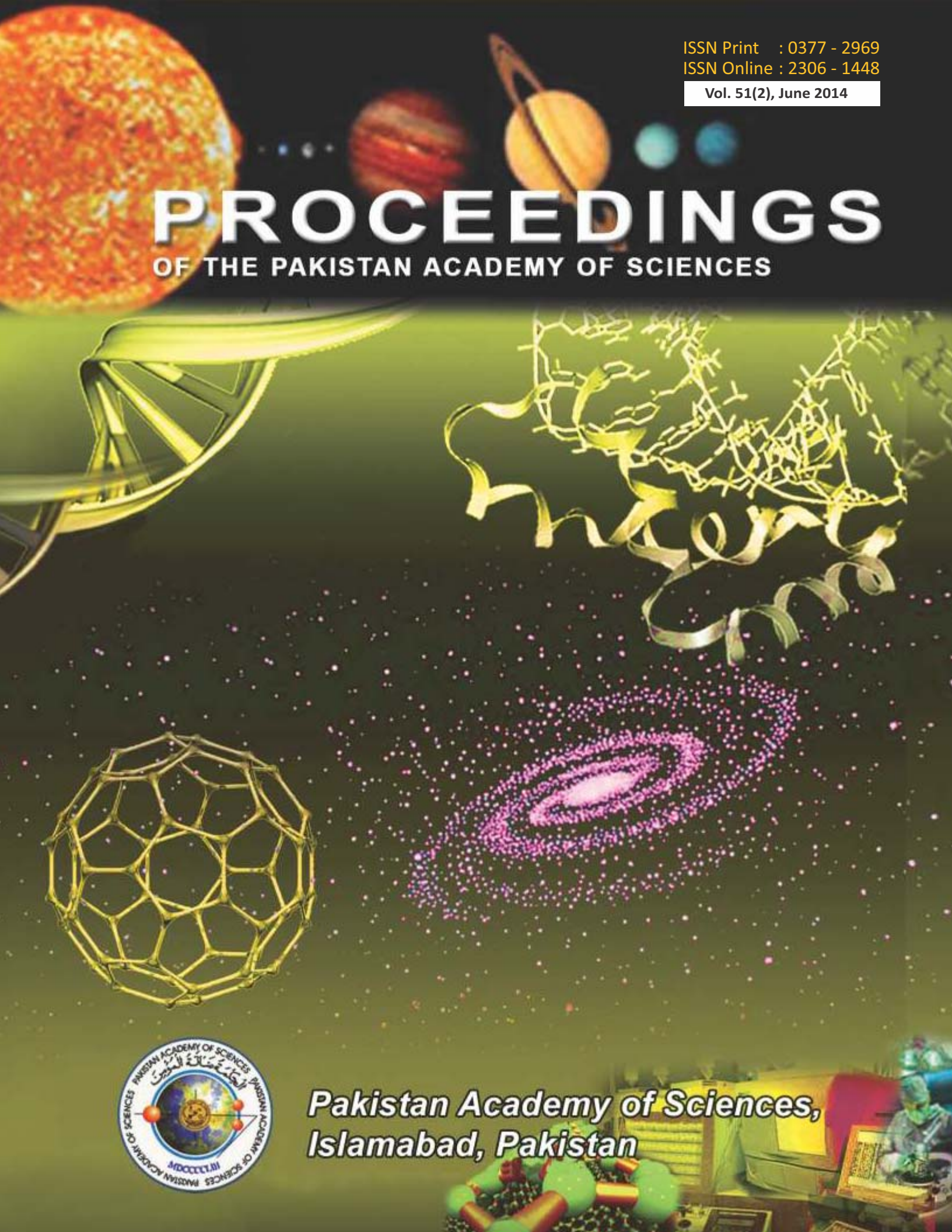

Pakistan Academy of Sciences,
Islamabad, Pakistan

Proceedings of the Pakistan Academy of Sciences, published since 1964, is official journal of the Academy, published quarterly. This open access journal publishes research papers and reviews in basic and applied sciences. All papers are peer reviewed. Authors are not required to be Fellows or Members of the Academy, or citizens of Pakistan.

Annual Subscription: **Pakistan:** Institutions, Rupees 2000/- ; Individuals, Rupees 1000/-
Other Countries: US$ 100.00 (includes air-lifted overseas delivery)

HEC Recognized, Category X; PM&DC Recognized

Published by **Pakistan Academy of Sciences**, 3 Constitution Avenue, G-5/2, Islamabad, Pakistan
Tel: 92-5 1-920 7140 & 921 5478; **Fax:** 92-51-920 6770; **Website: www.paspk.org; Email:** pas.editor@gmail.com

Printed at **PanGraphics (Pvt) Ltd.,** No. 1, I & T Centre, G-7/l, Islamabad, Pakistan
Tel: 92-51-220 2272, 220 2449; **Fax**: 92-51-220 2450; **Email**: pangraph@isb.comsats.net.pk

Proceedings
OF THE PAKISTAN ACADEMY OF SCIENCES

CONTENTS

Volume 51, No.2, June 2014 **Page**

Submission of Manuscripts: Manuscripts may be submitted online at www.paspk.org or as E-mail attachment. Authors must consult the ***Instructions for Authors*** at the end of this issue and at the Website: www.paspk.org

Proceedings of the Pakistan Academy of Sciences 51 (2): 101–114 (2014)

ISSN: 0377 - 2969 (print), 2306 - 1448 (online)

Pakistan Academy of Sciences

Research Article

The Jigsaw of Resource Description Framework (RDF) and Topic Maps Serialization Formats: A Survey

Fakhre Alam, Muhammad Abid Khan, Shaukat Ali* and Shah Khusro

Department of Computer Science,
University of Peshawar, Peshawar, Pakistan

Abstract: The dawn of the 21st century saw the emergence of a number of technologies which not only revolutionized human lives but also opened new avenues of research. Semantic Web technology is one of the technologies which attracted tremendous research attention around the globe. To successfully implement Semantic Web, technologies have been developed to effectively represent, create, and navigate metadata relationship among the Web resources. Resource Description Framework (RDF) and Topic Maps (TMs) emerged as the leading technologies of the newly envisioned Semantic Web. RDF and TMs are independent technologies using different mechanisms to represent semantic relationships between the Web resources. A number of serialization formats have been investigated by the researchers in the past few years for successful storage and transmission of RDF and TMs data. However, different representation mechanisms and serialization formats result into the problem of interoperability, potentially resulting in the division of the Semantic Web into two islands. This paper presents a comprehensive survey of the available serialization formats of RDF and TMs by categorizing, analysing, and evaluating them using a set of criteria. For evaluation purpose, simple book ontology is developed in both RDF and TMs formats. It has been observed that serialization formats vary in different aspects but are powerful enough to encode their respective data models and the interoperability among them is possible, subject to some additional effort. This investigation provides a compact platform for researchers to solve the interoperability problem among serialization formats to accelerate the growth of Semantic Web.

Keywords: Serialization, Semantic Web, Resource Description Framework (RDF), Topic Maps (TM), Extensible Markup Language (XML)

1. INTRODUCTION

The World Wide Web (WWW) [1] is an Internet system in which billions of web pages containing text, images, audio and videos are interlinked with each other through hypermedia links. Despite of all of the efforts for the perfection, advancement and widespread use, the information in the current Web is still presented in human readable format with lack of any semantic and annotation capabilities, enough for machines to deduce any new information from the existing by its own [2]. Today huge amount of information is available on the Web in different structural formats imposing the burden of retrieving and interpreting of relevant information on the users. Thus, making users overwhelmed while searching for specific information.

To overcome the limitations of the current Web, Tim-Berner-Lee[1] (inventor of the WWW) coined the idea of Semantic Web, also known as the modern Web. Semantic Web is an extension of the current Web, insisting the creation of implicit and meaningful relationships among the Web resource in a manner to be directly understandable by the machines [3]. In Semantic Web, machines will integrate information, apply computation on the information, and organize them into a format to be reusable across wide array of domains. Thus, will establish an environment where people and

Received, May 2013; Accepted, May 2014
* Corresponding author: Shaukat Ali; Email: shoonikhan@upesh.edu.pk

[1] http://www.w3.org/People/Berners-Lee/

machines will function in cooperation and will make the availability of right information at the right time and the right place possible.

The vision of Semantic Web revolutionized Web by taking it into new avenues of research. To light the lamp, researchers around the globe put forwarded their contributions for turning the Semantic Web vision into reality. To achieve the goals of Semantic Web, a list of technologies were proposed by the research communities which will not only help in understanding Semantic Web but will also accelerate the development rate of Semantic Web applications. Among the other technologies, Resource Description Framework (RDF) and Topic Maps (TMs) technologies developed respectively by W3C[2] and ISO[3] served as the backbone of Semantic Web and gained high level of popularity. An RDF model represents metadata enabled relationships among web resource in an explicit and precise manner to be easily interpretable by the machines [4]. Each RDF model is composed of statements where each statement relates two Web resources by using the analogy of subject, predicate, and object. The idea of Topic Maps was originally developed for the representation of back of the book index construction [5]. The original idea of Topic Maps was further extended by the researchers and used it for wider applications like to represent exchange and convey knowledge on the Semantic Web. Information in Topic Maps are represented in the form of topic, associations between topics and their occurrences.

Serialization is the process in which data in one format is semantically converted into another format for the storage and transmission purpose[6]. The convertible data can be reused later in another computing environment, regardless of any change in the original data format. It is due to the serialization that different types of data formats can be stored and run on different hardware platform regardless of their underlying architecture, thus, promoting interoperability. Serialization also provides simplicity and common I/O interface to store and transform data from one format to another. XML provides persistent method for the interchange of data on the web to be stored or communicated regardless of the programming languages in a human readable format [7]. A number of serialization formats are proposed by the research communities, academia, and organizations for RDF and TMs Semantic Web technologies with the view of expressibility, easy to create, easy to understand by both humans and machines, and take less network bandwidth while in transmission.

While being overwhelmed with a number of serialization formats, it is rather cumbersome for researchers and users to select an appropriate one and find solutions to problem of their inter-conversion. This research paper is aimed to provide a comprehensive overview and analysis of the available RDF and Topic Maps serializations formats, covering all of their possible aspects, and pros and cons. Main contributions of the paper are:

- The topic is almost unique in its integrity and opens new area of research.
- To provide a compact platform for the users and researchers to grab almost all of the relevant possible information about the topic in a single document.
- To organize and classify the available literature about the topic in an attractive manner to catch and boost interest of the new researchers in the area and take them into new avenues of research.
- To briefly explain and analyze the available serialization formats which are currently available in various domains and with their success stories and common reasons of failure.
- Gaining practical experience of inter-converting serialization formats belonging to the two Semantic Web islands.

2. EVALUATION FRAMEWORK AND METHODOLOGY

A serialization format is a way of encoding information that can be stored (e.g., in a file, or memory buffer) so that, when passed between machines, it can be parsed and understand, and reconstructed in the same or another computing environment. Resource Description Framework (RDF) and Topic Maps (TMs) technologies, fulfilling the vision of Semantic Web, enrich the scattered resources in the Web with metadata to solve the problem of knowledge sharing

[2] http://www.w3.org/
[3] http://www.iso.org/iso/home.html

and integration. Although RDF and TMs are independent technologies from different standard organizations but their goal is the same, which is to represent the semantic relationship between web resources. RDF and Topic Maps data needs to be stored in a data structure (i.e., file format) which can be transmitted through a network to be used in another computing environment without changing in the original data format. The notions used to record RDF and Topic Maps data in a data structure is called serialization format. Practically, serialization format and RDF/Topic Maps are two different things. A serialization format describes an encoding technique of information, whereas, a RDF/Topic Map represents a mental conceptual data model of information in a domain. But, to make a RDF/Topic Map data model understandable to both humans and computers (especially), it needs to be represented in a serialization format. In other words, serialization is like the grammar of a language, while the data model is the informational content behind words. For example, the word "Green" spoken aloud in English is the serialization, while a data model is a way to define the concept of

Table 1. Detailed analysis and evaluation of Resource Description Framework serialization formats using set of criteria.

Category	Serialization	Exp/Comp	Simplicity	Compactness	Tools Supp.	Applicability	Remarks
XML	**RDF/XML**	Very High	Simple and user friendlyz	Less Compact	Available	Small scale and large scale	Merge and interchange information from multiple sources, Used to create ontologies, Can be used with relational databases and RSS, Hard format, Difficult to implement, Not processable with some standard XML tools.
	TriX	High	Simple syntax	Compact	Available	Small scale	Represent RDF graph more consistently using XSLT, and Xquery, due to which processing speed is high and concise, Syntax can be extensible to represent any type of RDF graph, Verbose and poor human readable un-extended syntax, Inefficient transformation, Lack of hierarchy template match
Non-XML	**N3**	Medium	Simple and can easily parsed	Highly Compact	Available	Small scale and large scale	De facto standard, Optimize the logic and inference mechanism, Compact, persistent and readable syntax, Shorten absolute URI, Reduce verbose nature as compared to RDF/XML, Unknown and long term stability, Clear requirements for correlations of different features of N3 in RDF/XML format
	N-Triple	High	Simple and easier to read and write	Less Compact	Available	Large scale	Automated processing during the comparison of the actual results with our desired results, Store and transform RDF graph(Triples) data in plain text and lines, Easily processable with N3 and Turtle tools, Line by line Parsing, Redundancy in code and Lack of support for nested resources
	Turtle	High	Very Simple	Highly Compact	Available	Large scale	Contains all the capabilities of N-Triple, Compatible with N3, Encode any type of RDF graph, Greater conciseness and human readability, Used with the popular tools and API like Jena and OWL API, Reification of complex expressions and translations of OWL axioms into triples is difficult

Table 2. Detailed analysis and evaluation of Topic Maps serialization formats using set of criteria.

Category	Serialization	Exp/Comp	Simplicity	Compactness	Tools Supp.	Applicability	Remarks
XML	**XTM**	Very High	Simple	Not so Compact	Available	Small and large scale	Advance features than SGML, Flexible, user friendly, easily represent Knowledge Representation and navigation, Implemented on web browser, Cannot fully represent the whole Topic Maps paradigm, Occupy large space, Less effective in semantic integration and interoperability of Topic Maps constructs.
	CXTM	High	Complex	Less Compact	Available	Small scale	Provide test suite for testing different TM technology, Directly compare the two data structures, Provide more reliability then other formats, It is only the variation of XTM used for the judgment of two TMDM
Non XML	**HyTime**	Medium	Simple	Not Compact	Available	To any type of Hypermedia	Provides an abstract facility for the TM paradigm to be expressed in SGML, Link and organized related topics which are time and space critical, Fulfill the needs of addressing in a convenient way, General purpose and abstract standard
	CTM	Very High	Simple	Highly Compact	Available	Small and large scale	Short and simple text based notation, Represent the syntax of TMQL and TMCL precisely, Efficient parsing mechanism, Need special parser for TM constructs, Lack of support for item identifiers in TM constructs that are not topics
	GTM	High	Simple	Highly Compact	Not Available	Small and large scale	Easily modeled, presented and communicated between users Due to visual nature, Create similar view on TM for programmers, Can be used with UML in a single model yielding high level performance, Weak due to the separation of two levels one for TMDM and another for TMCL
	LTM	Low	Simple	Highly Compact	Available	Small scale	Simple and text based, Can be converted into XTM format, Efficient and take less space, User friendly and compact syntax, Not yet standardized, Superseded by CTM, Unsuccessful when come to the large TM

"Green" such that it is unambiguous whether you say "Green" or "Verde" or think about the color of a leaf [8]. A data model is an abstract model – it does not matter how one represent it as long as one stay true to its abstract properties. A serialization format typically encodes the information provided by the associated data modeling technology. To win the race, both of the competitors RDF and Topic Maps supports a variety of serialization formats varying in different aspects such as readability, expressibility, and compactness etc. for their data representation. However, a serialization format providing excellent overall results will not only help to boot the associated technology in the race but eventually the Semantic Web technology. In this paper, to give insight knowledge and understanding of the on hand RDF and Topic Maps serialization formats, they are evaluated against a set of criteria including

xml and non-xml, expressibility and computability, simplicity, applicability, compactness, tools and APIs support, and remarks. In order to compare the different serialization formats, simple book ontology is developed and serialized into different RDF and Topic Maps serialization formats to derive conclusions for the criteria (Table. 1 and Table. 2). Our book ontology covers most of the basic information related to a book as well as properties (.i.e., data properties and object properties), and objects. The overall ontological graphs in RDF and Topic Maps are shown in Fig. 1 and Fig. 2, respectively.

- ***XML-base and non-XML-based***: RDF and Topic Maps serialization formats can be classified into XML-based and non-XML-based. XML was the first serialization format used to produce text-based encoding which could not only be readable by humans and machines but could also be communicated between disjoint systems regardless of programming languages. XML-based encoding, however, lost more compact byte-stream-based encoding but the recent advancements in storage and communication capabilities made file size less of a concern. Binary XML was proposed more compact than regular XML but was not readable by plain-text editors and could not be exchanged between disjoint systems. Non-XML serializations were designed to be easier to write by hand and easier to follow because of using notions (.i.e., tabular notion etc), which encodes the underlying information in a document to be easily recognizable as compared to XML-based sterilizations. JavaScript syntax based serialization: JSON is another more compact and lightweight plain-text serialization proposed as an alternative to XML-based serialization.
- ***Expressibility***: The expressiveness power of a serialization format determines the level of constructs and features (.i.e., syntactic sugars) provided by the format to encode complex information. A serialization format with high expressive power is obviously a liked one but often result in low computational performance. Similarly, a highly expressive format can serialize any type of data model either valid or invalid. For example, Notion 3 and RDF/XML can serialize

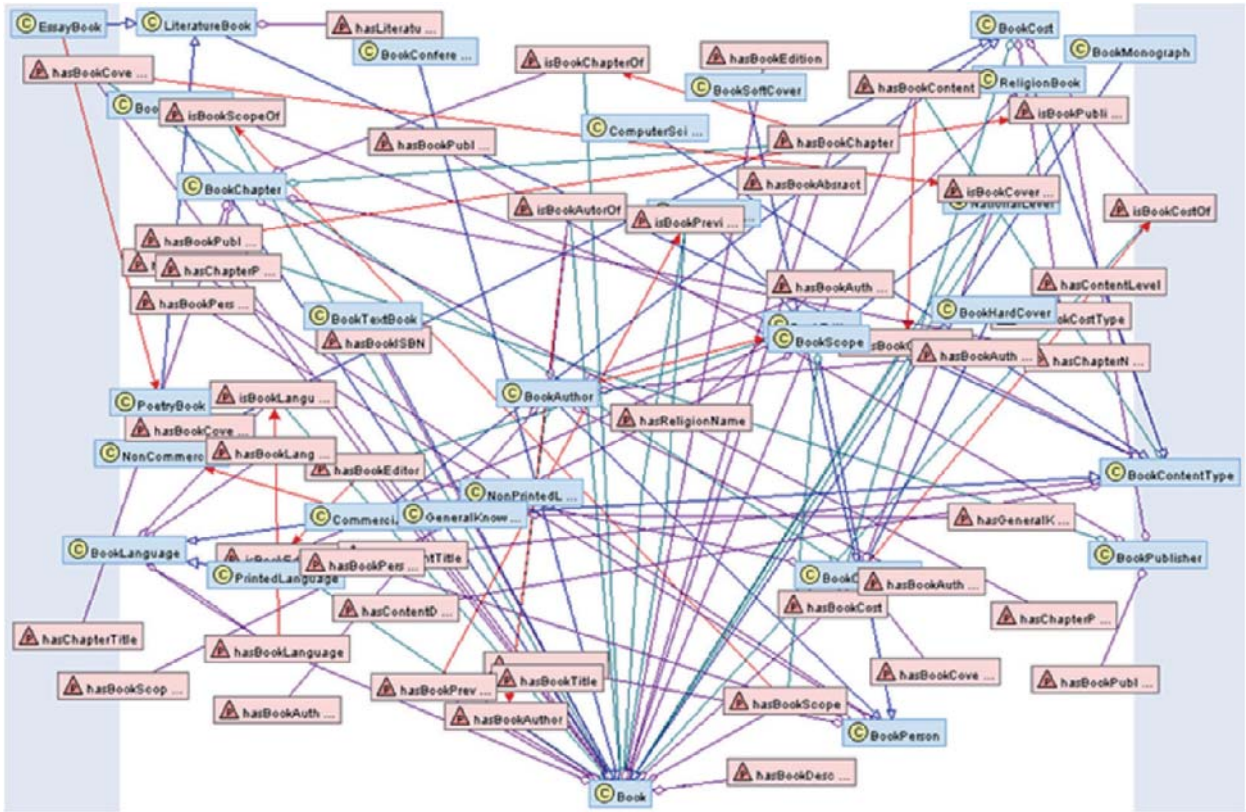

Fig. 1. Minimized RDF graph of book ontology.

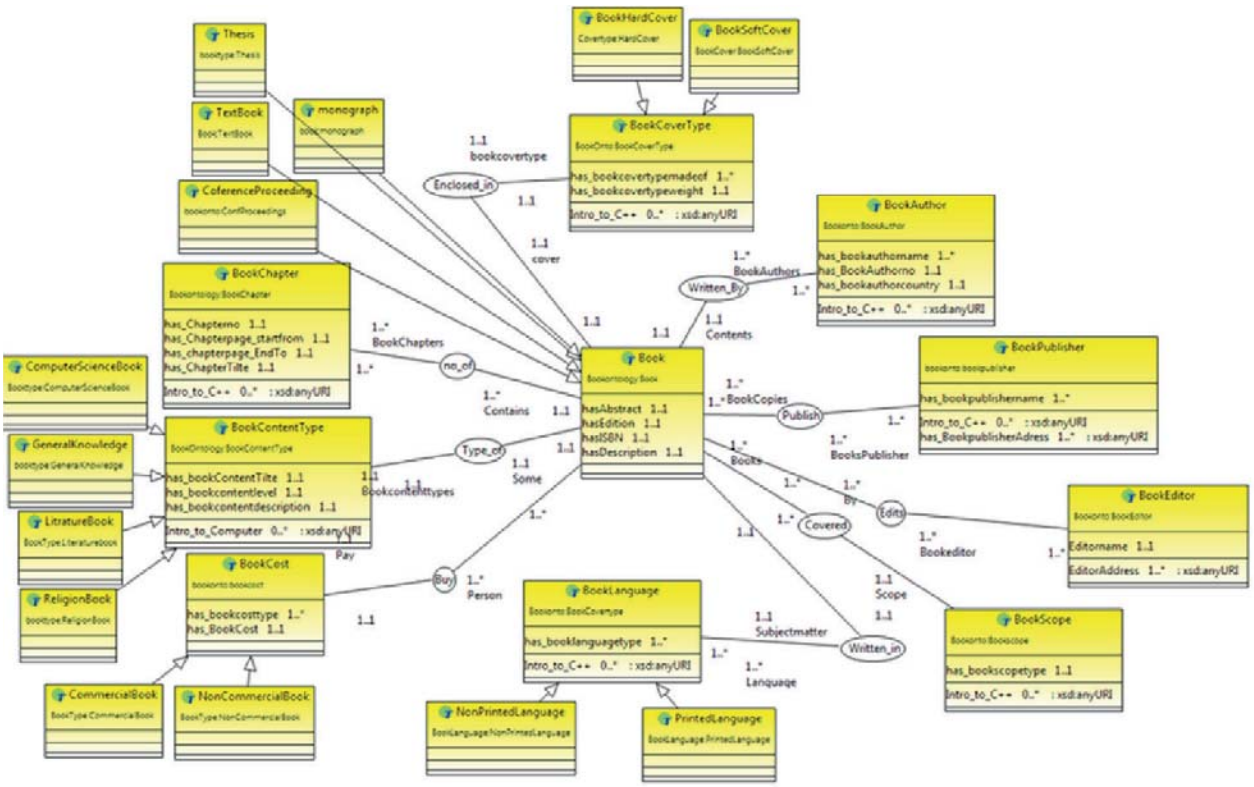

Fig. 2. Topic Maps schema of book ontology.

both valid and invalid RDF graphs but Turtle can serialize only valid RDF graphs [9]. For a useful serialization format to be rich enough to satisfy user requirements comprehensively whilst retaining good computational properties.

- ***Simplicity***: The simplicity of a serialization format defines how humane the format is: easy to understand by both humans and machines, quite readable/editable in raw form by humans, and relatively compact. However, compactness is not the critical requirement for simplicity because some serialization formats are quite simple but verbose such as N-Triples is a very simple but verbose serialization for RDF graphs [10]. Similarly, simplicity should not come at the cost of expressibility such as RDF/XML is very simple user friendly and highly expressive serialization format for RDF graphs.

- ***Compactness***: The compactness of a serialization format determines strength of the format to encode maximum information in small number of statements. The compactness of a serialization format typically depend on the encoding type (.i.e., XML-base and non-XML-based). XML based encodings are typically found more verbose (e.g., RDF/XML) and non-XML-based encodings are typically found more compact (e.g., Turtle [9]) but not necessarily (e.g., N-Triples [10]). XML-based serializations were plagued with non-compactness but current technological advancements in the storage and communication facilities made it of less concern. Compactness should not come at the cost of expressiveness. A Serialization format should be compact enough while retaining the desired expressiveness level. Similarly, simplicity should not be effect by compactness, a serialization format should use various methods to compact the data while still leaving it readable [10]. However, majorly simplicity affects compactness because compactness increases complexity while decreasing simplicity (e.g., N-Triples, and RDF/XML). Furthermore, using heavy compact encoding can impact encoders and decoders performances negatively.

- ***Tools Support***: For a serialization format to be accepted by users needs strong support from software tools and APIs paradigms. A tool or an API provides an environment for users to create,

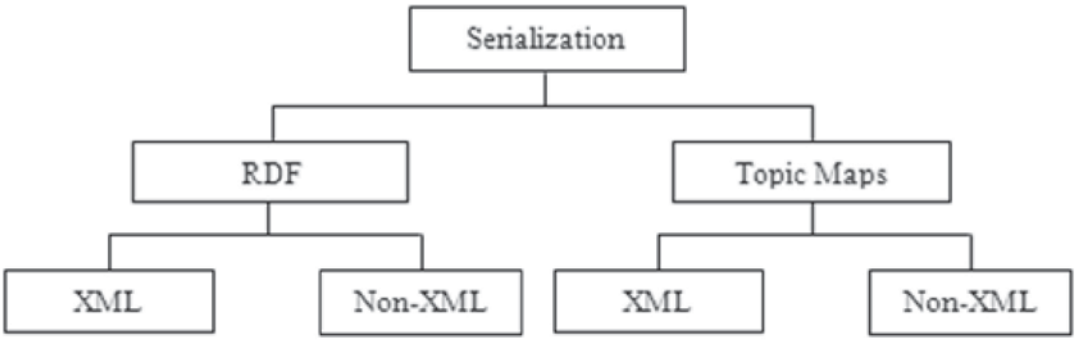

Fig. 3. Classification of RDF and Topic Maps serializations formats.

store, edit, maintain, and visualize a data model in a serialization format. However, hard coding in serialization format directly is a cumbersome task, therefore, tools and APIs should provide graphical user interface for users to interact with the data models in a click and play environment while producing the resultant serialization code automatically. For example, Protégé for RDF data model, and Ontoa for Topic Maps. An editor should support various serialization formats enabling users to select the required one. The more a serialization format is supported by the tools and APIs, the higher will be its market value.

- ***Applicability***: The applicability of a serialization format determines to address which scale of data models: small scale or large scale. The scale of a RDF model is measured by the number and types of objects and relations, whereas, of Topic Maps by the number and types of concepts, occurrences, and associations. The higher the number of ingredients the complex will be the model and the higher the will be the scale. However, large scale models are difficult to create and maintain, therefore, designers typically recommend a serialization format application for a specific scale level.
- ***Remarks***: In addition to the above criteria, several other features found during serialization formats investigation are highlighted in the remarks.

3. TYPES OF SERIALIZATION

A number of RDF and Topic Maps serialization formats are introduced by the Semantic Web researchers in the past several years. The available serialization formats of RDF and Topic Maps can be broadly divided into two categories: XML based and Non-XML based (as shown in Fig. 3) using the structure of serialized documents. Serialization formats belonging to both of the categories provides flexibility, user friendless and web centric application syntax while keeping the expressive power of both RDF and Topic Maps. Knowledge representation and navigation can also be done with simplicity and flexibility due to its support for different types of software and implementation on multiple platforms.

2.1. Resource Description Framework Serialization Formats

Resource Description Framework (RDF) represents data in the form of graph model which is not suitable for storage and manipulation. To efficiently store, transmit, manipulate, and reuse RDF data on the Internet or in local computer several types of serialization formats were researched by the Semantic Web researchers with the aims of providing flexibility and compactness. Using the underlying serialization structures, they are classified into XML based and Non-XML based serialization formats, as shown in Fig. 4.

2.1.1. XML Based Serialization

XML is a meta language standardized by the W3C, which stores, structures, and relates the contents of Web resources in a way to be easily accessible and interpretable by the machines [11]. To easily and efficiently interchange RDF documents on the Semantic Web, XML based Serialization like RDF/XML and Triples in XML (TriX) etc have been introduced by the Semantic Web researchers.

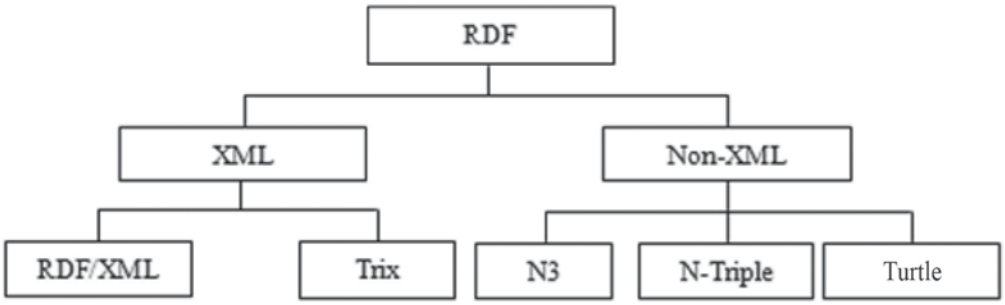

Fig. 4. Classification of RDF serialization formats.

***RDF/XML**:* RDF/XML is W3C standardized serialization format for the merging and interchangeability of information from multiple sources. Web resources can be expressed more meaningfully by RDF/XML Serialization. The expressive power of RDF/XML is much high, and the syntax is computable, simple, and user friendly. The parsing mechanism is quick and produces the output files in the same or another format by serializing the RDF triples [12]. One of the reasons of its popularity is the availability of numerous visual editing tools written in Java, like IsaViz etc [13]. As compared to other RDF serialization formats (e.g., N3, and Turtle, etc), RDF/XML based documents are less compact due to being lengthy, and larger in sizes [14]. But, on the other are more readable, easy to understand, and easy to implement as compared to them. Although RDF/XML is more flexible providing opportunities for representing RDF resource in multiple of ways, but results into making the syntax and format hard to read and implement [15]. Therefore, sometimes it is not processable with standard XML tools and creates difficulty while implementing some general types of RDF Graphs.

***Triples in XML (TriX)**:* TriX is a XML based serialization format which represents RDF graph (subject, predicate, and object) in a highly consistent and normalized way [16]. The reason of its high consistency and normalization is due to the use of XML tools like XSLT[4], and Xquery[5] etc for the manipulation of RDF graphs. TriX can express and serialize RDF named graphs as well, which are the combination of various RDF graphs in a single document represented by URIs. The syntax of TriX is more user friendly due to its unique features: relative URIs, and qnames. These features establish an environment where RDF documents can be easily read and write by eliminating redundant information and easing URI abbreviation. Supporting XSLT, TriX provides extensible syntax to express, represent and manipulate RDF graphs [16]. On the negative side, the syntax of TriX is incoherent and un-extended, therefore, decreases human readability. Despite of the fact that TriX documents are translatable using XSLT, but due to its lack of efficiency for hierarchal representation, each pattern match must query the entire document.

2.1.2. Non-XML Based Serialization

Although XML is well enough to provide interoperability, and platform independency but it suffers from numerous problems majoring that XML documents are normally larger in size by containing a number of words, which will not only create problems while transmission but will also severely effect human readability and understandability. To eliminate these problems researchers tried to find another way of representing RDF documents which is SGML. In the past several years, a wide array of non-XML based (SGML based) serialization formats for RDF documents including Notation-3 (N3), N-Triple, Terse RDF Triple Language (Turtle) are introduced by the research communities. It is argued that they have the potential to overcome the limitations and, in specific, the verbose nature of XML based serialization.

***Notation-3 (N3)**:* N3 is a de-facto standard developed by Tim Berners Lee and published by W3C in 2008 [17]. The basic idea was to optimize the logic and inference mechanism as compared to the other notations. The main reason behind the popularity of

[4] http://www.w3schools.com/xsl/
[5] http://www.w3schools.com/xquery/default.asp

N3 is because of its compactness, readability, and following many key features of Semantic Web not available in RDF/XML [18]. The distinguishable features of N3 include its simple and persistent syntax, expressive power, and ability to abbreviate URIs using prefixes. The expressive power of N3 in open web based environment is high and can express rules and logic by combining RDF properties with N3's extensions of RDF by including variables and nested graphs. The development of N3 notation for RDF has optimized the computability of data and logic due to its short notation and abbreviations used for representing RDF graph. N3 can parse RDF data quickly while its syntax is compact and can also be extended for much wider applications. N3 format has low redundancy, describe URI prefix at the beginning of file, shorthand notations are available in it and provides an abbreviation for both URI prefixes and base URI. Several types of visual and text editors and convertors are available for N3 which can create, edit and convert N3 document into another format both online and locally inside the system. The unknown and long term stability of N3 and its clear requirements for correlations of different features of N3 in RDF/XML format is the main limitation of this format [18]. The power of N3 is also limited in a situation when a user wants to make a statement about statement (reification).

***N-Triple**:* Dave Beckett at the University of Bristol and Art Barstow at the W3C developed serialization format called N-Triple to solve the problem of automated processing while comparing the actual results with desired results [19]. RDF graph data can be stored and transmitted in N-Triple serialization format in the form of plain text and line. N-Triple syntax is easier to read and write and represents a single triple (subject, predicate and object) in a single line. N-triple is suitable in a situation when user want to store millions of triples. Although this serialization format is the subset of N3 and Turtle, however, it is easier to generate, merge, and parse in memory as compared to its predecessors. N-Triple serialization format can express RDF test cases and describe the association between RDF/XML serialization and the RDF abstract syntax. Parsing is also done in N-Triple file, line by line and a large file which cannot fit into main memory at once can be loaded one line at a time [20]. However, N-Triple is not as compact as RDF/XML and Turtle due to its lack of support for nested resources and elimination of repetitions of the resources URIs.

***Terse RDF Triple Language (Turtle)**:* Turtle is a W3C's recommendation for representing almost every type of RDF graph data in a plain and compact text format [21]. Turtle is the extension of N-Triple and subset of N3, therefore, supporting any system which N3 and N-Triple supports. Turtle represents triples in the form of <subject >, <relationship>, and <object>. Some of the most promising features of Turtle includes high expressive power, user friendly than RDF/XML, and the availability of open source online editors and conversion tools. Apart from them popularity of Turtle serialization can be attributed to its wider use, greater conciseness, human readability, ease of generation, and use by the popular tools and APIs including Jena and OWL API[22]. Turtle suffers from the same limitations as RDF/XML having triple based syntax, where reification becomes necessary while translating complex expressions and OWL axioms into triples. Thus, makes the resulting RDF document more disruptive and unpleasant.

2.2. Topic Maps Serialization Formats

In Topic Maps serialization (TMs), data is semantically converted into a suitable format to be stored and transmitted over Internet and reused in a different computing environment, without requiring any change in the original data format. Topic Maps can be represented in a number of serialization formats including XTM, CTM, TM/XML, and LTM etc (as shown in Fig. 5), which could be exported into another computing environment conveniently. A number of applications (e.g., TM4J[6], and Wandora[7] etc) have been invented by the research communities which not only facilitate representing Topic Maps data in afore mentioned serialization formats but also provides consistent methods for interchanging data from one format into another. Using the underlying serialization structures, Topic Maps serialization formats are classified into two broad categories: XML based and non-XML based.

[6] http://tm4j.org/
[7] http://www.wandora.org/www/

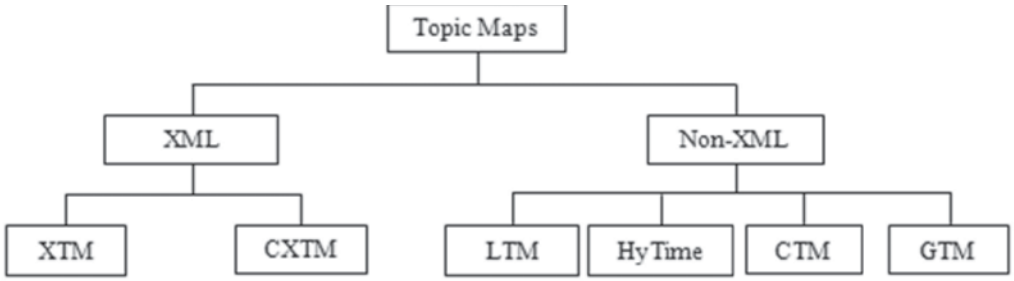

Fig. 5. Classification of Topic Maps serialization formats.

2.2.1. XML Based Serialization

XML based Serialization provides an efficient, easily implementable, and easily interchangeable syntax for Topic Maps documents, due to fact of its working on the lower layer of Topic Maps and direct insertion of any XML tag into Topic Maps information source. A number of XML oriented serialization formats are available, with the capability of smooth interchange of Topic Maps data into another format.

XML Topic Maps (XTM)*:* Knowledge Representation in SGML Topic Maps was suffered for numerous problems including difficult to understand and create, application dependent, and lack of interchangeability. Therefore, a group of researchers in topicmaps.org developed a new syntax with more advanced features than SGML, called XTM 1.0 (XML Topic Maps version 1.0), which uses XML as a storage method and URL for linking and references [23]. Due to its flexibility, software support, and accessible in diverse domains and platform, XTM was standardized by ISO and published as XTM DTD[8] in October 2001. The prominent features of XTM includes simplicity, open architecture, flexibility, user friendly web-centric applications syntax, high expressive power, high level of computability, and the availability of editing and conversions tools [24]. XTM is inherently implemented in the web browser, therefore, knowledge representation, accessibility, and navigation on the Web across applications can be easily done irrespective of scale. The automatic translation process of XTM is made simple by the availability of CAT[9] tool, Translation Management System (TMS)[10] tool, and its support for all common file types. Beside several advantages provided by XTM for its users to create Topic Maps for the World Wide Web, XTM suffers from a number of problems including cannot fully represent the whole Topic Maps paradigm, less compact due to the verbose nature of XML, occupy large space as compared with other Topic Maps serialization formats, and not so much effective in semantic integration and interoperability of Topic Maps constructs [25].

Canonicalization of XML Topic Maps (CXTM)*:* CXTM was developed to overcome the lack of canonicalization in XTM serialization. Canonicalization can be used for immediate comparison of two data model instances to find out correspondence and equality by comparing their canonical serialization [26]. CXTM is XML based serialization format standardized by the ISO/IEC-4 in 2009. The unique feature which distinguishes it from XTM is that the instances of two corresponding Topic Maps data models will generate byte by byte identical serializations at every time and the two Topic Maps data models dissimilar instances will generate different serialization [27]. Test suite for testing different Topic Maps technologies to show the existence of some particular set of behaviours can be effectively created using CXTM. The availability of editing and conversion tools makes the reading, writing, and parsing of CXTM documents pretty much easy. Despite of its good aspects, CXTM is very complex to understand, and is not user friendly. CXTM is only a variation of XTM useful for comparing two Topic Maps data models, which could be done with XTM, indeed.

2.2.2. Non XML Based Serialization

To overcome the limitations and the verbose nature of XML based serialization, several types of non

[8] http://www.topicmaps.org/xtm/1.0/xtm1.dtd
[9] http://www.metatexis.com/cat.htm
[10] http://cmswithtms.net/what-is-a-translation-management-system/

XML serialization formats have been researched for the interchange of Topic Maps data into another format.

Linear Topic Map (LTM): LTM serialization format for Topic Maps was developed by Ontopia[11] in 2001 and refined by Lars Marius Garshol [28]. LTM provide a unique Topic Maps textual editor, which isolates users from the syntactical details of the interchange format unlike that of XTM. Representation of LTM is simple, efficient and takes less space as compared to XTM. This interchange syntax is suitable for small scale Topic Maps constructs especially for personal use like email and chat discussions etc. The computability of LTM is ideal, the syntax is compact, and simple, having user friendly interface as compared to XTM, easily convertible to XTM format, and has efficient parsing mechanism. The expressive power of LTM is low than XTM because of its lack of representing the whole Topic Maps data model [29]. LTM did not succeeded in obtaining standard from any official body (i.e., ISO, etc), therefore, superseded by another Topic Maps serialization format called CTM[12].

Hypermedia/Time-based Structuring Language (HyTime): HyTime is another ISO standard interchange format for Topic Maps, based on SGML (Standard Generalize Mark-up Language, a language which describe the contents of documents rather than its look) [30]. HyTime provides an abstract facility for the Topic Maps paradigm to be expressed in SGML format. Originally HyTime was used to link and organize related topics which are time and space critical, but later on used for any types of Topic Maps representation as well. The expressive power of HyTime is much better, therefore, any sort of virtual notation can be used to express addressing [31]. The architecture of HyTime is flexible, providing simple and user friendly ways for defining new applications, having efficient parsing mechanism, provides convenient way to fulfill the addressing needs, and applicable to any type of hypermedia concepts [32]. The main limitation of HyTime is the lack of support for real SGML because currently there are several SGML systems having limited capability for the support of HyTime standard [33].

Compact Topic Maps (CTM)*:* Compact Topic Maps (CTM) is a text based notation standardized by ISO for representing Topic Maps data. CTM replaces LTM and AsTMa because of its compact syntax and unique feature of supporting TMQL's insert operation [34]. CTM provides several features including its short and simple notation, easy and maximum readability, and providing a common background for TMCL and TMQL. Due to these features CTM can represent any type of Topic Maps resources and their relationships as a simple test pattern. The CTM notation uses CTM processor for the precise computation, enabling users to interact with Topic Maps and perform several data operations such as evaluation, editing, and changing etc. according to user's rights on data. The editing facility provided by CTM is efficient, the transformation and parsing mechanism is fast, and supports all types of character encoding. The limitations of CTM includes the need of special parser for transforming Topic Maps constructs, and the lack of support for item identifiers in the constructs which are not topics.

Graphical Notation for Topic Maps (GTM)*:* Standardized by the ISO, GTM was developed for visual representation and creating similar views of Topic Maps instances and ontologies. The graphical modeling features of GTM are similar to UML, represents topics and associations using rectangles and edges respectively [35]. Names and occurrences of topic's classes are indicated in the lower part of each rectangle. In GTM compositional shapes are available for the representation of topics, associations, labels, occurrences and reification [36]. Due to its visual notation and compact syntax ontologies, TMDM and TMCL can be expressed and understood easily while designing, explaining, and instructing peoples. GTM is simple, user friendly, easy to read in paper form, and can parsed into other formats like XTM and LTM without any change in its original information or addition of new elements. GTM is applicable to both small scale and large scale Topic Maps instance data and ontologies. The unavailability of editors and authoring system, due to its early stages of development is major problem faced by the GTM users.

[11] http://www.ontopia.net/
[12] http://www.isotopicmaps.org/ctm/

4. COMPARISON OF RDF AND TOPIC MAPS SERIALIZATIONS

After thorough analysis it is not difficult to decide that both Resource Description Framework (RDF) and Topic Maps (TMs) are the finest examples of human's efforts for representing objects/concepts and their relationships/associations on the Web not only in human readable form but for the machines equally. To further refine the vision, researchers contributed their massive efforts in developing unique and powerful serializations formats not only to ensure interoperability but to provide flexibility, and strength at extreme levels. In the preceding sections of this paper, the available serialization formats for both of the technologies are highlighted in extreme. To further refine the idea and increase the strength of understanding, the discussed RDF and Topic Maps serializations are evaluated using the evaluation criteria describe in section 2.

A detail comparison of the main features of the RDF serializations is presented in Table 1. It is obvious from the table that every serialization format has their own capability to describe RDF graphs in their own formats. However, as a conclusion of analysis, the most appropriate serialization format to represent RDF graphs is Notation-3 (N3). The superiority of Notation-3 over its companion is due to a number of its reasons including: (1) logic and inference mechanism, (2) compact, persistent and readable syntax, (3) advanced parsing mechanism, (4) availability of open source visual and text based editors, (5) and its expressive power to represent any RDF graph.

Likewise, detailed comparisons of the main features of Topic Maps serialization formats are presented in Table 2. It is find out that every serialization format provides their own facilities, and potentials to represent Topic Maps constructs in different formats effectively. However, as a conclusion of analysis, it is deduced that the most appropriate serialization format to represent Topic Maps documents is XTM. The superiority of XTM over its companions is attributed due to some of its prominent features including: (1) having advanced features than SGML, (2) user friendly and flexible architecture, (3) high expressibility due to XML based syntax, (4) simple interface, (5) automatic translation facility, (6) availability of simple and efficient visual editors, (7) and its applicability for both small scale and large scale projects. Knowledge representation and navigation on the Web can also be done easily by XTM as compared to other serialization formats.

After analysis and comparison of the facts about the RDF and Topic Maps serializations formats presented expressively in the above two tables, it not difficult to reach at a solid conclusion. It is found that both RDF and Topic Maps serialization formats either XML based and non-XML based can be compared using evaluation criteria. Although the two sets of serialization formats have some degree of differences but have majority ratio of similarities, therefore, can be deemed as inter-convertible with the introduction of some technology. The list of similarities among both of the technologies includes it XML based syntax, its representation and navigation on the web, the computation of internal and external resources, advanced automatic translation facility, availability of visual and text based editors, online open source conversion software, and their flexible nature to be represented in any type of languages and their underlying formats.

The two non- XML based serialization formats (i.e., N3 and LTM) for RDF and Topic Maps respectively have also several commonalities and have the possibilities to be used together. Both of the formats can write their own technologies in a simple text editor, availability of prefixes for URIs, having high speed of computability, and represents information in simple and efficient documents requiring less space. Therefore, using the underlying facts it is easy to conclude that we can use RDF serialization formats for encoding Topic Maps data and vice versa with the provision of requiring development of advanced tools and technologies supporting both of the technologies.

5. CONCLUSIONS

The freedom of World Wide Web has lead into exponential growth of web pages containing enormous contents such as text, images, videos, and hyperlinks etc, resulting into the increase of human's cognitive overload. To elevate the problem

and convert the web contents into machine readable and interpretable format Semantic Web is deemed as the ideal solution. To achieve the goals of Semantic Web, a number of technologies are invented by the research communities in the past several years having their foundations in RDF and Topic Maps. To further refine the ideas and achieve high level of interoperability and machine readability, a number of serialization formats are put forwarded by the researchers.

In this paper we presented a comprehensive overview of the taxonomy of Resource Description Framework (RDF) and Topic Maps (TMs) serialization formats by classifying them into XML based and non XML based. RDF and Topic Maps data can be serialized into XML, non-XML, or any other customized format. Thus, providing flexibility, and user friendliness for creating web centric applications while pertaining the expressive power of RDF and Topic Maps paradigms. It was augmented by the critics that the leading factor effecting RDF and Topic Maps interoperability is the underlying serialization formats used by the technologies. Therefore, to turn the vision of their interoperability into reality, a common XML based serialization syntax is needed which should be understandable to both of the technologies. But, in our investigation we came up with finding a number of commonalities which could be exploited effectively with the addition of novel advanced technologies to turn the idea of interoperability into possible. However, the introduction of such advanced technologies is not pretty easy and still needs a massive amount of research contributions from the research communities.

6. REFERENCES

1. World Wide Web. world wide web. [Online]. Internet Available: http://en.wikipedia.org/wiki/World_Wide_Web (Accessed: November 20, 2012).
2. Singh, D.R.K. Mishra & Chandrashekhar. Exploring semantic web using ontologies. *Stem Cell* 2: 11-15 (2012).
3. Berners-Lee, T.J. Handler & O. Lassila. The semantic web. *Scientific American* 284*:* 34-43 (2001).
4. Kaminski, P. *Integrating Information on the Semantic Web Using Partially Ordered Multi Hyperset.* MS thesis, Department of Computer Science, University of Victoria, Canada (2002).
5. Pepper, S. *Topic Maps: Encyclopedia of Library and Information Sciences 3rd ed*. Taylor & Francis Group, New York, USA (2010).
6. Serialization. Serialization [Online]. Internet Available: http://en.wikipedia.org/wiki/Serialization (Accessed: November 22, 2012).
7. Manoj, K.V. What is serialization in .NET, types of serialization and why we need it while developing an application? [Online]. Internet Available: http://www.c-sharpcorner.com/interviews/answer/499/ (27 July, 2006) (Accessed: October 24, 2012).
8. Gonzalez, R. RDF vs. XML [Online]. Inernet Available: http://www.cambridgesemantics.com/semantic-university/rdf-vs-xml (2007) (Accessed: May 17, 2012).
9. Benson, E. A Quick Tutorial on the Turtle RDF Serialization. Internet Available: http://haystack.csail.mit.edu /blog/2008/11/06/a-quick-tutorial-on-the-tutrle-rdf-serialization/ (2008) (Accessed: May 20, 2012).
10. Segaran, T., C. Evans, J. Taylor, S. Toby, E. Colin, & T. Jamie. *Programming the Semantic Web*. O'Reilly Media (2009).
11. W3school. XML tutorial. [Online]. Internet Available: http://www.w3schools.com/xml/default.asp (Accessed: October 14, 2012).
12. Lapalme, G. XML: Looking at the forest instead of the trees [Online]. Internet: http://www.igt.net/~ngrenon/ UdeM/cours/IFT3220/ForestInsteadOfTheTrees.pdf (18 November, 2005) (Accessed: September 13, 2012).
13. Powers, S. *Practical Resource Description Framework (RDF) (First ed.)*. O'Reilly & Associates, North Sebastopol, Canada (2003).
14. Yu, L. *A Developer's Guide to the Semantic Web*. Springer Publishing Company, Berlin Heidelberg, Germany (2010).
15. Jeni. RDF chimera [Online]. Internet Available: http://www.jenitennison.com/blog/node/171 (30 June, 2012) (Accessed: October 24, 2012).
16. Carroll, J.J. & P. Stickler. TriX: RDF triples in XML. *Proceedings of the 13th international World Wide Web Conference on Alternate Track Papers & Posters*: p. 412- 413 (2004).
17. Berners-Lee, T. & D. Connolly. Notation3 (N3): A readable RDF syntax [Online]. Internet: http://www.w3.org/ TeamSubmission/2011/SUBM-n3-20110328/ (28 March, 2011) (Accessed: October 28, 2012).
18. Grlicky, V. An overview of RDF model representation formats. *M. Bieliková (Ed.), IIT.SRC 2005*: 242-248 (2005).
19. N-Triples. N-Triples [online]. Internet: http://en.wikipedia.org/wiki/N-Triples (Accessed: December 11, 2012).

20. Heath, T. & C. Bizer. *Linked Data, Evolving the Web into a Global Data Space (First Edition)*, Morgan & Clay- pool publishers, USA (2011).
21. Beckett, D. & T. Berners-Lee. Turtle - terse RDF triple language [Online]. Internet Available: http://www.w3. org/TeamSubmission/turtle/ (28 March, 2011) (Accessed: January 12, 2013).
22. Horridge, M. OWL syntaxes [Online]. January 22, 2010. Internet Available: http://ontogenesis. knowledgeblog. org/88 (22 January, 2010) (Accessed: December 24, 2012).
23. Tolksdorf, R. C. Bizer. R. Eckstein. & R. Heese. Business to consumer markets on the semantic web. *Proceedings of the On The Move to Meaningful Internet Systems (OTM 2003) Workshops, Catania, Sicily, Italy*: p. 816-828 (2003).
24. Marshall, M. The semantic web & its implications on search marketing [Online]. July 27, 2007. Internet Available: http://www.searchenginejournal. com/the-semantic-web-its-implications-on-search-marketing/ 5390/ (27 July, 2007) (Accessed: December 26, 2012).
25, Pepper, S. & G. Moore. XML Topic Maps (XTM) 1.0 [Online]. Internet Available: http://www. topicmaps.org/ xtm/ (08 June, 2001) (Accessed: November 13, 2012).
26. Ahmed, K. Topic maps — canonicalization [Online]. Internet Available: http://www.isotopicmaps.org/ cxtm/ 2004-11-01/ (11 January, 2004) (Accessed: October 17, 2012).
27. Lee, J. L.M. Garshol. & M. Naito. Topic maps — canonicalization [Online]. Internet Available: http://www.isotopicmaps.org/cxtm/cxtm.html (27 January, 2009) (Accessed: October 17, 2012).
28. Garshol, L.M. The linear topic map notation: definition and introduction, Version 1.3 [Online]. Internet Available: http://www.ontopia.net/download/ ltm.html (17 June 2006) (Accessed: December 10, 2012).
29. LTM. LTM [Online]. Internet Available: http://xsiteable.sourceforge.net/standard-ltm.html (Accessed: October 17, 2012).
30. Fierz, W. & R. Grutter. The SGML standardization framework and the introduction of XML *Journal of Medical Internet Research* 2: e12 (2000).
31. Biezunski, M. & S.R. Newcomb. Differences between XTM 1.0 and the HyTime-based meta-dtd [Online]. Internet Available: http://www.topicmapslab.de/ publications/differences_between_xtm_10_and_ hytime-based_meta-dtd (18 December, 2001) (Accessed: October 18, 2012).
32. Rutledge, L. J. V. Ossenburgen. L. Hardman. & D.C. A. Bulterman. A framework for generating adaptable hypermedia documents. *Proceedings of the Fifth ACM international conference on Multimedia, Seattle, Washington, USA*, p. 121-130 (1997).
33. Newcomb, S. R. Using the information addressing model of HyTime (ISO 10744) to add hypermedia functionality to legacy data and systems. *Proceedings of the Second International Workshop on Incorporating Hypertext Functionality into Software Systems held in conjunction with the ACM Hypertext '96 conference, Washington, USA* (1996).
34. Hopmans, H. & O. Pepper. WD 13250-6: Topic maps – compact syntax [Online]. Internet Available: http://lingo.uib.no/trond/TopicMaps/CTM Working Draft.pdf (15 September, 2006) (Accessed: January 22, 2013).
35. Witt, T. Conception and Implementation of a Visual Editor for Topic Maps [Online]. Diploma thesis, Department of Institut für Informatik Ludwig-Maximilians-Universität München, Germany (2009).
36. Thomas, H., T. Redmann, M. Pressler & B. Marksscheffel. GTMalpha – Towards a graphical notation for topic maps. *Proceedings of the Fourth International Conference on Topic Maps Research and Applications (TMRA 2008) - Subject-centric computing, Leipzig, Germany,* p. 56-66 (2008).

Proceedings of the Pakistan Academy of Sciences 51 (2): 115–119 (2014)

ISSN: 0377 - 2969 (print), 2306 - 1448 (online)

Pakistan Academy of Sciences

Research Article

Cost Analysis of Aluminum Winding Transformer for Electrical Distribution Network of Pakistan

Umar T. Shami[1*] and Muhammad A. Shahid[2]

[1]Department of Electrical Engineering, University of Engineering and Technology, G.T. Road, Lahore, Pakistan
[2]Transformer Design Section, PEL, 14-km Ferozepur Road, Lahore, Pakistan

Abstract: Aluminum winding transformers have not yet been introduced in the distribution network of Pakistan. This paper evaluates the use of electrolytic aluminum in oil immersed distribution transformers to be used by electric utilities of Pakistan. Specifications for distribution transformers in terms of size and losses are examined. A particular rating from the specification is selected for transformer design with copper and aluminum winding separately. The cost of aluminum winding transformer was compared with the conventional copper winding transformer for the same technical performance parameters. Feasibility of aluminum winding transformer in the distribution network is presented and its viability is established through analyzing a practical unit.

Keywords: AC utilities, aluminum winding transformer, distribution transformer

1. INTRODUCTION

Globally, rise in cost of copper has affected the total transformer cost considerably. The design and manufacture of aluminum transformers is inadequate in Pakistan. Consequently, the relevant utilities in the country are purchasing bulk quantity of distribution transformers from local manufacturers with copper windings only. In June 2010, WAPDA revised the iron and copper losses for distribution transformers which are now about 20% less than the previously defined losses (Amendment # 5 of WAPDA Specs. DDS 84:2007) [1]. This reduction in losses has caused considerable increase in the price of transformer as the transformers procured are still of copper winding. Many researchers of the power engineering field have recommended the use of aluminum winding transformers instead [2]. In addition, many transformers manufacturing companies abroad have commenced aluminum winding transformer manufacturing [3]. Up till now local utilities have shown little interest for the procurement of aluminum winding transformers. Also, none of the Pakistani transformer manufacturers have worked out on this option.

In order to get approval as per standards for the distribution transformers, individual transformer manufacturer has to go through the type testing of that particular rating transformer. These type tests include impulse, temperature rise and short circuit test from an independent laboratory, such as WAPDA's High Voltage and Short Circuit Laboratory at Rawat in Punjab province, Pakistan. The short circuit test has to be repeated every year on an approved prototype transformer [2]. After the short circuit test, average temperature of winding should not exceed 200ºC for aluminum winding transformer, and 250ºC for copper winding transformer. In addition, no physical deformation in the core-coil assembly of the transformer should be observed [4]. In this scenario, the risk of failure for an aluminum winding transformer is higher as the thermal conductivity and tensile strength of aluminum is less than copper (thermal conductivity – 210 vs 398 W/mK and tensile strength – 46.5 Vs. 124 MPa).

Received, November 2013; Accepted, April 2014
*Corresponding author: Umar T. Shami; Email: ushami@ymail.com

2. COST ANALYSIS

For medium range distribution transformers, i.e., up to 3000kVA, the tensile strength of aluminum can withstand the forces arising due to short circuit. For power transformers, where the short circuit forces are high, use of aluminum causes problems [5].

The percentage cost of materials in a transformer depends upon the losses and dimensions of the transformer required by the customer. The cost of materials in percentage for optimum defined losses is given in Table 1 [6].

The high voltage (HV) winding of a transformer can be constructed using either enameled aluminum wire or paper insulated aluminum conductor. For low voltage (LV) winding, due to high current, aluminum foil is required which is imported. Paper insulated aluminum wire can also be used in the LV of transformer; however, the use of foil eliminates the axial short circuit forces during a short circuit condition [7]. The failure rate of aluminum wound distribution transformers is greater in haphazardly expanded network where frequent switching and external short circuits occur [8]. To avoid this problem, the winding should be manufactured with interlayer varnish in both LV and HV windings. This will bond the winding together to minimize the risk of failure in the field short circuit. Also the pressure blocks should be seated properly on the windings to keep them rigidly within the clamping structure.

AA1050 is the aluminum grade to be used in transformer winding. It consists of 99.15% of Al and the remaining 0.85% includes Cu, Mg, Si, Fe, Mn, Zn and Ti [9]. In an aluminum winding transformer, the winding resistance calculation to convert it to a reference temperature (θ_r) for winding losses evaluation is different from a copper winding transformer. In the case of copper or aluminum, the winding losses R_r is calculated with the aid of a reference temperature θ_r. For copper winding, R_r is expressed as,

$$R_r = R_1\left(\frac{235+\theta_r}{235+\theta_1}\right), \quad (1)$$

Whereas for aluminum, R_r is expressed as,

$$R_r = R_1\left(\frac{225+\theta_r}{225+\theta_1}\right) \quad (2)$$

Where, both eq. (1) and (2), resistance of winding R_1 is taken at a temperature θ_1 [10].

A comparison of copper and aluminum temperature graph for distribution transformers during short circuit test for 4s is displayed in Fig. 1 [10]. Normally, the resistivity of aluminum is about 1.8 times greater than the resistivity of copper. Therefore, higher cross-sectional area of aluminum conductor is required to achieve the same winding losses to that of copper winding transformer. The greater volume of aluminum winding transformer would require more core, insulation, oil and a larger tank size. However, there is a considerable cost difference between the prices of copper and aluminum and winding is the most expensive part of the transformer. As per current (Sept., 2013) LME (London Metal Exchange) prices, the cost of copper is US $/Ton 7,170.50 and that of aluminum US $/Ton 1,780.50 [11]. Mass density of Aluminum is approximately 3.3 times less than the mass density of copper; therefore, less mass of aluminum is consumed to achieve the same winding losses to that of copper winding transformer.

A comparison of copper and aluminum prices from the period from 2007 to 2013 is given in Fig. 2 [11-13]. As can be seen from the graph that at any point aluminum is about 3.5 times economical than copper over the period of past seven years.

There are nine types of ratings defined in the WAPDA specifications for distribution transformers. The ratings from 5kVA to 200kVA are pole mounted whereas 400 and 630kVA are platform mounted transformers. As per latest revision of WAPDA specifications [4] DDS 84:2007, the losses are defined as in Table 2.

There is no mandatory requirement in WAPDA specification that the winding of the transformer should be of copper only. The approval of prototype transformer from WAPDA involves physical verification of materials and its mass; therefore, any manufacturer cannot claim an aluminum winding transformer as copper winding transformer. Hence it is not possible to bid a transformer on copper price and manufacture aluminum winding transformers. 630kVA is the largest rating in the WAPDA distribution network. The material cost comparison of 630kVA transformer with both aluminum and

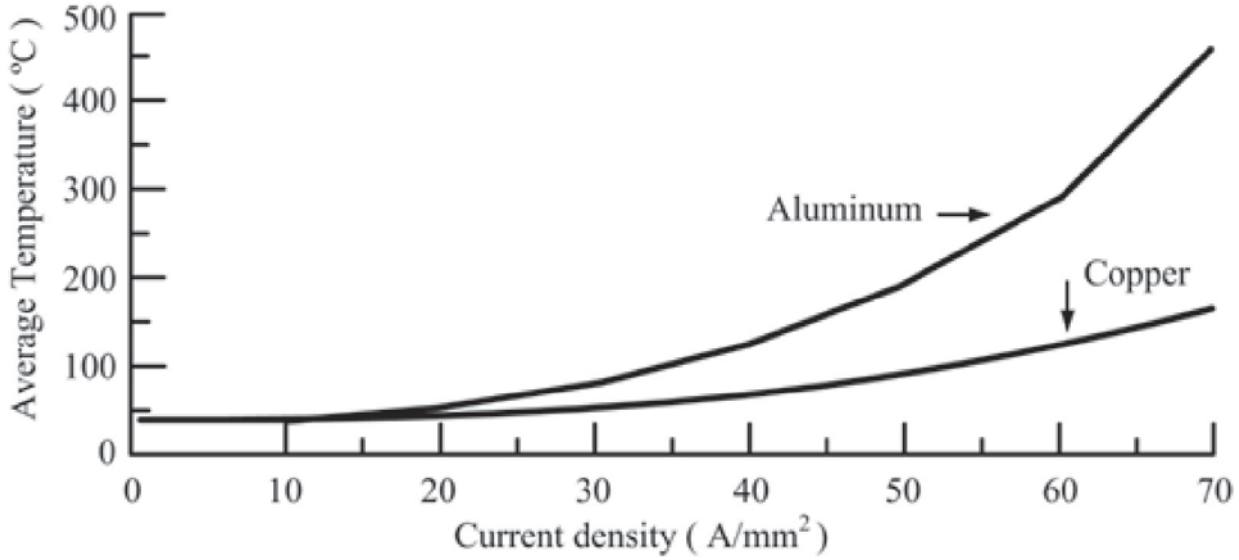

Fig. 1. Comparison of copper and aluminum temperature graph for distribution transformers during short circuit test for 4s [1].

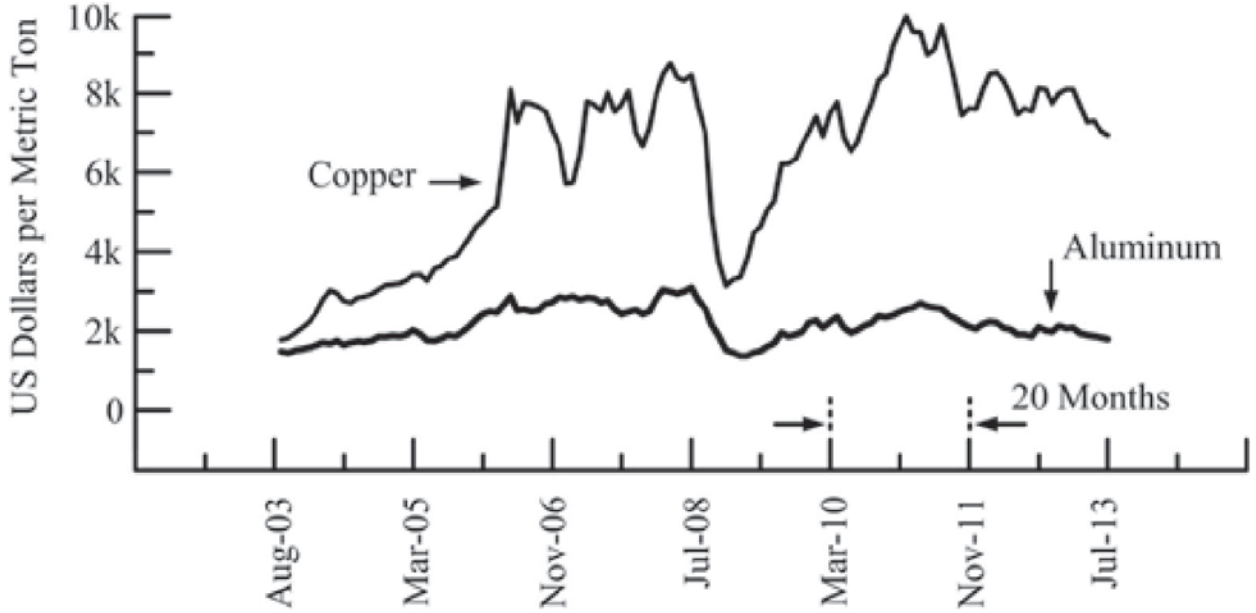

Fig. 2. Comparison of copper and aluminum per metric ton price from the period 2003 to 2013[10-12].

copper winding transformers are presented in Table 3, where the material cost is determined by keeping the performance parameters same for both copper and aluminum winding transformer as defined in WAPDA Specification DDS 84:2007 amended to date.

Table 1. Distribution transformer material costs in percentage.

Material	% Cost	Tolerance
Silicon Steel Sheet	22	±5
Windings	32.5	±6
Insulation	14.1	±5.5
Tank Structure	16.4	±8.5
Tap changer, bushings, etc.	15	±9

Table 2. Distribution transformer kVA rating with losses.

kVA	5	10	15	25	50	100	200	400	630
Fe Losses (W)	44	52	68	98	140	248	396	740	1080
Cu Losses (W)	140	256	348	512	936	1616	2728	4480	6520

Table 3. Assembled 630kVA distribution transformer cost comparison (as of Sept. 2013).

Material	Cost of Copper Winding Transformer	Cost of Aluminum Winding Transformer
Winding	Rs. 266801	Rs. 56792
Core	Rs. 167461	Rs. 177776
Oil	Rs. 87640	Rs. 105280
Steel Structure	Rs. 66159	Rs. 67280
Insulation & Accessories	Rs. 71769	Rs. 76052
Miscellaneous (4% of total cost)	Rs. 26393	Rs. 19276
Total Cost of Transformer	Rs. 686223	Rs. 502507
Total Cost of Transformer	US $ 6474	US $ 4741

3. DISCUSSION

Approximate comparison of copper winding and aluminum winding complete assembled 630 kVA distribution transformers is summarized in Table 4. The cost of aluminum winding transformer is 26.9% less than the cost of copper winding transformer based upon same performance parameters. The cost of core, coil, steel structure and Insulation is more in aluminum winding transformer as compared to copper winding transformer but there is a 78.7% reduction in the material cost of winding which is ultimately resulting in reduction in the overall material cost of aluminum winding transformer.

It is evident that the aluminum winding transformer is feasible for the distribution network of Pakistan as far as cost comparison with copper winding transformer is concerned. For Pakistani distribution network where utilities are spending enormous budget on purchasing a large quantity of transformers (approximately 40,000 to 45,000 transformers per year), this can be an attractive solution saving millions of rupees. Manufacturing issues such as brazing of aluminum wire with the tap changer pins, where aluminum being brittle material, may break easily at this point.

Frequent switching and short circuits occurring in electric distribution network may severely affect the aluminum winding transformer. Special care is to be taken during manufacturing of aluminum winding transformer. The winding has to be tightly wound with varnish used within each layer. The clamping structure should hold the windings tightly and aluminum conductor should be annealed before manufacturing the winding.

4. CONCLUSIONS

Winding being most expensive component of the transformer plays an important role in determining the total cost of the transformer. Replacing copper with aluminum in a transformer increases the overall volume of the transformer, however, still aluminum winding transformer turns out to be 26.9% less expensive than copper winding transformer for 630 kVA rating as per WAPDA specs. DDS 84:2007, amended to date.

For developing countries, like Pakistan, where capital cost of transformers matters, switching over to aluminum winding transformers is an optimized solution. By observing some precautions in manufacturing, these can suit the distribution network not only of Pakistan but in any developing country.

5. REFERENCES

1. WAPDA specification DDS84:2007. *Oil Immersed Distribution Transformer 11 / 0.415kV.* Water and Power Development Authority, Pakistan (2010).
2. Olivares-Galván, J.C., F.de León, P.S Georgilakis, & R. Escarela-Pérez, Selection of copper against aluminum windings for distribution transformers. *IET Electric Power Applications* 4: 474-485(2010).
3. Siemens, A.G. *Power Transmission and Distribution Transformers Division*. GEAFOL cast-resin Transformers. http://www.energy.siemens.com/br/pool/br/transmissao-de energia/transformadores/Geafol_ing.pdf
4. IEC Standard 60076-5. Power transformers: Part 5 – ability to withstand short circuit. *International Electrotechnical Commission (IEC)* (2006).
5. Tipton, E.W. Experiences with the use of aluminum in windings for dry-type power transformers. *Transactions of the American Institute of Electrical Engineers. Part III. Power Apparatus and Systems* 74: 1201–1204 (1955).
6. Olivares, J.C., Y. Liu, J.M. Cañedo, R. Escarela-Pérez, J. Driesen, & P. Moreno. Reducing losses in distribution transformers. *IEEE Transactions on Power Delivery* 18: 821-826 (2003).
7. Hori, Y. & K. Okuyama. Axial vibration analysis of transformer windings under short circuit conditions. *IEEE Transactions on Power Apparatus and System* PAS-99(2): 443-451(1980).
8. Beniwal, N.S., R. Rani, H.O. Gupta, & D.K. Dwivedi. Effect of temperature on tensile and creep characteristics of aluminum wire used in 25 kVA distribution transformers. *IPEC Conference Proceedings* 6(2): 205–208 (2010).
9. Chemical Composition of Aluminum Alloy 1050. http://www.azom.com/article.aspx?ArticleID=2798#_Chemical_Composition
10. IEC Standard 60078-1. Power Transformers - Part-1, General. *International Electrotechnical Commission(IEC)*, Amendment No. 1 (1999).
11. Aluminum Monthly Price - US Dollars per Metric Ton. http://www.indexmundi.com/commodities/?commodity=aluminum&months=120
12. London Metal exchange official price for copper. http://www.lme.com/metals/non-ferrous/copper/#tab2
13. London Metal exchange official price for aluminum. http://www.lme.com/metals/non-ferrous/aluminium/#tab2

Proceedings of the Pakistan Academy of Sciences 51 (2): 121–127 (2014)

ISSN: 0377 - 2969 (print), 2306 - 1448 (online)

Pakistan Academy of Sciences

Research Article

New Fungal Records on Guava (*Psidium guajava*) from Pakistan

Syed Qaiser Abbas[1], Mubashir Niaz[1], Thereema Iftakhar[1], Abida Perveen[1], Alia Abbas[2]* and Sana Riaz[1]

[1]Department of Botany, Government College University, Allama Iqbal Road, Faisalabad, Pakistan
[2]Department of Botany, Federal Urdu University, Karachi, Pakistan

Abstract: *Rutola graminis* (Desm.) Crane & Schokn., *Cladosporium nigrellum* Ellis & Everh. and *Gliomastix* state that *Wallrotheilla subiculosa* Hohn. are reported for the first time on *guava (Psidium guajava* L.) from Pakistan. *Alternaria tenuissima* (Kunze ex Pers.) Wiltshire is also reported for the first time on guava from Faisalabad, Pakistan.

Keywords: *Rutola graminis* (Desm.) Crane & Schokn, *Cladosporium nigrellum* Ellis & Everh. *Gliomastix* state of *Wallrotheilla subiculosa* Hohn, *Alternaria tenuissima* (Kunze ex Pers.) Wiltshire

1. INTRODUCTION

In a project on survey and surveillance of fungal associations to the flora in district Faisalabad, Pakistan, a detailed survey of the area was carried out for guava (*Psidium guajava* L.; local name, *Amrood*).

Guava is a small tree or shrub, belonging to family *Myrtaceae*, about 6 m tall. In Pakistan guava is cultivated on more than 62.5 thousand hectares [11] and in the Punjab province, Pakistan on 50.3 thousand hectares; its annual production in the country is 421.3 thousand tones [9]. Guava fruit contains 0.7% protein, 11% carbohydrates and appreciable amounts of certain vitamin A, B1, B2 and C and some minerals [10]. The ripened fruit is eaten in fresh and is used in jams, juices and sauces. Guava may boost natural immunity and is thought to provide antioxidant protection for heart and against cancer.

Guava is grown worldwide and its growth and production is reported to be stressed by a number of diseases [24]. Among the diseases which attack guava plant, wilt is very destructive. This disease is characterized by yellowing and browning of leaves and the tips of the twigs. Another important disease which is reported recently in Pakistan is anthracnose of guava, caused by *Gloeosporium psidii* which attacks all the above ground plant parts resulting in death of the branches. [25]. In India, guava decline due to fungal attack is the most serious and devastating disease, destroying thousands of trees annually, thus attaining the status of a national problem [27].

Twenty one (21) fungi have been reported to infect guava plants in Pakistan, viz., 1) *Phytopthora parasitica* in Faisalabad [12]; 2) *Capnodium sp.*, on guava in Karachi [18]; 3) *Glomerella cingulata* Stonem.) Spauld & Schrenk, on guava fruit in Karachi [20]; 4) *Alternaria alternata* on bark of guava in Pattoki and Sharqpur [17]; 5) *Alternaria tenuissima*. (Kunze ex Pers.) Wiltshire, on guava leaves in Karachi [18]; 6) *Cladosporium sp.* on leaves in Karachi [19] and on guava's twigs in Pattoki and Sharqpur [17]; 7) *Curvularia* sp. on tree branches in Pattoki and Sharqpur [17]; 8) *Fusarium solani* in Larkana, [11] ; 9) *Fusarium solani f. f. sp. psidi ava* in Faisalabad [12]; 10)

Received, March 2012; Accepted, February 2014
*Corresponding author: Alia Abbas; Email: abbasalia@ymail.com

Fusarium oxysporum on tree branches in Pattoki and Sharqpur [17] ; 11) *Fusarium oxysporum f. f. sp. psidi* in Faisalabad [12]; 12) *Gleosporium psidii*, on plant twigs of in Pakistan, [19]; 13) *Penicillium sp.* on tree bark in Pattoki and Sharqpur [17]; 14) *Pestalotiopsis brevista* Sacc. on leaves and fruit in Karachi [18,20]; 15) *Phomopsis sp*. on fruit in Karachi [18,20]; 16) *Phoma psidii* Ahmad on dead branches in Lahore and Karachi [3, 6, 18]; 17) *Diplodia psidii* Ahmad on tree branches in Bhawalpur [5, 7]; 18) *Stagnopsis psidii* on branches *in* Bhawalpur [5,7]; 19) *Pestalotia psidii* Pat., on dead twigs in Pakistan [26]; 20) *Lasiodiplodia undulata* (Pat). Abbas, Sutton, Ghaffar, and Abbas [1] (as *Botryodiplodia theobromae* Pat) on dead branches of *Psidium guajava* in Tandojam [21] and Faisalabad [12, 18]; and 21) *Polyporus sp.* on tree anches in Haripur (Hazara) [19].

2. MATERIALS AND METHODS

Methodology of the study was the same as described elsewhere [2]. Samples of infected *Psidium guajava* were collected from the different areas of Faisalabad city, i.e., G.C. University, Faisalabad; University of Agriculture, Faisalabad; and Sheikh Colony, Faisalabad. Identification of fungi, up to species level, was carried out [8, 13, 15, 16, 22].

3. RESULTS

The fungus found on *Psidium guajava*, specimen number 18 belonged to *Rutola graminis* (Desm.) Crane & Schokn.

1) ***Rutola graminis*** (Desm.) Crane & Schokn., *Can. J. Bot.,* **55** (24): 3015 (1978) (1977)

   = *Torula graminis* Desm. *Annls Sci. nat.,* 11, **2**: 72 1834.

Description of the Identified Fungus

Mycelium immersed. Cronate conidiogenous cells absent, Conidia brown, minutely verruculose, conidia in a long chain, sometimes branched chains which break up into 0, 1, 2, 3 or more segments. Conidia. 0-septate, almost spherical but often slightly broader than long, 4 - 4 .8 x 4.2 – 5.8 µm.

The fungus under study was compared with *Rutola graminis* (Desm.) Crane & Schokn. It was observed that it closely resembled to *Rutola graminis.* Resembelence lies in conidial size and absence of cronate conidiogenous cells. In *Rutola graminis* conidia were 4-5 x 4-6 µm, where as in the fungus under study conidia were 4 - 4. 8 x 4.2 – 5.8 µm, therefore fungus under study was identified as, *Rutola graminis* (Desm.) Crane & Schokn.

Crane & Schokn, 1978 [14] erected genus *Rutola* based on *Torula graminis* Desm. Crane & Schokn studied the type specimen of *Torula graminis* Desm. (1834), they observed that the distinguining character "cronate conidiogenous cells" of genus *Torula* Persoon ex Fries was not present in *Torula graminis* Desm. Therefore they erected a new hyphomycetous genus *Ratula* Crane & Schokn based on *Torula graminis* Desm. This is a monotypic genus with only one species *Rutola graminis* (Desm.) Crane & Schokn.

In the present study, genus *Torula* was first time replaced in Pakistan. *Psidium guajava* is a new host record of *Rutola graminis* from Faisalabad, Pakistan.

Specimens Examined

Rutola graminis, on branches of *Psidium guajava*, collected from University of Agriculture, Faisalabad: August 19, 2007; S.Q. Abbas and Abida Perveen; G.C.U.F.M.H# 18.

The fungus found on *Psidium guajava*, specimen # 19, was identified as *Cladosporium nigrellum* Ellis Everh.

2) ***Cladosporium nigrellum*** Ellis Everh: 1894 (1893), *Proc. Acad. N. Sci. Philad.* : 463, Ellis More Dematiaceous Hyphomyctes: 329 (1976). Fig. 2 (A-B).

Description of the identified fungus: Mycelim brown, septate. Conidiophore septate, brown, 240 - 250 x 5 - 9.32 µm. Conidia smooth, brown, conidia ellipsoidal, cylindrical, oval and 0-3 septate. 5.32-15.31 x 4- 7 µm.

Cladosporium nigrellum Ellis Everh., *C apicale* Berk. & Brown, *C. uredinicola* Speg., *C. macrocarpum* Preuss, *C. variable* (Cooke) de Vries and *C. brassicae* (Ellis & Barthol) Ellis., have 0-3 septate conidia. The fungus under study on *Psidium guajava* also has 0-3 septate conidia. In spite of

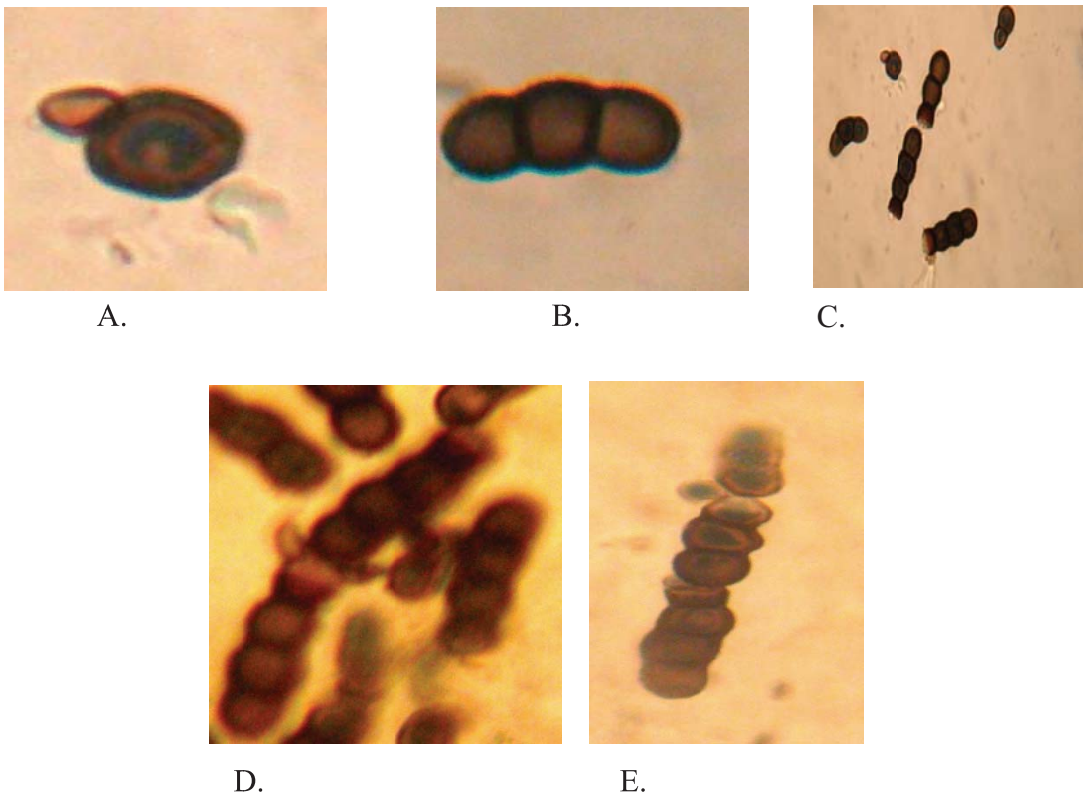

Fig. 1. *Rutola graminis* (A-E), A. Conidia 1000X, B. Conidia in a chain of three cells (400X), (C.D.E), Conidia in a chain of more than nine cells (1000X).

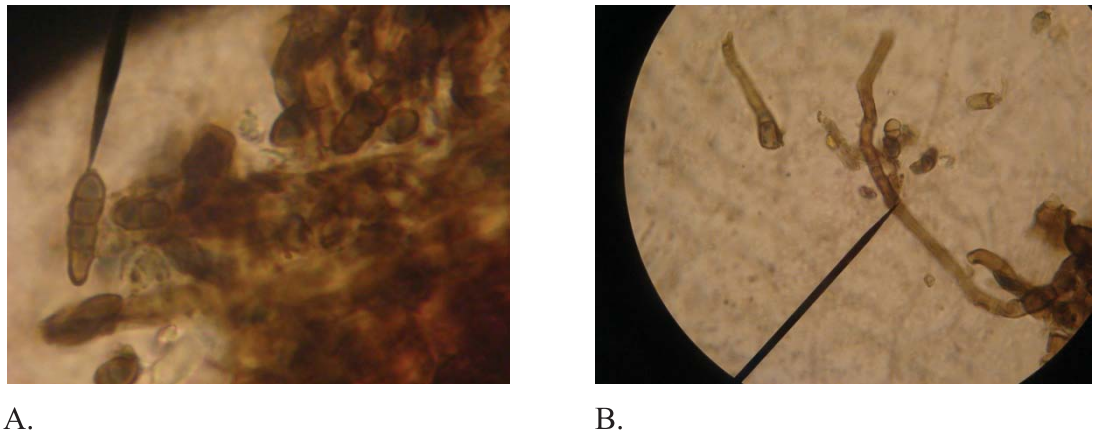

Fig. 2. (A-B): *Cladosporium nigrellum* A. 1-septate, 2-septate and 3-septate conidia 1000X, B. conidia and conidiophore 400X.

similarity in having 3 septate conidia, there are some differences among them; *C. brassicae* have shorter conidiophores 150 x 6-9 µm with terminal and intercalary swellings of diameter 10-12 µm than the fungus under study which has conidiophores of 240 - 250 x 5 - 9.32 µm. Similarly *C. apicale* also have longer and wider conidiophores 260 x 6 - 8 µm than the fungus under study 240 - 250 x 5 - 9.32 µm. Whereas *C. variable* have longer conidiophores 350 x 6 - 8 µm than the under study fungus. *C. macrocarpum* differs from under study fungus in having longer but less wider conidiophores 300 – 4 - 8 µm with terminal and intercalary swellings of diameter 9 - 11 µm. Furthermore *C. uredinicola* also differs from under study fungus in having longer and less wider conidiophores 300 x 3 - 5µm than

the under study fungus where the conidiophores are of 240 - 250 x 5 - 9.32 µm. Conidiophores in *Cladosporium nigrellum* are wavy, smooth, reddish brown, septate, 240 - 250 x 5 - 9.32 µm. and conidia are lemon shaped to cylindrical, narrowing at the ends, , in simple or branched chains, smooth walled, light brown, 5 - 15 x 4 - 7 µm.

After comparative studies, it was concluded that *Cladosporium nigrellum* closely resembled with fungus under study found on *Psidium guajava*, from Faisalabad, Pakistan. Therefore, it is identified as *Cladosporium nigrellum*.

Eighteen (18) species of *Cladosporium* were identified from Pakistan; however, *Cladosporium nigrellum* was not previously reported from Pakistan [8].

In this report *Cladosporium nigrellum* is reported for the first time from Faisalabad, Pakistan. Further more, *Psidium guajava* is an addition to the list of hosts of *Cladosporium nigrellum* from Faisalabad, Pakistan.

Specimens Examined

Cladosporium nigrellum on the branches of *Psidium guajava*; Sheikh Colony, Faisalabad, August 21, 2007: S.Q.Abbas and Abida Perveen G.C.U.F.M.H. # 19.

The fungus found on branches of *Psidium guajava*; G.C.U.M.H.# 20 was *Gliomastix* state of *Wallrothiella subiculosa* Hohn.

3) ***Gliomastix* state of *Wallrothiella subiculosa*** Hohn., *Sber. Akad. Wiss. Wien*, Math. aturw. Kl., Abt. 1,**121**: 381(1912), Ellis, Dematiaceous Hyphomycetes CAB, IMI Kew: 520, (1971) Fig. 3, (A-D).

Description of the Identified Fungus

Conidiophore branched, sometimes simple, usually brown in colour. The base of conidiophore is darker than the upper part, septate. Conidia light brown, oval, some times globose, smooth walled, 3.8-4.1-7.6 x 2.68-3.84 µm. Conidia formed endogenously from the tip of the conidiophore and aggeregated in a mucilaginous sheath.

The fungus under study closely resembled with *Gliomastix* state of *Wallrothiella subiculosa.* The surface and the shape of conidiophore of both were the same, the base of conidiophores are more darker than the upper region and septate. Further more the conidia of both are smooth and aggeregated in slimy mass. Conidial length and breadth were also same. In *Gliomastix* state of *Wallrothiella subiculosa* conidia are (3-8 x 2-4. µm) and conidia in the fungus under study are (3.8- 7.6 x 2.68-3.84 µm), Therefore the fungus under study was identified as *Gliomastix* state of *Wallrothiella subiculosa.* Hohn.

The species under study was also compared with *Gliomastix murorum* Hughes, which resembles with *Gliomastix* state of *Wallrothiella subiculosa*. In both species conidia arising from the apex of conidiophores which act as conidiogenous cells, but differes that the conidiophores of *Gliomastix murorum* are not septate, while they are septate in *Gliomastix* state of *Wallrothiella subiculosa.* Conidia of *Gliomastix murorum* are smaller (2.5 - 5.5 x 2 - 4.5 µm) than the conidia of *Gliomastix* state of *Wallrothiella subiculosa.* (3.8 - 7.6 x 2. 68 - 3.84 µm).

Gliomastix state of *Wallrothiella subiculosa*a also resembles with *Gliomastix ceralis, Gliomastix cereale* (Karst) Dickinson. In both species conidia fromed from the tip of the conidiophore, which act as conidiogenous cells. Further more similarity also lies in having septate conidiophores. Howevere they differe in that, conidial surface are verruculose in *Gliomastix ceralis* and smooth. in *Gliomastix* state of *Wallrothiella subiculosa*

Four species of *Gliomastix* have been reported from Pakistan on different hosts/substrate, but was not reported earlier on *Psidium guajava*, viz.: 1) *G .mororum* (Corda) Hughes; 2), *G. convoluta* (Harz) Mason; 3) *Gliomastix cerealis* (Krast) Dickinson. 4) *G.luzulae* (Fucekl) Mason ex Hughes.

Correct name of *G. mororum* (Corda) Hughes is *Gliomastix murorum* (Corda). var. *murorum* Hughes and *G. convoluta* (Harz) Mason is the synonmys of *Gliomastix murorum* (Corda). var. *murorum* Hughes; thus the reported species of *Gliomastix* remained three. 1) *Gliomastix cerealis* (Krast) Dickinson from soil of Alpine meadow, Mt Gilpur (Nangaparbat) [23]; 2) *G. Gliomastix murorum* (Corda). var. *murorum* Hughes (as *G. Gliomastix murorum* (Corda) Hughes), from

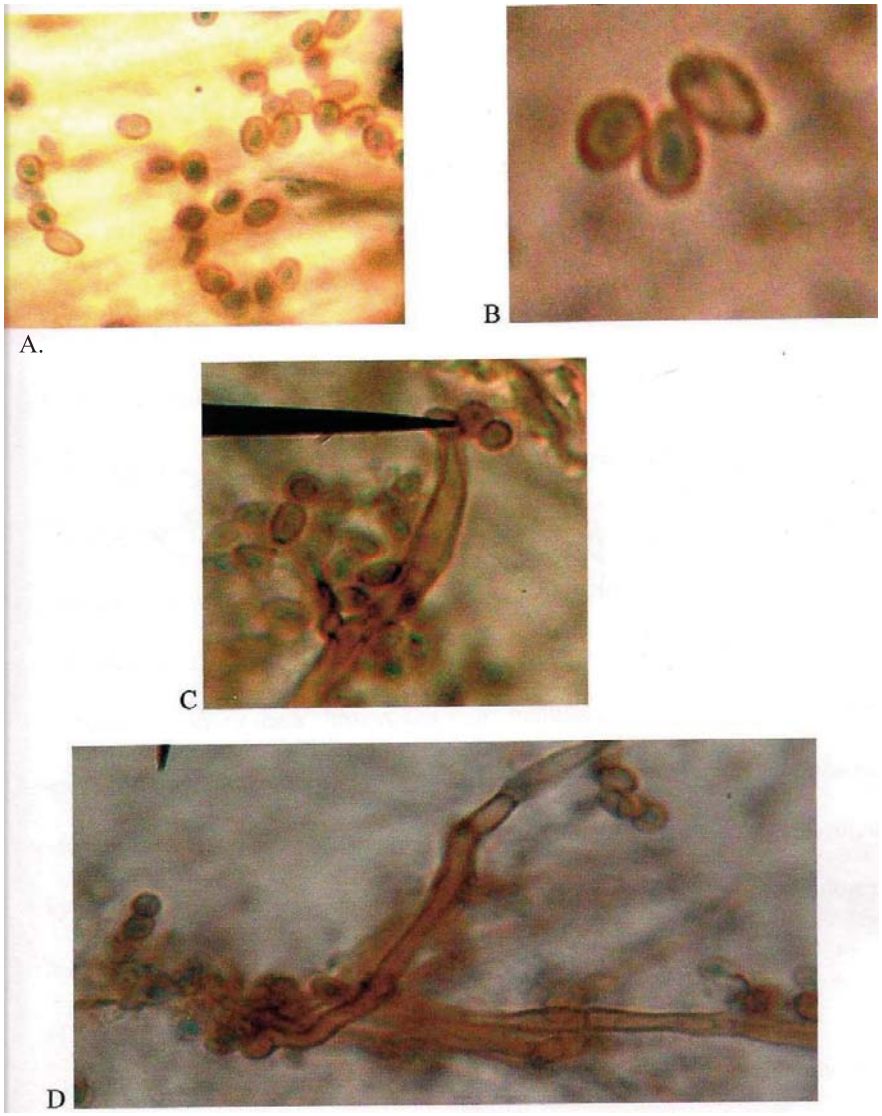

Fig. 3. *Gliomastix* state of *Wallrothiella subiculosa* (A-D) A. Conidia 400X, B. Conida 1000X C. Conidia with conidiophore 400 x. D. septate Conidiophore 400x.

A. B.

Fig. 4. (A-B): *Alternaria tenuissima* A. Conidia 1000X, B. Conidia 400X.

coniferous soil; Mansehra (Swat) [23]; and (as *G. convoluta* (Harz) Mason) on *Polyporus sp*., Kaghan vally, Sarhan [4]; 3) *G.luzulae* (Fucekl) Mason ex Hughes from bush soil; Margalla (Islamabad) [23].

Gliomastix state of *Wallrothiella subiculosa* was not reported from Pakistan [8]; Howevere it was reported on bamboos, oil palm, *Phormium, Solanum, Theobroma* etc. and isolated from the soils of Europe, Java, Hong Kong, New Zealand and West Africa [16]. In the present study, *Gliomastix* state of *Wallrothiella subiculosa* is reported on *Psidium guajava,* from Pakistan (Faisalabad) and is an addition to mycoflora of Pakistan.

Specimen Examined

Gliomastix state of Wallrothiella subiculosa on branches of *Psidium guajava*; Jhang Road garden, Faisalabad; September 4, 2007: S.Q. Abbas and Abida Perveen. G. C. U. M. H. # 20.

4) The fungus on *Psidium guajava* specimen No. 16 belongs to *Alternaria tenuissima* (Kunzeexpers) Wiltshire.

Alternaria tenuissima (Kunze ex pers) Wiltshire, [as (Fr.) Wiltshir] *Trans. Br. Mycol. Soc.***18**: 157 (1933.) Fig. 4 (A-B)

=*Helminthosporium tenuissimum* Kunze in C.G. & T.F.L. Nees,, *Nova Acta Acad. Caesar. Leop.* Carol; ***9***: 242, (1818); Persoon, *Mycol. Eur*; **1**: 18. (1822).

=*Macrosporium tenuissimum* Fr; *Syst. Mycol*; **3**: 374. (1832

Description of the Identified Fungus

Mycelium well developed septate branched pale brown. Conidiophore solitary or in groups, simple and branched, septate and thick walled, smooth, brown; 84 - 117 x 4.2 - 5.9 µm thick. Conidia usually smooth, sometimes minutely verruculose, generally with 3-7 transverse and 0-4 longitudinal septa, brown in colour. Sometimes slightly constricted at the position of septa. 22.75 – 97 x 10.5 - 17.5µm thick in the broadest part, beak of conidia 2.8 - 4.2µm thick, swollen at apex 4.2 - 4.9 µm wide.

The fungus under study is identified as *Alternaria tenuissima*; (Kunze ex pers) Wiltshire

Fungus under study can easily be distinguished from *A. dianthicolla, A. longissima, A. brassicae, A. solani, A. crassa, A. porri, A. carthami, A. dauci, A. passiflorae, A. cucumerina* by having very long transversely septate beak.

Furthermore this species is also compared with *Alternaria sonchi* Davis. Conidiophores of *Alternaria sonchi* are up to 80 x 5-9 µm, while the conidiophores of *Alternaria tenuissima* are up to 115 x 4-6 µm. Similarly conidia of *Alternaria sonchi* are 60-130 (77) x 15-26 µm (20) thick in the broader part; beak 4- 10 µm wide, while conidial length of the under study fungus is 23 - 98 x 10.5-17.5 µm thick in broader part; beak is 2.8-4.2 µm clearly differed from *Alternaria sonchi.*

The fungus under study differs from *Alternaria raphani* Groves & Skolko. The conidia in *A. raphani* are more longer and more wider (50 - 130 (70) x 14 -30 µm (22) µm.) than the conidia of under study fungus (22.75- 97 x 10.5-17.5 µm.). Both species are different from each other. The fungus under study closely resembled with *Alternaria tenuissima* in number of septa, in conidia, their Length and thickness. Conidia in *Alternaria tenuissima* are (22.75- 97 x 10.5-17.5 µm), and have 3-7 transverse septa resembled with *Alternaria tenuissima* where as conidia are (22-95 x 8-19 µm and 4-7 transverse septa. Similarly measurements of conidiophores also resembled with the fungus under study. Conidiophores in fungus under study are (84-117 x 4.2-5.9µm) and are115 x 4-6 µm in *Alternaria tenuissima.*

Alternaria tenuissima is a common fungus in Pakistan and found on more than 54 different plant belonging to different families including *Psidium guajava*, but not reported on *Psidium guajava* from Faisalabad [8]

In the present report, *Alternaria tenuissima* is for the first time reported on *Psidium guajava* from Faisalabad, Pakistan.

Specimen Examined

Alternaria tenuissima; on fruit of *Psidium guajava*; G.C. University, Faisalabad; July 27, 2007; S.Q. Abbas and Abida Perveen, G. C. U. M. H. # 16.

4. REFERENCES

1. Abbas, S.Q., B.C. Sutton, A. Ghaffar & A. Abbas. Reassesment of *sphaeropsis undulate. Pakistan Journal of Bot*any 36(1): 209-218 (2004).
2. Abbas, S. Q., M. Naiz, R. Ayesha, T. Iftikhar & I. Ali. New fungal records on *Morus alba* from Faisalabad, Pakistan. *Pakistan Journal of Botany* 42: 583-592 **(**2010).
3. Ahmad, S. *Fungi of Pakistan: Monograph* 1: 1-126. Biological Society of Pakistan, Lahore (1956).
4. Ahmad, S. Further contributions to the fungi of Pakistan: Π. *Biologia* 6:117-136 (1962).
5. Ahmad, S. Contributions to the fungi of Pakistan: V. *Biologia* 13: 15-42 (1967).
6. Ahmad, S. Further contributions to the fungi of Pakistan: VΠ. *Biologia* 14: 1-11 (1968).
7. Ahmad, S. *Fungi of Pakistan: Monogarph* 5: 1- 110. Biological Society of Pakistan, Lahore, Pakistan **(**1969).
8. Ahmad, S.**,** S.H. Iqbal & A.N. Khalid. *Fungi of Pakistan.* Sultan Ahmad Mycologi**c**al Socie**t**y of Pakistan, Department of Botany, University of the Punjab, Lahore*,* Pakistan (1997).
9. Anonymous. *Agricultural Statistics of Pakistan, 2010–2011.* Ministry of Food, Agriculture and Co-operatives. Govt. of Pakistan, Islamabad, Pakistan (2011).
10. Baradi, E.I. Tropical fruits *Psidium guajava*. *Abstracts on Tropical Agriculture* 1: 16 (1975).
11. Bhatti, A.G., N.J. Ismail, A.M. lodhi & W.A. Maitlo. Isolation and identification of fungi causing deteriotion of guava (*Psidium guajava*) L.) in Larkana, Sindh. In: Abstracts "*Challenges and Options for Plant Health Management*", 8th National Conference of Pakistan Phytopathological Society, 28-29 November 2011, University of Agriculture, Faisalabad, Pakistan, p. 64 (2011).
12. Bokhari, A.A. & S.T. Sahi. Studies on Guava decline and disease management Pakistan. In: Abstracts "*Challenges and Options for Plant Health Management*", 8th National Conference of Pakistan Phytopathological Society, 28-29 November 2011, University of Agriculture, Faisalabad, Pakistan, p. 64 (2011).
13. Carmichael, J.W., W.B. Kendrick, I.L. Conners & L. Sigler. *Genera of Hyphomycetes*. The University of Alberta Press, Edmonton, Canada, 386 pp. (1980).
14. Crane, J. L. & J.D. Schoknecht. Revision of *Torula* species. *Rutola*, a new genus for *Torula graminis. Canadian Journal of Botany* 55(24): 3013-3039. (1977).
15. Ellis, M.B. Dematiaceous Hyphomycetes. Imperial Mycological Institute, Commonwealth Agricultural Bureau, Kew, Surrey, England, 608 pp. (1971).
16. Ellis, M.B. *More Dematiaceous Hyphomycetes*. Imperial Mycological Institute, Commonwealth Agricultural Bureau, Kew, Surrey, England, 507 pp. (1976).
17. Fateh, F.S., M.R. Kazmi, I. Ahmad & T. Mukhtar. Common fungi found in decline affected Mango and Gauva orchids in Punjab. In: Abstracts "*Challenges and Options for Plant Health Management*", 8th National Conference of Pakistan Phytopathological Society, 28-29 November 2011, University of Agriculture, Faisalabad, Pakistan, p. 30 (2011).
18. Ghaffar, A., A. Kafi. Fungi of Karachi. *Pakistan Journal of Sci*ence 20: 5-10 (1968).
19. Ghafoor, A., S.A. J. Khan. *List of Diseases of Economic Plants in Pakistan*. Department of Plant Protection, Ministry of Food, Agriculture and Under Developed Area, Government of Pakistan, 85 pp. (1976).
20. Kafi, A., Z.A. Siddique. Russetting of guava in Karachi Malir area. Abstracts *Pakistan Science Conference* A: 56 (1964).
21. Khan, S.A., M. Kamal. The Fungi of South West Pakistan, Part 1. *Pakistan Journal of Scientific & Industrial Research* 11**:** 1-8 (1968).
22. Kirk, P.M. *Species Fungorum*. Centre for Agriculture and Bioscience International, CABI, UK (2012), Available from: http://www.speciesfungorum.org.
23. Matsushima, T. List of Micro fungi from Pakistan soils. In: In: *Cryptogamic Flora Pakistan,* Vol. 2., T. Nakaike & S. Malik (Ed.), p. 43 – 63. National Science Museum, Tokyo (1993).
24. Pathak,V.N. *Diseases of Fruit Crops, 2nd ed*., Oxford & IBH Publishing Company, New Delhi, India, 309 pp. (1980).
25. Shakir, A.S., M.A. Nasir & S.T. Sahi. *Anthracnose* of Guajava (*Psidium guajava)* a new record in Pakistan. *Pakistan Journal of Agricultural Sci*ence 28: 211-212 (1991).
26. Saleem, A., M. Hussain and M. Ansar. A report on *Pestalotia* dieback of Guava plant in Pakistan. *Pakistan Journal of Forestry* 41 **(**3-4):38 (1988).
27. Singh, S.J. D*iseases of Fruit Crops in India. 1st ed*. Kalyani Publisher, New Delhi (1996).
28. Snowdon, A.L. General introduction and fruits. In: *A Colour Atlas of Post Harvest Diseases and Disorders of Fruits and Vegetables, Vol. 1*. Wolfe Scientific, London, 302 pp. (1991).

Proceedings of the Pakistan Academy of Sciences 51 (2): 129–138 (2014)

ISSN: 0377 - 2969 (print), 2306 - 1448 (online)

Pakistan Academy of Sciences

Research Article

Removal of Coliform Bacteria from Municipal Wastewater by Algae

Farooq Ahmad[1]*, Aqsa Iftikhar[1], Adnan Skhawat Ali[1], Syed Ahtisham Shabbir[1], Abdul Wahid[2], Nazish Mohy-u-Din[1] and Abdul Rauf[3]

[1]Sustainable Development Study Centre, GC University, Lahore, Pakistan
[2]Department of Environmental Science, Bahauddin Zakariya University, Multan, Pakistan
[3]Department of Zoology, University of Agriculture, Faisalabad, Pakistan

Abstract: The present work was conducted in Sustainable Development Study Centre, Government College University, Lahore. The focus of the study was the removal of coliform bacteria from municipal wastewater by *Rhizoclonium implexum,* a freshwater algal species. Experiments were conducted on the basis of pond size, algal and water quantity and optimum conditions were determined i.e. Pond size (P2), algal quantity (150 g) and wastewater quantity (7 liters). In this study maximum percent reduction for Chemical oxygen demand (99.4%), Biochemical oxygen demand (99.5%), Total solids (95.1%), Total dissolved solids (97.2%), Total suspended solids (96.1%), Total Kjeldahl nitrogen (98.2%), Total phosphorus (96.8%), Total coliforms (100%) and Faecal coliforms (100%) were obtained. Increase in accumulation of nitrogen (10.75 to 34.9mg/g), phosphorus (257.40 to 268.1ppm) and organic matter (290 to 315.3mg/g) in algal biomass were also observed besides other operating parameters. Biochemical oxygen demand (BOD) and chemical oxygen demand of treated sewage were found in NEQS (2000) permissible limits while total coliform and faecal coliform were totally removed from sewage by *Rhizoclonium implexum* therefore, it could be an efficient technique for sewage effluent treatment.

Keywords: Coliform bacteria, municipal wastewater, sewage, faecal coliforms, algae

1. INTRODUCTION

Human activities are continuously affecting the quality and quantity of water. Water after adversely affected in its quality by various anthropogenic activities is termed as wastewater. It includes an extensive range of waste in the form of pathogens, metals and other contaminants from domestic, agricultural, industrial and other activities. Studies revealed that the major cause of water pollution is the discharge of sewage into rivers and irrigation canals. Release of wastewater without any treatment directly into water bodies is a destructive act because it badly pollutes the water resources. After treating wastewater, it can safely be released into water bodies because treated wastewater is not as much harmful as wastewater without treatment but safe for water bodies [1].

Mainly the municipal wastewater contains various categories of pathogenic agents including bacteria, helminthes, viruses and several protozoan and fungi. Sewage containing these pathogens causes many health problems including water borne diseases especially in the developing nations. There are a number of harmful diseases that can caused by these categories of pathogens which are commonly exist in municipal wastewater. Pathogens of bacteria are very injurious for health and they are source of deaths especially in those regions where sanitation is deprived or improper. In municipal wastewater pathogenic bacteria are specifically in large quantity [2].

Pakistan was already struck with a similar kind of outbreak in 2006 reported by ADB [3]. There is wide range of pathogenic contamination

Received, December 2013; Accepted, April 2014
*Corresponding author: Farooq Ahmad; Email address: fagondal82@yahoo.com

includes in municipal wastewater. There is group of bacteria known as coliform bacteria which are used as indicators for various disease producing pathogens. This group of indicator bacteria consists of *Escherichia coli* along with other type of bacteria that are found in human faeces or originated from other sources. Water quality can checked for disease causing pathogen of human by the presence of faecal coliform bacteria which are mostly used as an indicator to assess water contamination [4].

Although, there are large number of wastewater techniques and facilities such as adsorption methods, chemical techniques, precipitation, constructed wetlands and other processes are present but the most suitable is biological method because of its least expensiveness for developing countries particularly [5]. Algal-based wastewater treatment method is a better option for areas where expensive conventional methods are not affordable [6].

As algae plays a significant role in removing nutrients, pathogens, heavy metals and other pollutants from the sewage and this type of treatment process is easy to handle, more effective and environment friendly. Another benefit of algal use is that nutrient extraction from sewage by means of algae provides useful biomass that can be used to biofuels. Open ponds and closed photobioreactors of various designs are used for algal growth but microalgae grow efficiently in ponds containing wastewater [7].

Wastewater treatment ponds are considerably used for sewage treatment in most of the developing countries where wastewater treatment plants are not available. In such settings biological treatment systems using algae are useful. It has many advantages because they are inexpensive, easy to assemble, manage and no skilled labor is required to run it. Particularly, the removal of pathogens must be stressed in developing areas because of vulnerability towards various diseases in such areas due to improper ways of sanitation. In this perspective, wastewater treatment ponds are considered to be more efficient and effective as compared to other conventional treatment systems [2]. Major objectives of the study were to determine the presence of total coliform and faecal coliform in municipal wastewater and their removal by algae based treatment methods.

2. MATERIALS AND METHODS

2.1. Experimental Layout

Aquatic cultures were conducted in synthetic ponds with dimensions of 0.15 x 0.15 x 0.3 m^3 having maximum capacity of 6.75 liters; the dimensions of second pond were 0.3 x 0.3 x 0.15 m^3 with maximum capacity of 13.5 liters, and 0.9 x 0.15 x 0.45 m^3 were the dimensions of third pond with maximum capacity of 60.75 liters.

2.2. Wastewater Sampling

Water samples were collected in plastic cans from sewage drain passing through Shadman, Lahore by grab sampling methods then these (samples collected at morning, noon, afternoon and evening) were mixed with each other to form composit sample. Tests were performed immediately or the sample was refrigerated (at 12 ^{0}C) for further analysis.

2.3. Algal Sampling

Algal samples were collected from Botanic Garden of GC University Lahore and forms of Department of Fisheries near Manawa police station Lahore. These samples were grown in wastewater ponds for experiments to optimize the conditions for wastewater treatment.

2.4. Identification and Inoculation of Algae

Collected algae were first identified and then kept at room temperature as local outdoor cultures. Inocula of algae were transferred in previously mentioned ponds for sewage treatment. The rate of growth of these algal species was measured by the estimation of fresh weight. These samples were dried in an oven at 60 °C for 48 hours to calculate its dry weight.

2.5. Wastewater Analysis

2.5.1. *Physical Analysis of Wastewater*

Temperature and pH were determined immediately after sample collection with digital meter as mentioned in APHA [8] standard methods.

2.5.2. *Total Coliform*

Sample was analyzed for biological parameter i.e.

total coliform. It was determined throughout the experiment by MPN/100 method. Culture media was prepared by adding 17.5 g LT-broth into 500 mL of distilled water and 5 mL from this culture was put into the required number of pre sterilized test tubes. All the test tubes were cotton plugged. Test tubes were autoclaved at 120 ºC for 20 minutes after covering them with aluminium foil. After removing from autoclave these were cooled at room temperature and filled with wastewater sample i.e. 0.1 mL, 1 mL and 10 mL in separate test tubes except one which served as a blank. Put them in an oven at 35 ºC for 48 hours. After the incubation period these were compared with blank to count the total coliform MPN/100 [8].

2.5.3. *Faecal Coliform*

Samples were analyzed for faecal coliform bacteria following the standard procedures [8] and reported as MPN/100 mL.

2.6. Algal Analysis

Algal samples were dried in an oven at 60-80 ^{0}C for 48-72 hours. This dried algae was weighed and then crushed by grinder and after grinding samples were weighed again. These powdered algal samples were utilized for further study.

2.7. Total Nitrogen Determination

Nitrogen is determined by Kjeldahl method [8].

Calculations

%N = (V-B) ×N×R×E×100/ Wt

V = Volume of 0.01 N H_2SO_4 titrated for the sample (mL)

B = Blank titration volume (mL)

R = Ratio between total volume of the extract and extract volume used for titration.

N = Normality of H_2SO_4 solution.

Wt = Weight of air dry algae (g)

E = Atomic weight of Nitrogen

2.8. Phosphorus Test

Available phosphorous was determined by Olsen method [8] and ammonium molybdate-developed color intensity was measured colorimetrically using spectrometer 0-D.

2.9. Organic Matter

Organic matter was determined by Walkley-Black method [8].

2.10. Experimental Setup on the Basis of Variation in Pond Size

Experimental setup was conducted on the basis of variation in pond size. Where the algal and water quantity were taken constant i.e. 150 g and 7 L, respectively. Pond size was varied from P1 to P3.

2.11. Experimental Setup on the Basis of Variation in Algal Quantity

Second experimental setup was conducted on the basis of variation in algal quantity. In this setup, the water quantity and pond size were constant i.e. 7 L and P2 respectively. P2 was selected on the basis of its efficiency in comparison to P1 and P3. Three replicates of each experiment were conducted to minimize error. Different Algal quantities used in this setup were; 50 g, 100 g, 150 g and 200 g.

2.12. Experimental Setup on the Basis of Variation in Water Quantity

Third experimental setup was performed on the basis of water quantity, where pond size and algal quantity were remained constant i.e. P2 and 150 g respectively. This algal quantity showed maximum removal of pollutants from municipal wastewater therefore it was selected for further experiments. In this setup, different water quantities were used in four ponds of similar dimensions (3 L, 5 L, 7 L and 9 L).

2.13. Experimental Setup on Monthly Basis

This setup was conducted to observe the effect of seasonal variation on percent reduction of various parameters. In this regard, 100 g of Algae was taken with 5 liters of water in P2. Chemical oxygen demand (COD), Biochemical oxygen demand (BOD), Faecal coliforms (FC), Total coliforms (TC), Total Kjeldhal nitrogen (TKN), Total phosphorus (TP),

Total solids (TS), Total suspended solids (TSS) and Total dissolved solids (TDS) were observed after each month from September to July.

3. RESULTS AND DISCUSSION

3.1. Pollutant Load in the Samples

Sample collected from the sewage drain was found to be rich in pollutants. The results shown in Table 1 indicated that the concentrations of the parameters were above National Environmental Quality Standards (2000). Table 1 also compared the concentrations of pollutants in untreated sample immediately after collection with concentration of pollutants after treatment with algae and control setup conducted without inoculation of algae. The alga used in the current study was identified as *Rhizoclonium implexum.*

3.2. Mechanism for the Removal of Coliforms from Wastewater by Algae

In wastewater ponds of algae, sunlight give rise to those processes which are related with dissolved oxygen, pH and sedimentation. It can play a key role in pathogen removal. If there are high amounts of protozoa present, it can be significant to overcome the bacterial population. There are some mechanisms of pathogen removal from wastewater by algae as under:

- Nutrient competition of algae with coliform bacteria.
- Increase in pH due to CO_2 consumption which is lethal for pathogens.
- Algae produce toxins of long chain fatty acids which kill pathogens.
- Aeration (addition of O_2 by algae) enhances faecal coliform die-off rates.
- Adhesion/Attachment to the algal cells [2].

3.3. Effect of Treatment on Total Coliforms Reduction

In this experiment, the measurement of total coliform (TC) reduction was done to observe the effect of pond size with varying treatment duration but fixed algal and water quantity (150 g and 7 L, respectively). Reduction in TC was detected to be maximum in pond P2 (100%) low percentage

Table 1. Wastewater analysis before and after treatment and its comparison with National Environmental Quality Standards (2000).

Parameter	Unit	Sewage analysis, before treatment	Reduction after treatment (%)	Without treatment reduction (%)	NEQS 2000
Colour	---	grayish	---	---	---
Odour	---	Irritating	---	---	---
pH	---	6.7	0.1±0.08	0.4±0.2	6-9
Temperature	^{0}C	25±3	---	---	≥3 ^{0}C
Chemical oxygen demand	mg/L	580±20	99.4±0.02	13±1.2	150
Biological oxygen demand	mg/L	321±15	99.5±0.01	15±2.4	80
Total solids	mg/L	5720±20	95.1±0.05	10±0.6	3700
Total dissolved solids	mg/L	4500±20	97.2±0.07	4±2.5	3500
Total suspended solids	mg/L	1220±15	96.1±0.11	3±1.6	200
Total Coliforms	MPN	1.6×10^3	100±0	8±1.9	---
Fecal Coliforms	MPN	1.6×10^3	100±o.06	11±1.5	---
Total Kjeldahl nitrogen	mg/L	30.2±2.1	98.2±0.12	4±0.8	---
Total phosphorus	mg/L	13±1.6	96.8±0.24	5±1.3	---

reduction was observed in pond P3 (89.5%) whereas the percentage reduction was decreased to 78.3 % in pond P1, as a result pond P2 was selected for further study (Fig. 1).

In this experiment, the effect of variation in algal quantity was observed for total coliform (TC) reduction with alteration in treatment time at constant water quantity and pond size (7 L and P2 respectively). Maximum TC reduction was indicated with 150 g and 200 g algal quantity i.e. 100% and 100% respectively whereas lower TC reduction was found with 50 g and 100 g algal quantity i.e. 79.6% and 86.3% respectively. Since the percentage reduction was similarly observed with 150 g and 200 g of algae thus, for 7 liters of water quantity, 150 g of algae were found to be most favorable (Fig. 2).

Percent reduction in total coliform (TC) was also observed with variation in treatment time at constant pond size and algal quantity (P2 and 150 g respectively). Maximum percent reduction was found with 3L, 5L and 7 L of wastewater i.e. 100%, 100% and 100% respectively however the reduction percentage was decreased with 9liters of wastewater (89.4%). Therefore, for further study 7 liters of wastewater was selected (Fig. 3).

3.4. Effect of Treatment on Faecal Coliforms Reduction

In this experiment, the measurement of fecal coliform (FC) reduction was done to observe the effect of pond size with varying treatment duration but fixed algal and water quantity (150 g and 7 L, respectively). Reduction in FC was detected to be maximum in pond P2 (97.8%) low percentage reduction was observed in pond P3 (84.6%) whereas the percentage reduction was decreased to 77% in pond P1, as a result pond P2 was selected for further study (Fig. 4). 100% reduction of all fecal indicator bacteria was observed by [9] during the 6.6-day system residence time. In the presence of sunlight, fecal coliforms removal increased because sunlight promoted their inactivation.

In this experiment, the effect of variation in algal quantity was observed for fecal coliform (FC) reduction with alteration in treatment time at constant water quantity and pond size (7 L and P2 respectively). Maximum FC reduction was indicated with 150 g and 200 g algal quantity i.e. 100% and 100% respectively whereas lower FC reduction was found with 50 g and 100 g algal quantity, i.e., 78.3% and 86.1% , respectively. Since the percentage reduction was similarly observed with 150 g and 200 g of algae thus, for 7 liters of water quantity, 150 g of algae were found to be most favorable (Fig. 5). 100% reduction of all fecal indicator bacteria was observed by [9] during the 6.6-day system residence time. In the presence of sunlight, fecal coliforms removal increased because sunlight promoted their inactivation. Attachment of fecal coliforms along with other bacteria on the surface significantly enhanced the fecal coliform die-offs [2].

Percent reduction in fecal coliform (FC) was also observed with variation in treatment time at constant pond size and algal quantity (P2 and 150 g respectively). Maximum percent reduction was found with 3L, 5L and 7 L of wastewater i.e. 100%, 99.9% and 100% respectively however the reduction percentage was decreased with 9liters of wastewater (87.7%). Therefore, for further study 7 liters of wastewater was selected (Fig. 6). [10] reported phosphorus reduction almost 96.2%.

100% removal of all fecal indicator bacteria was observed by [9] during the 6.6-day system residence time. In the presence of sunlight, fecal coliforms removal increased because sunlight promoted their inactivation. Attachment of fecal coliforms along with other bacteria on the surface significantly enhanced the fecal coliform die-offs [2].

3.5. Effect of Treatment on Reduction of Pollutants

The effect of seasonal variation on percent reduction was observed in wastewater parameters with 150 g of algal quantity and pond P2. In November, maximum percent reduction of parameters was found. Nearly, same results were observed in the month of March whereas results obtained in other months were not satisfactory. Therefore, month of November is found to be favorable for percent reduction in wastewater parameters (Fig. 7). Kadam [11] reported percent reduction of biochemical oxygen demand (BOD), total kjeldahl nitrogen

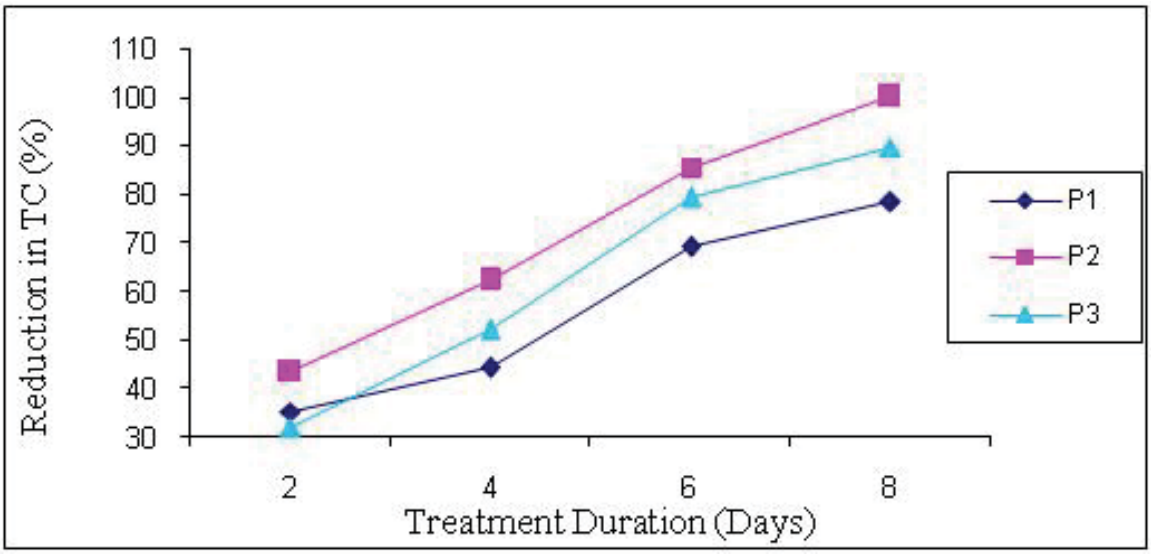

Fig. 1. Effect of pond size and treatment duration on percent reduction in total Coliforms (TC) with 7 liters of water and 150 g of algae.

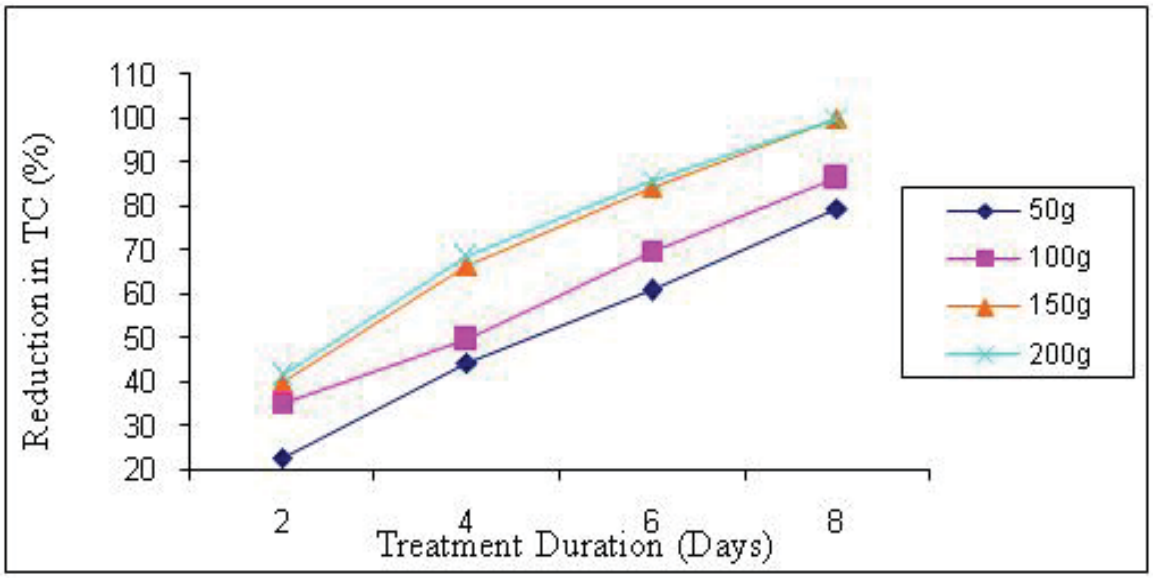

Fig. 2. Effect of algal quantity and treatment duration on percent reduction in total Coliforms (TC) with 7 liters of water in P2.

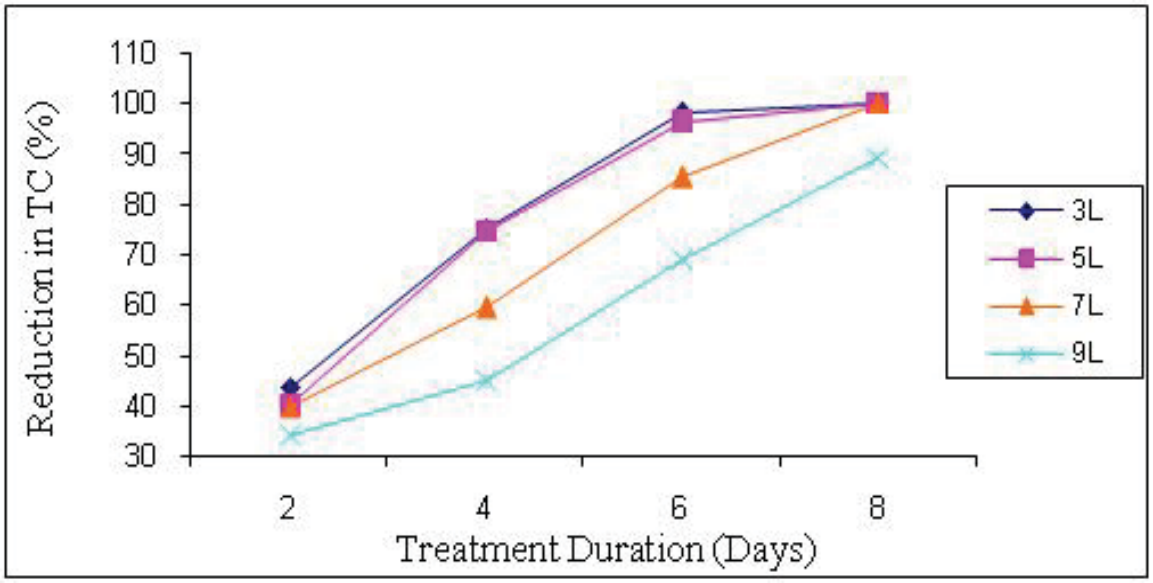

Fig. 3. Effect of water quantity and treatment duration on percent reduction in total Coliforms (TC) with 150 g of algae in P2.

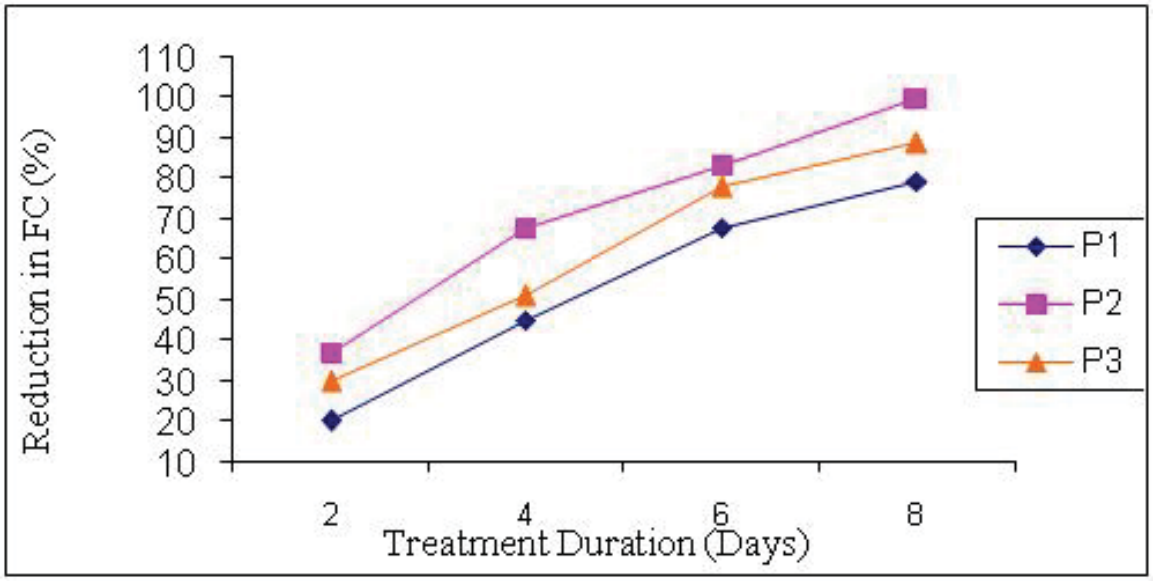

Fig. 4. Effect of pond size in percent reduction of Faecal Coliforms in 7 litres of water and 150 g of algae.

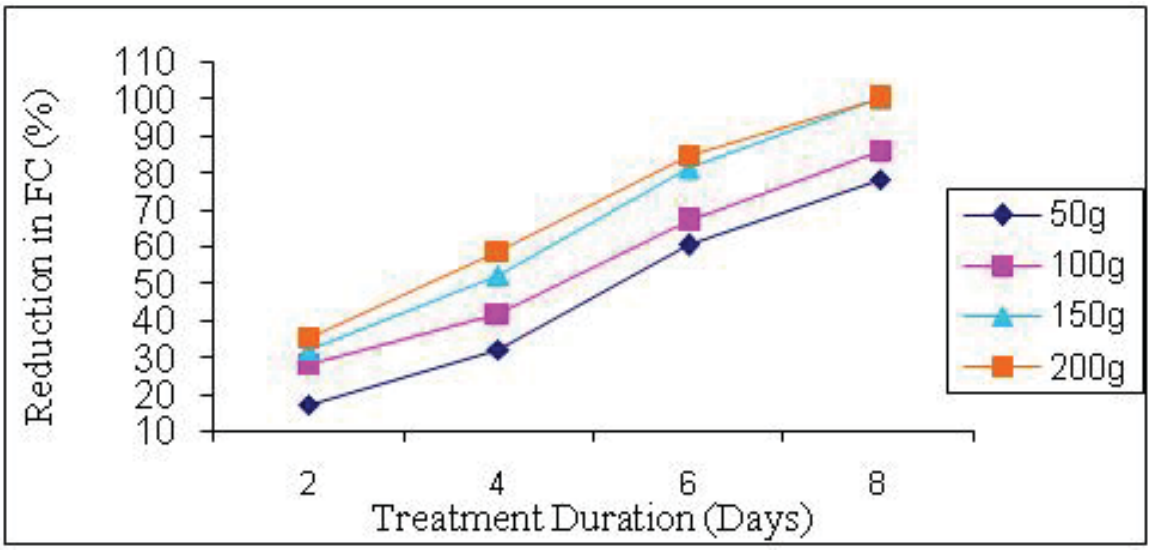

Fig. 5. Effect of algal quantity and treatment duration in percent reduction of Faecal Coliforms with 7 liters of water in P2.

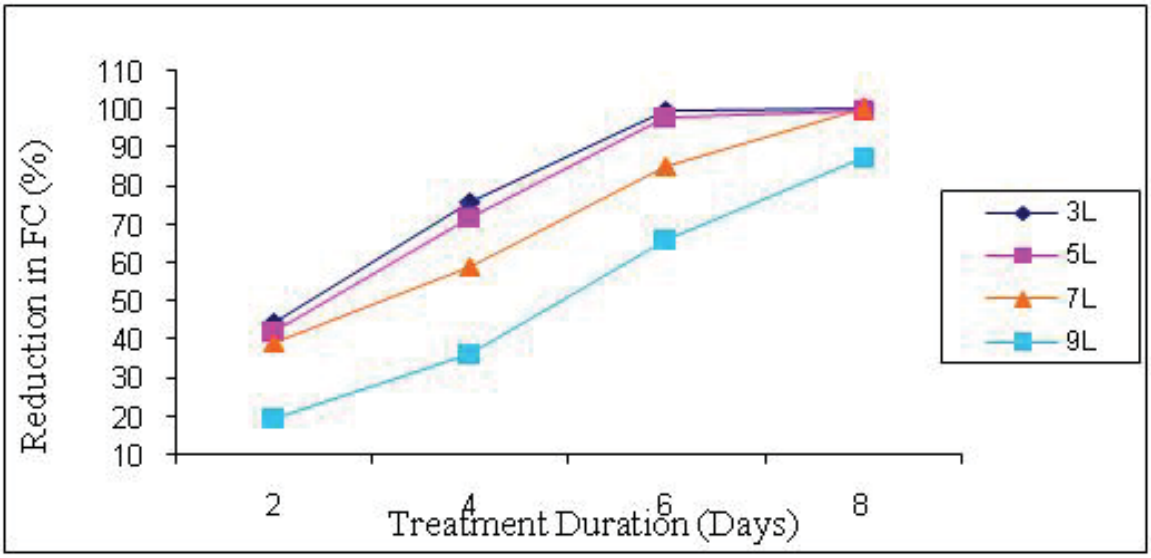

Fig. 6. Effect of water quantity and treatment duration in percent reduction of Fecal Coliforms with 150 g of algae in P2.

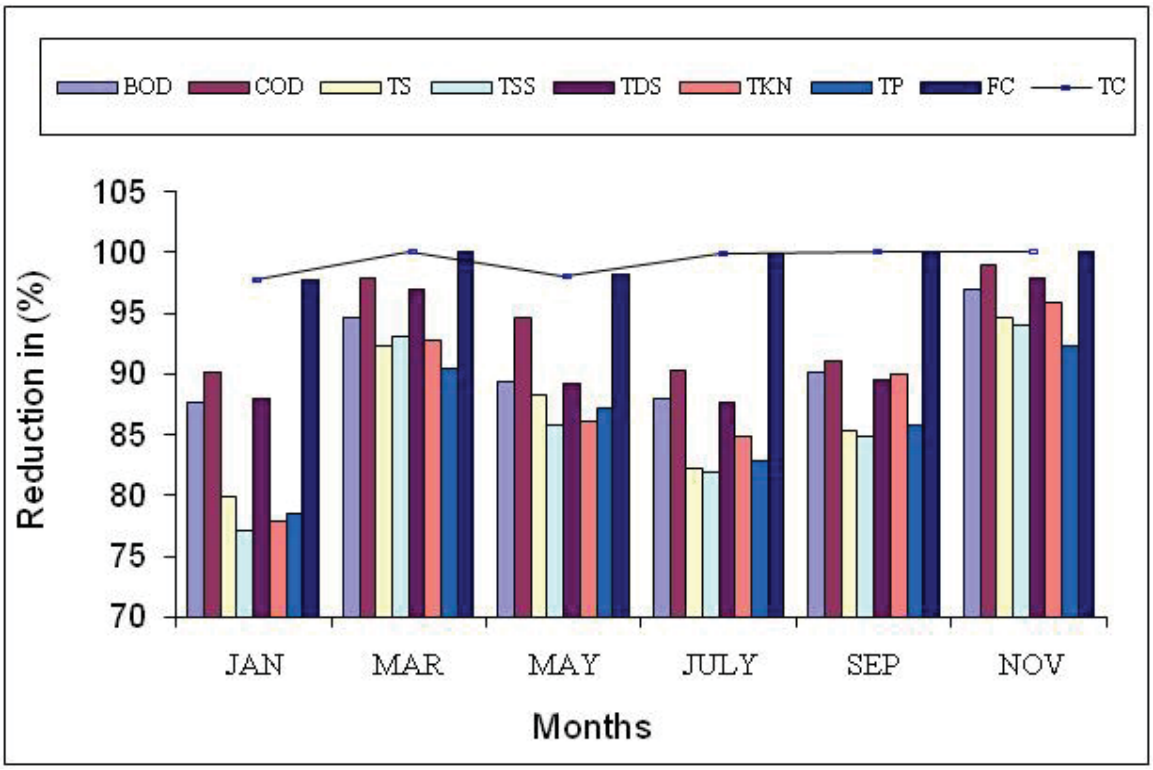

Fig. 7. Percent reduction of wastewater parameters in alternative months of the year under optimum conditions.

Table 2. Mean accumulation of nitrogen and phosphorous in algae with change in treatment duration under optimum conditions.

Parameters	Treatment duration (Days)				
	0	2	4	6	8
Nitrogen (mg/g)	10.75±1	13.5±1.7	23.3±0.8	32.2±0.6	34.9±2
Phosphorus (µg/g)	257.40±2.9	259.4±3.2	264.4±2.2	267.6±2.6	268.1±1.7
Organic matter (mg/g)	290±2	293.2±3.1	299±4	314.5±1.5	315.3±2.1

(TKN) and chemical oxygen demand (COD) as 83% 21% and 68%, respectively.

3.6. Accumulation of Nitrogen and Phosphorous in Algal Biomass

In this experiment, total nitrogen, total phosphorus and organic matter was calculated in algae with the change in treatment duration and it was observed the accumulation of both these nutrient increase with increase in treatment time. Maximum nitrogen, phosphorous and organic matter accumulation was found on the final day of treatment i.e. 34.9mg/g, 268.1ppm, 315.3mg/g respectively (Table 2).

4. CONCLUSIONS

Present study revealed that algae for wastewater treatment are very effective for reduction of coliform bacteria along with other various parameters from municipal wastewater. Algal based wastewater treatment system was proved to be a good alternative

to the conventional wastewater treatment systems in many ways, due to its efficiency in pollutant removal, cost-effectiveness and other advantages. It not only gives 100% removal efficiency but also bring other pollutants into their permissible limits. Consequently, this wastewater treatment process can become very cheaper and efficient.

Based on the results of this study, it is recommended that algae-based wastewater treatment system is a cost-effective and environment friendly way to remove pathogens. It is more efficient system as compared to other conventional treatment systems. The optimum conditions obtained in the current study can become very helpful in launching this technique at pilot scale. The natural biomass produced can also be utilized for production of biofuels. The process consume CO_2 a major green house gas for pollutant removals. Therefore, it is recommended to take these aspects for future studies in developing countries like Pakistan. There is need to identify the algal species with high oil content and wastewater treatment efficiency so that dual benefits can be obtained from this natural resource.

5. ACKNOWLEDGEMENTS

The authors acknowledge Government College University, Lahore for providing funding for the study. The research work was done in laboratories of Sustainable Development Study Centre and Department of Chemistry of GC University, Lahore.

6. REFERENCES

1. Ruin-Marin, A., L.G. Mendoza-Espinosa & T. Stephenson. Growth and nutrient removal in free and immobilized green algae in batch and semi-continuous cultures treating real wastewater. *Bioresource Technology* 101 (1): 58- 64 (2010).
2. Awuah, E. *Pathogen Removal Mechanisms in Macrophyte and Algal Waste Stabilization Ponds.* Doctoral Dissertation, UNESCO-IHE Institute for Water Education, Taylor and Francis Group/ Balkema. Rotterdam, The Netherlands, (2006).
3. ADB. *Asian Development Bank Annual Report*. http://www.adb.org/documents/adb-annual-report-2007 (2007).
4. Abreu-Acosta, N & L. Vera. Occurrence and removal of parasites, enteric bacteria and faecal contamination indicators in wastewater natural reclamation systems in Tenerife- Canary Islands, Spain. *Ecological Engineering* 37: 496- 503 (2010).
5. Wei, X., R.C. Viadero, Jr & S. Bhojappa. Phosphorus removal by acid mine drainage sludge from secondary effluents of municipal wastewater treatment plants. *Water Research* 42: 3275-3284 (2008).
6. Zhang, K. & K. Farahbakhsh. Removal of native coliphages and coliform bacteria from municipal wastewater by various wastewater treatment processes: Implications to water reuse. *Water Research* 41: 2816–2824 (2007).
7. Oswald, W.J. Ponds in the twenty-first century. *Water Science and Technology* 31: 1-8 (1995).
8. APHA (American Public Health Association), *Standard Methods for the Examination of Water and Wastewater,* 20th ed. American Public Health Association, American Water Works Association, Water Pollution Control Federation, Washington, DC, USA (1998).
9. Winfrey, B.K., W.H. Strosnider, R.W. Nairn & K.A. Strevett. Highly effective reduction of fecal indicator bacteria counts in an ecologically engineered municipal wastewater and acid mine drainage passive co-treatment system. *Ecological Engineering,* 36: 1620-1626 (2010).
10. Hammouda, O., A. Gaber & M.S. Abdel-Hameed. Assessment of the effectiveness of treatment of wastewater-contaminated aquatic systems with *Lemna gibba. Enzyme Microbial Technology* 17: 317-323 (1995).
11. Kadam, A.M., G.H. Oza, P.D. Nemade & H.S. Shankar. Pathogen removal from municipal wastewater in constructed soil filter. *Ecological Engineering* 33: 37- 44 (2008).

Proceedings of the Pakistan Academy of Sciences 51 (2): 139–144 (2014)

ISSN: 0377 - 2969 (print), 2306 - 1448 (online)

Pakistan Academy of Sciences

Research Article

Cellular Stress Response Induced by Low Dose Gamma Radiation

Inayat ur Rahman[1]*, Naeem Ullah Jan[1], Hamid Rasul Niazi1[2] and Haroon Rahim[3]

[1*]Gandhara College of Pharmacy, Gandhara University, Peshawar, KPK, Pakistan
[2] Wazir Mohammad Institute of Paramedical Technology, Gandhara University, Peshawar, KPK, Pakistan
[3]Department of Pharmacy, Sarhad University of Science and Technology, KPK, Pakistan

Abstract: Low dose radiation-induced damages to DNA are mainly repaired by poly (ADP-ribose) polymerase (PARP-1 and PARP-2) system present in the cell. Suppression of neoplastic transformation of human hybrid cells by low doses of low linear energy transfer (LET) radiation is abrogated by PARP enzyme inhibitors and this presents a new tool in radiotherapy for cancers. The aim of this study was to investigate DNA damages by low doses of gamma rays (2.4 mGy/h) in the presence of inhibitors, 3-aminobenzamide (3-AB) and amino naphthalimide (ANI), with control. Cultured human fibroblast (VH10 cells) were irradiated with Cs^{137} γ-source at a dose rate of 2.4 mGy /hour for total doses of 50 mGy or 100 mGy in the presence of 3-AB and ANI and cell damage was detected through Comet assay. Compared to control, the presence of ANI did not inhibit PARP function at 50 mGy of 2.4 mGy/hr but there was increased tail moment in the presence of 3-AB and this might be due to differences in their concentrations. However, at 100 mGy dose, the tail moment increased in the presence of both 3-AB and ANI with the later showing greater increase. These results show that PARP inhibitors sensitized the cells to low dose γ radiation by abrogating the activity of PARP enzyme. DNA repair process reduced and the tail moment increased.

Keywords: Gamma radiation, PARP, 2.4 mGy, 100 mGy

1. INTRODUCTION

Ionizing radiations are atomic particles or electromagnetic waves that cause ionization of atoms and molecules. Particulate radiation is alpha-particle, beta particle, and neutron while electromagnetic waves (photons) include ultraviolet radiation, x-rays and gamma rays. Sources of ionizing radiations are radioactive materials, particle accelerator, x- ray tubes and the environment [1]. The Ionizing radiation energy is transferred to atoms and molecules in the cellular structure and ionizes or excites them. Both ionization and excitation produces free radicals which break chemical bond of molecules and form new chemical bonds. Vital molecules of cells (DNA, RNA and proteins) are damaged as a result of such energy transfer mechanism. Production of reactive oxygen species (ROS) is the result of water radiolysis in cells that cause a major damage to these macro molecules. This oxidative stress is the cause of different biological phenomena and diseases [2, 3]. Low level of radiation effects are small that could be repaired by different ways of DNA repair mechanisms. DNA damages induced by low dose rate radiation are repaired or cell may go through apoptosis to eliminate the potential genetic lesions. If the lesion is not so large because of low dose, it may lead to cancer due to error prone DNA repair processes [4].

Poly (ADP-ribose) polymerase or PARP is a family of proteins of 17 members involved in different functions. There are four domains of PARP including, catalytic domain, DNA binding domain, cleavage domain and auto-modification domain. These domains are responsible for different functions of the PARP enzyme. PARP-1 and PARP-2 are most important in DNA repair process. DNA-ribose polymer is synthesized from nicotinamide adenine dinucleotide (NAD) on PARP-1 activation. DNA single strand break (SSB)

Received, July 2013; Accepted, May 2014
*Corresponding author: Inayat ur Rahman; Email: marwax07@yahoo.com

is detected by PARP-1 and binding to SSB recruits base excision repair proteins (BER), i.e., XRCC1, DNA pol beta, DNA ligase and kinase to break sites. PARP-1 is oligomerized by PARP-2 in the repair mechanism [5]. It has been noted that low doses of low linear energy transfer (LET) radiation could suppress neoplastic transformation of human hybrid cells in vitro. This suppression is abrogated by using 3- aminobenzamide (3-AB), an inhibitor of PARP enzyme [6]. PARP inhibitors, 3-AB and 4-Amino-1, 8-naphthalimide (ANI) competitively inhibit the catalytic domain of PARP from binding to NAD and prevent ribosylation. In this way, the DNA breaks will not be repaired by PARP enzyme and cells will die. In radiotherapy for tumor cells, the effect of ionizing radiation is potentiated by using PARP inhibitors [7, 8]. Inhibitors act by increasing the sensitivity of mammalian cells to low doses of ionizing radiation [9, 10]. The use of PARP inhibitors in cancers in which BRCA 1/2 are mutated is a novel approach in cancer therapy [8, 11]. In treatment of glioblastoma, the sensitivity of rapidly proliferating glioma cells to ionizing radiation is enhanced by using PARP inhibitors [12, 13]. Inhibition of PARP enzyme represents a new tool in radiotherapy for cancers and gives promising results [14, 15]. The aim of this study was to investigate the induction of DNA damages by low doses of low dose rate gamma radiation by inhibiting poly (ADP-ribose) polymerase (PARP) protein, a DNA repair enzyme.

2. MATERIAL AND METHODS

2.1 Cell Culture

The adherent human fibroblast VH10 cell line was cultured in Minimum Essential Medium Eagle (MEM) supplemented with antibiotics (1 % penicillin-streptomycin 10000 IU) and 10 % bovine calf serum. For experiments, cells were washed 2x with Hanks Balanced Salt Solution (HBSS) and trypsinized with 1 ml trypsin-EDTA for 5-7 min at 37 °C. Then 10ml MEM was added to neutralize trypsin and the cell suspension was put on shaker in order to prevent cell attachment. The number of cells was counted 3 times by cell counter and 0.2 x 10^6 cells were seeded into 25 cm^2 flasks containing 8 ml MEM. Cells were grown overnight in a humidified 95 % air and 5 % CO_2 atmosphere at 37 °C.

2.2 Irradiation Conditions

After overnight incubation, cell medium was changed with fresh 8 ml MEM containing 5 mM 3-AB or 10 μM ANI, respectively. One sample was used without inhibitor as control. Flasks were incubated in the specially designed low dose rate radiation incubator with the Cs^{137} γ-source underneath at a dose rate 2.4 mGy /hour for total doses of 50 mGy or 100 mGy. Irradiation was carried out as described earlier [16].

2.3 Comet Assay

After irradiation, cells were washed with HBSS and trypsinized. The cell suspension was kept on ice and cell number was counted for each sample. Then 200μl of cell suspension with 0.2 x 10^6 cells/ml was mixed with 2 % low melting agarose in same ratio (1:1), 80 μl of each sample were applied on the slides coated with 0.5 % normal melting agarose and covered with cover slips. In cold room, all slides were put in lysis buffer (2.5M NaCl + 100mM Na2EDTA + 10 mM Tris Base) of pH 10 for 1 hour. After one hour, slides were washed, shifted to electrophoresis tank filled with unwinding buffer (3M NaOH + 10 mM Na2EDTA) of pH 10 and voltage to 32.5V, left for 1 hour for unwinding process. After one hour, keeping the voltage constant, switched on the power of electrophoresis for 25 min. Then rinsed slides 3 x 5 min in neutralizing buffer of pH 7.5 (0.4M Tris Base). The slides were stained with 50μl DAPI stain and covered with cover slips. All slides were analyzed on next day.

2.4 Statistical Methods

The values are expressed as means ± SD. Statistical analyses were performed using SAS statistical software, version 8.0 (SAS Institute, Cary, NC, USA) for Windows®. A p-value <0.05 was considered to be statistically significant.

3. RESULTS AND DISCUSSION

3.1 Effect of Inhibitors on VH10 Cell at 50mGy of 2.4 mGy/h Gamma Rays

The present study was conducted to detect the effect of low dose of low dose rate gamma rays (2.4 mGy/h) in the presence of inhibitor, 3-AB

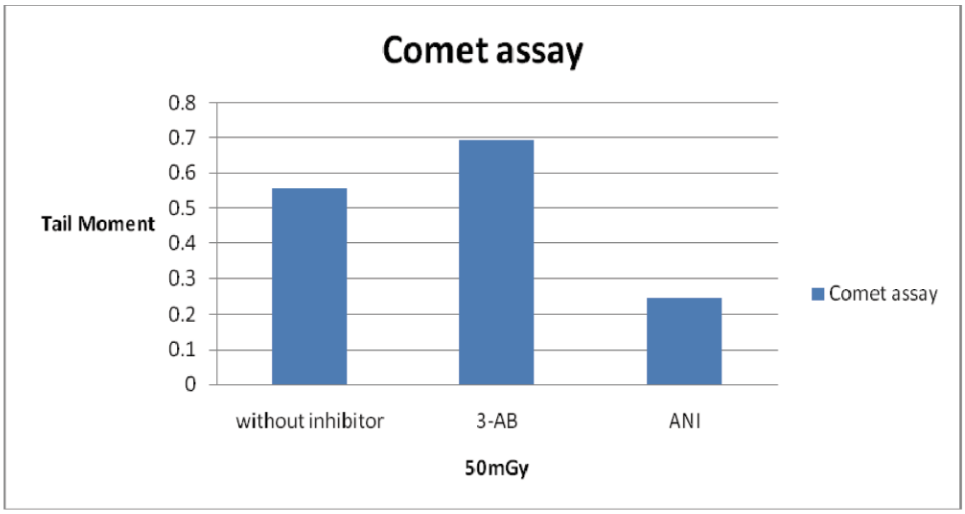

Fig. 1. Effect of 50 mGy dose of low dose rate (2.4 mGy/h) gamma radiation on cell DNA in the absence and presence of inhibitors, 3-aminobenzamide (3-AB) and ANI. Data are mean of 2 independent experiments.

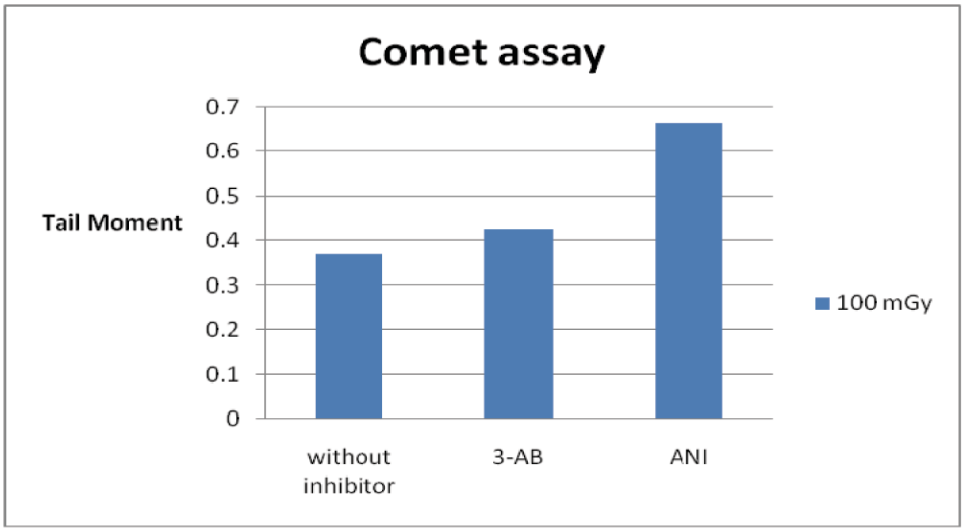

Fig. 2. Effect of 100 mGy dose of low dose rate (2.4 mGy/h) gamma radiation on cell DNA in the absence and presence of inhibitors, 3-aminobenzamide (3-AB) and ANI.Data are mean of 2 independent experiments.

and ANI with control. Comet assay was used to detect cell damage. In this technique, individual cell DNA damage and its migration was identified in the form of tail moment. There was increased tail moment in the presence of 3-AB as compared to control (Fig. 1). These results are supported by previous study that shows increased sensitization of cells to gamma radiation by treatment with 3-AB [17]. This method is more flexible and sensitive, requires less number of cells and has low cost. In genotoxicity, it is frequently used to identify mutagenic agents to human i.e. ionizing radiation [18]. Incubation with 3-AB (100 mM) on 50 mGy dose reduced DNA repair process (tail moment increased). In the presence of inhibitors the tail movement was more than without inhibitor. In contrast, ANI did not show inhibition of PARP function due to some unclear error (Fig. 1, 3). This is probably due to low concentration of ANI compared to 3-AB (8µl and 400µl respectively) used with the dose of 50 mGy. The effect of ANI is shown to be concentration dependent [18].

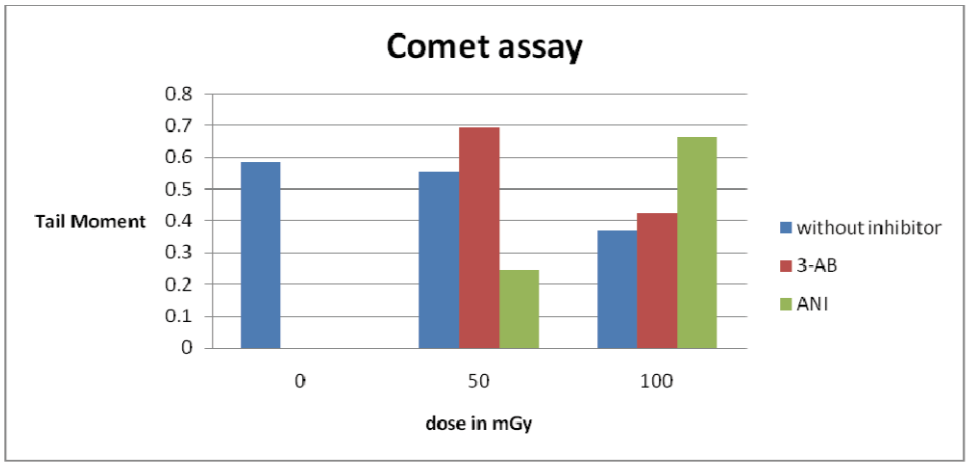

Fig. 3. Effect of low dose rate γ–radiation on cells in the presence and/or absence of PARP 3-AB and ANI. Data are mean of 2 independent experiments.

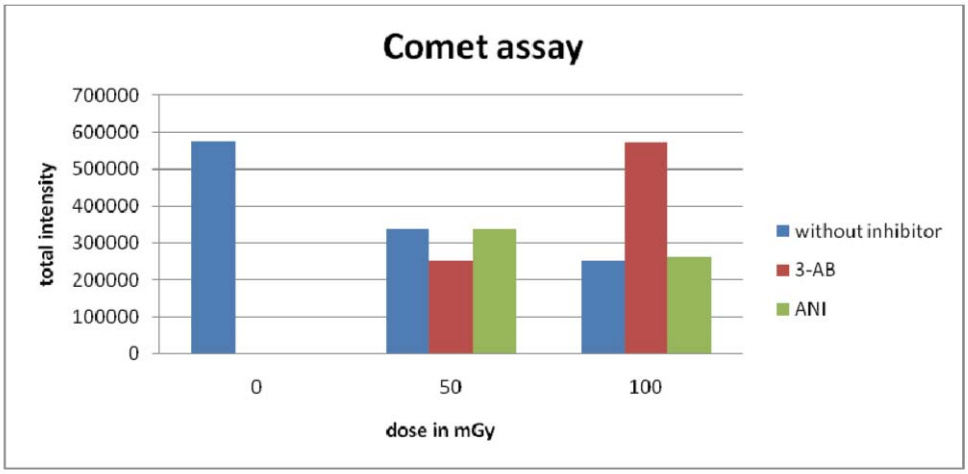

Fig. 4. Total intensity of DNA of γ-irradiated cells in the presence and/or absence of 3-AB and ANI. Data are mean of 2 independent experiments.

Radiosensitiztion mostly depends on the phase of cell cycle. Moreover, inhibiting DNA repair by ANI radiosnsitization is studied specifically in S phase. In this experiment, confluent VH10 cells were used that repaired DNA damage irradiated before S phase or on G2-M and G1 phases [7, 19].

3.2 Effect of inhibitors on VH10 cell at 100 mGy of 2.4 mGy/h Gamma Rays

Figure 2 represents the radiosensitizing effect of both PARP inhibitors during irradiation of 100 mGy dose. Compared to control, tail moment of cell DNA was more with inhibitors ANI and 3-AB. Further, the effect of ANI on PARP inhibition was much larger at 100mGy dose (Fig. 2, 3). It has been shown that 3-AB and ANI are radiosensitizing the culture cells which abrogate the activity of PARP enzyme, ANI is highly specific to inhibiting PARP activity in DNA repair and more potent than 3-AB [20, 21].

3.3 Effect on Total Intensity

Low dose and low dose rate of gamma radiation effect showed decreased total intensity of cellular DNA. It also decreased with inhibitors, but in the presence of 3-AB (0-100mGy), the total intensity was equal to control sample (without radiation and inhibitors). The irradiated cells were mostly examined for apoptosis, which might then be proposed that total intensity was affected (Fig.

4). This study of radiosensitization with PARP inhibitors on confluent fibroblasts is generally agreed with previous observations [7, 16, 17, 22, 23].

4. CONCLUSIONS

The study concludes that PARP inhibitors are concentration dependent and the dose and dose rate affects the DNA damage to large extent. Moreover, the killing of cells by low dose of low dose rate gamma radiation is improved in the presence of PARP inhibitors.

5. ACKNOWLEDGEMENTS

The authors are thankful to Gandhara College of Pharmacy, Gandhara University, Peshawar for providing the required facilities and supporting the research project.

6. REFERENCES

1. Hall, E.J. & A.J. Giaceia. *Radiobiology for the Radiobiologist,* 6th ed. Lippincott Williams & Wilkins, Philadelphia, Pennsylvania, USA, p. 1-15 (2005).
2. Goodhead, D.T. Initial events in the cellular effects of ionizing radiations: clustered damage in DNA. *International Journal of Radiation Biology* 65: 7-17 (1994).
3. Robert, A. Fosbinder & D. Orth. *Essentials of Radiologic Science*, Part-1. Lippincott Williams & Wilkins, Pennsylvania, Pennsylvania, USA, p. 1-20 (2011).
4. Little, J.B. Radiation Carcinogenesis. *Carcinogenesis* 21: 397-404 (2000).
5. Chalmers, A.J., M. Lakshman, N. Chan & R.G. Bristow. Poly (ADP-ribose) polymerase inhibition as a model of synthetic lethality in developing radiation oncology targets. *Seminars in Radiation Oncology* 20(4): 274-281 (2010).
6. Pant, M.C., X. Y. Liao, Q. Lu, S. Molloi, E. Elmore & J.L. Redpath. Mechanisms of suppression of neoplastic transformation in vitro by low doses of low LET radiation. *Carcinogenesis* 24(12): 1961-1965 (2003).
7. Noel, G., C. Godon, M. Fernet, N. Giocanti, F. Meqnen-Channet & V. Favaudon. Radiosensitization by the poly(ADPribose) polymerase inhibitor, 4-amino-1,8-naphthalimide is specific of the S phase of the cell cycle and involves arrest of DNA synthesis. *Molecular Cancer Therapeutics*. 5: 564-574 (2006).
8. Davar, D., J.H. Beumer2, L. Hamieh & H. Tawbi. Role of PARP inhibitors in cancer biology and therapy. *Current Medicinal Chemistry* 19(23): 3907–3921 (2012).
9. Chalmers, A., P. Johnston, M. Woodcock, M. Joiner & B. Marples. PARP-1, PARP-2, and the cellular response to low doses of ionizing radiation. *International Journal of Radiation Oncology* 58: 410-419 (2004).
10. Chalmers, A.J. Poly (ADP-ribose) Polymerase-1 and Ionizing Radiation: sensor, signaller and therapeutic target. Clinical Oncology 16: 29-39 (2004).
11. Evers, B., R. Drost, E. Schut, M. de Bruin, E. van der Burg, P.W.B. Derksen. Selective inhibition of BRCA2-deficient mammary tumor cell growth by AZD2281 and cisplatin. *Clinical Cancer Research* 14: 3916-3925 (2008).
12. Dungey, F.A., D.A. Loser & A.J. Chalmers. Replication-dependent radiosensitization of human glioma cells by inhibition of poly (ADP-Ribose) polymerase: mechanisms and therapeutic potential. *International Journal of Radiation Oncology Biology Physics* 72(2): 1188-1197 (2008).
13. Zheng, Y.D., X.Q. Xu, F. Peng, J.Z. Yu & H. Wu. The poly (ADP-ribose) polymerase-1 inhibitor 3-aminobenzamide suppresses cell growth and migration, enhancing suppressive effects of cisplatin in osteosarcoma cells. *Oncology Reports 25:* 1399-405 (2011).
14. Albert, J.M., C. Cao, K.W. Kim, C.D. Willey, L. Geng. D. Xiao & H. Wang. Inhibition of poly (ADP-ribose) polymerase enhances cell death and improves tumor growth delay in irradiated lung cancer models. *Clinical Cancer Research* 13(10): 3033-3042 (2007).
15. Zhang, J., K. Yanyan, T. Yongjie, W. Zhe & Z. Jie. Effects of poly (ADP-ribosyl) polymerase (PARP) inhibitor on cisplatin resistance & proliferation of the ovarian cancer C13 cells. *Indian Journal of Medical Research* 137: 527-532 (2013).
16. Gilbin, R., A. Frederic & G. L. Jacqueline. Effects of chronic external gamma irradiation on growth and reproductive success of Daphnia magna. *Journal of Environmental Radioactivity* 99: 134-145 (2008).
17. Thraves, P., K.L. Mossaman, T. Brennan & A. Dritschilo. Radiosensitization of human fibroblasts by 3-aminobenzamide: an inhibitor of poly (ADP-ribosylation). *Radiation Research* 104 (2 Pt 1): 119-127 (1985).
18. Tice, R. R., E. Agurell, D. Anderson, B. Burlinson, A. Hartmann & H. Kobayashi. Single cell gel/Comet assay: Guidelines for in vitro and in vivo genetic toxicology testing. *Environmental and Molecular Mutagenesis* 35: 206-221 (2000).
19. Staff, E., B. Karl, H. Siamak, C. Joanna & W. Andrzej. Gamma-H2AX foci in cells exposed to a

mixed beam of X-rays and alpha particles. *Genome Integrity* 3: 8 (2012).

20. Schlicker, A., P. Peschke, A. Bürkle, E.W. Hahn & J.H. Kim. 4-Amino-1,8-naphthalimide: a novel inhibitor of poly(ADP-ribose) polymerase and radiation sensitizer. *International Journal of Radiation Biology* 75: 91-100 (1999).
21. Pereira, S., V. Malard, R.J. Luc, H.D. Anne, A. Jean, F. Nicolas & A.G. Christelle. Low doses of gamma-irradiation induce an early bystander effect in Zebra fish cells which is sufficient to radioprotect cells. *PLOS ONE* 9(3): e92974 (2014), doi:10.1371/journal.pone.0092974
22. Hirai,T., H. Shirai, H. Fujimori, R. Okayasu, K. Sasai & M. Masutani. Radiosensitization effect of poly(ADP-ribose) polymerase inhibition in cells exposed to low and high liner energy transfer radiation. *Cancer Science* 103: 1045-1050 (2012).
23. Postiglione, I., A. Chiaviello & G. Palumbo. Twilight effects of low doses of ionizing radiation on cellular systems: a bird's eye view on current concepts and research. *Medical Oncology* 27: 495–509 (2010).

Proceedings of the Pakistan Academy of Sciences 51 (2): 145–155 (2014)

ISSN: 0377 - 2969 (print), 2306 - 1448 (online)

Pakistan Academy of Sciences

Research Article

New Integral Inequalities of the Hermite-Hadamard Type through Invexity

Shahid Qaisar[1], Muhammad Muddassar[2]* and M. Iqbal[3]

[1]College of Mathematics and Statistics, Chongqing University,
Chongqing, 401331, P. R. China
[2] Department of Mathematics, University of Engineering and Technology,
Taxila, Pakistan
[3] Department of Mathematics, University of Engineering and Technology,
Lahore, Pakistan

Abstract: In this paper, we establish some new inequalities of Hermite-Hadamard type based on preinvexity for differentiable mapping that are linked with the illustrious Hermite-Hadamard type inequality for mappings whose derivatives are preinvexity. Also a parallel development is made base on concavity. Applications to some special means of real numbers are found. Also applications to numerical integration are provided. This contributes to new better estimates than presented already.

Keywords: Hermite-Hadamard inequality; preinvex function;H ö lder Integral Inequality; power mean inequality.

AMS Subject Classification(2000): 26D15; 26D10

1. INTRODUCTION

One of the cornerstones of analysis is the Hadamard inequality, if $[a,b]$ with $a<b$ is a real interval and $f:[a,b]\to\mathbb{R}$a convex function, then

$$f\left(\frac{a+b}{2}\right)\leq\frac{1}{b-a}\int_a^b f(x)dx\leq\frac{f(a)+f(b)}{2} \qquad (1.1)$$

Over the last decade this has been extended in a number of ways. An important question is the estimating the difference between the middle and rightmost term in the (1.1). In recent years, this classical inequality has been improved and generalized in a number of ways and a large number of research papers have been written on this inequality [see 5-8, 10-13, 15-16, 20] and the references therein. The following identity is a useful building block.

In recent years, lots of efforts have been made by many mathematicians to generalize the classical convexity. For example, Ben-Israel and Mond [4] discuss the role of invexity in optimization; some more researchers extended the idea of this generalization [1, 3, 14, 15, 17-19, 21].These studies include among others the work of Hanson [8], Weir and Mond [18]. Noor [13, 14] has studied basic properties of the preinvex functions and their role in optimization, variational inequalities and equilibrium problems. Hanson in [9], introduced invex functions as a significant generalization of convex functions. Ben-Israel and Mond [4] gave the concept of preinvex function which is special case of invexity. Let us first recall the definition of pre-invexity and some related results.

Let K be a closed set $\mathbb{R}^n$and let $f:K\to\mathbb{R}$and $\eta:K\times K\to\mathbb{R}$be continuous functions. Let $x\in K$, then the set K is said to be invex at $x$with respect to $\eta(.,.)$.

Received, November 2013; Accepted, May 2014
*Corresponding author. E-mail address: malik.muddassar@gmail.com.

If $x + t\eta(y,x) \in K.\ \forall\, x,y \in K\ , t \in [0,1]$

K is said to be invex set with respect to η if K is invex at each $x \in K$. The invex set K is also called a η-connected set.

Definition 1[16]**.** The function f on the invex set K is said to be preinvex with respect to η, if

$$f\big(x + t\eta(y,x)\big) \le (1-t)f(x) + t\,f(y), \forall\, x,y \in K, t \in [0,1]$$

The function f is said to be preconcave if and only if $-f$ is preinvex.

It is to be noted that every convex function is preinvex with respect to the map $\eta(\mathrm{x},\mathrm{y}) = \mathrm{x} - \mathrm{y}$ but the converse is not true [17-18] and [21].

Dragomir and Agrawal [7] established the following result connected with the Hadamard inequality, as well as to apply them for some elementary inequalities for real numbers and numerical integration.

Lemma 1. Let $f: I^o \subseteq \mathbb{R} \to E$ be differentiable function on I^o $, a,b \in I^o$, with $a < b$. If $f' \in L^1[a,b],\ then$

$$\frac{f(a) + f(b)}{2} - \frac{1}{b-a}\int_a^b f(x)dx$$

$$= \frac{(b-a)}{2}\int_0^1\int_0^1 \begin{pmatrix} f'(ta + (1-t)b) - \\ f'(ua + (1-u)b) \end{pmatrix}(u-t)dtdu.$$

Definition 2 [10]**.** A function $f: [0,\infty) \to \mathbb{R}$ is said to be s-convex or f belongs to the class K_s^i if

$$f(\mu x + \nu y) \le \mu^s f(x) + \nu^s f(y)$$

holds for all $x,y \in [0.,\infty)$ and $u,v \in [0,1]$, for some fixed $s \in (0,1]$.

Note that, if $\mu^\alpha + \nu^\alpha = 1$, the above class of convex functions is called s-convex functions in first sense and represented by K_s^1 and if $\mu + \nu = 1$ the above class is called s-convex in second sense and represented by K_s^2

It may be noted that every 1-convex function is convex.

This paper is in the continuations of [12], which provides more general and refine results aspresented in [12].This paper is organized as follows: after Introduction, we discuss some new s-preinvex-Hermite Hadamard type inequalities for differentiable function in Section 2, and in Section 3 we give some applications for some special means of real numbers of the results formulated in Section 2. In Section 4 we gave some applications to quadrature formulae. Finally conclude our results and applications in Section 5.

2. MAIN RESULTS

Before proceeding towards our main theorem we need the following equality which is the generalization of Lemma 1 for invex sets. We begin with the following Lemma.

Lemma 2[3]**.** Let $K \subseteq \mathbb{R}$ be an open invex subset with respect to $\eta: K \times K \to \mathbb{R}$ and suppose $f: K \to \mathbb{R}$ be differentiable function. If $|\boldsymbol{f}'|$ is integrable on the η-path $P_{ac}, c = a + \eta(b,a)$,then following inequality holds:

$$\left|\frac{f(a) + f\big(a + \eta(b,a)\big)}{2} - \frac{1}{\eta(b,a)}\int_a^{a+\eta(b,a)} f(x)dx\right|$$

$$\le \frac{\eta(b,a)}{2}\int_0^1 |1-2t|\,\boldsymbol{f}'\big(a + t\eta(b,a)\big)dt$$

Theorem 2. Let $K \subseteq \mathbb{R}$ be an open invex subset with respect to $\eta: K \times K \to \mathbb{R}$suppose that $f: K \to \mathbb{R}$be differentiable function. If$|\boldsymbol{f}'|^{\mathbf{q}}$ is preinvex on$K$, then the following inequality holds:

$$\left|\frac{f(a) + f\big(a + \eta(b,a)\big)}{2} - \frac{1}{\eta(b,a)}\int_a^{a+\eta(b,a)} f(x)dx\right|$$

$$\le \frac{\eta(b,a)}{2^s}\left[\frac{s.2^s}{(s+1)(s+2)}\right][|\boldsymbol{f}'(a)| + |\boldsymbol{f}'(b)|] \quad (2.6)$$

For $\mathrm{q} \ge 1$and everya, $\mathrm{b} \in$ Kwith $\eta(b,a) \ne 0$.

Proof. By using Lemma 2, we get

$$\left|\frac{f(a) + f\big(a + \eta(b,a)\big)}{2} - \frac{1}{\eta(b,a)}\int_a^{a+\eta(b,a)} f(x)dx\right|$$

$$\le \frac{\eta(b,a)}{2}\int_0^1 |1-2t|\,\boldsymbol{f}'\big(a + t\eta(b,a)\big)dt$$

since$|\boldsymbol{f}'|$ is s-preinvex on K for everya, $\mathrm{b} \in$ Kand $\mathrm{t} \in [0,1]$.we have

$\boldsymbol{f}'\big(a+t\eta(b,a)\big) \le (1-t)^s|\boldsymbol{f}'(a)| + (t)^s|\boldsymbol{f}'(b)|.$

$$\left|\frac{f(a)+f\big(a+\eta(b,a)\big)}{2} - \frac{1}{\eta(b,a)}\int_a^{a+\eta(b,a)} f(x)dx\right|$$

$$\le \frac{\eta(b,a)}{2}\int_0^1 |1-2t|\,[(1-t)^s|\boldsymbol{f}'(a)| + (t)^s|\boldsymbol{f}'(b)|]dt \quad (2.7)$$

Where we use the fact

$$\int_0^1 |1-2t|\,(1-t)^s dt = \int_0^1 |1-2t|\,t^s dt = \left[\frac{s.2^s}{(s+1)(s+2)}\right] \quad (2.8)$$

By (2.8), and (2.7),we get (2.6).

Theorem 3. Let the assumption of Theorem 2 are satisfied with $\mathrm{p} > 1$,such that $\mathrm{q} = \frac{\mathrm{p}}{\mathrm{p}-1}$ if the mapping $|\boldsymbol{f}'|^{\mathbf{q}}$is concave on $[a,b]$.then,

$$\left|\frac{f(a)+f\big(a+\eta(b,a)\big)}{2} - \frac{1}{\eta(b,a)}\int_a^{a+\eta(b,a)} f(x)dx\right|$$

$$\le \frac{\eta(b,a)}{2}(p+1)^{\frac{1}{\mathrm{p}}}\left|\boldsymbol{f}'\frac{a+b}{2}\right|. \quad (2.9)$$

Proof. By using Lemma 2, we obtain

$$\left|\frac{f(a)+f\big(a+\eta(b,a)\big)}{2} - \frac{1}{\eta(b,a)}\int_a^{a+\eta(b,a)} f(x)dx\right| \le$$

$$\frac{\eta(b,a)}{2}\int_0^1 |1-2t|\,\boldsymbol{f}'\big(a+t\eta(b,a)\big)dt \quad (2.10)$$

By applying Hölder'sinequality on the right side of (2.10). we have,

$$\int_0^1 |1-2t|\,\boldsymbol{f}'\big(a+t\eta(b,a)\big)dt \le$$

$$\left(\int_0^1 |1-2t|^p\,dt\right)^{\frac{1}{\mathrm{p}}}\left(\int_0^1 \left|\boldsymbol{f}'\big(+t\eta(b,a)\big)\right|^q dt\right)^{\frac{1}{\mathrm{q}}} \quad (2.11)$$

Here

$$\int_0^1 |1-2t|^p\,dt = \int_0^{\frac{1}{2}} (1-2t)^p\,dt =$$

$$\int_{\frac{1}{2}}^1 (2t-1)^p\,dt = \frac{1}{p+1}, (2.12)$$

Since$|\boldsymbol{f}'|^{\mathbf{q}}$isconcave, by applying Jensen's integral inequality on the second integral of R.H.S of (2.11.) we have

$$\int_0^1 \left|\boldsymbol{f}'\big(a+t\eta(b,a)\big)\right|^q dt \le \left(\int_0^1 t^0 dt\right)$$

$$\left|\frac{\int_0^1 \left|\boldsymbol{f}'\big(a+t\eta(b,a)\big)\right|^q dt}{\int_0^1 t^0 dt}\right| = \left|\boldsymbol{f}'\frac{a+b}{2}\right|^q \quad (2.13)$$

By (2.10), and (2.12),and (2.13)we get (2.9).

Theorem 4. Let the assumption of Theorem 2 are satisfied with $\mathrm{p} > 1$,such that $\mathrm{q} = \frac{\mathrm{p}}{\mathrm{p}-1}$ if the mapping $|\boldsymbol{f}'|^{\mathbf{q}}$is s-preinvex on $[a,b]$.then,

$$\left|\frac{f(a)+f\big(a+\eta(b,a)\big)}{2} - \frac{1}{\eta(b,a)}\int_a^{a+\eta(b,a)} f(x)dx\right|$$

$$\le \frac{\eta(b,a)}{2(p+1)^{\frac{1}{\mathrm{p}}}}\left(\frac{|\boldsymbol{f}'(a)|^q + |\boldsymbol{f}'(b)|^q}{s+1}\right)^{\frac{1}{\mathrm{q}}}. (2.14)$$

Proof. By using Lemma 2, we obtain

$$\left|\frac{f(a)+f\big(a+\eta(b,a)\big)}{2} - \frac{1}{\eta(b,a)}\int_a^{a+\eta(b,a)} f(x)dx\right|$$

$$\le \frac{\eta(b,a)}{2}\int_0^1 |1-2t|\,\boldsymbol{f}'\big(a+t\eta(b,a)\big)dt \quad (2.15)$$

By applying Hölder's inequality on the right side of (2.15). we have,

$$\int_0^1 |1-2t|\,\boldsymbol{f}'\big(a+t\eta(b,a)\big)dt \le$$

$$\left(\int_0^1 |1-2t|^p\,dt\right)^{\frac{1}{\mathrm{p}}}\left(\int_0^1 \left|\boldsymbol{f}'\big(a + t\eta(b,a)\big)\right|^q dt\right)^{\frac{1}{\mathrm{q}}} (2.16)$$

since $|\boldsymbol{f}'|$ is s-preinvex on K for everya, b $\in$ Kand t $\in [0,1]$. we have

$$\left|\boldsymbol{f}'\big(a+t\eta(b,a)\big)\right|^q$$

$$\le (1-t)^s|\boldsymbol{f}'(a)|^q + (t)^s|\boldsymbol{f}'(b)|^q.$$

And

$$\int_0^1 |1-2t|^p\, dt = \int_0^{\frac{1}{2}} (1-2t)^p\, dt$$

$$= \int_{\frac{1}{2}}^1 (2t-1)^p\, dt = \frac{1}{p+1},$$

$$\int_0^1 \left|\boldsymbol{f}'\big(a+t\eta(b,a)\big)\right|^q dt =$$

$$\frac{|\boldsymbol{f}'(a)|^q + |\boldsymbol{f}'(b)|^q}{s+1} \qquad (2.17)$$

By (2.16), and (2.17), we get (2.14).

Corollary 5. From theorem 4 the assumption of Theorem 2 are satisfied with $\mathrm{p} > 1$,such that $\mathrm{q} = \frac{\mathrm{p}}{\mathrm{p}-1}$ if the mapping $|\boldsymbol{f}'|^{\mathbf{q}}$is s-preinvex on $[a,b]$.then,

$$\left|\frac{f(a)+f\big(a+\eta(b,a)\big)}{2} - \frac{1}{\eta(b,a)}\int_a^{a+\eta(b,a)} f(x)dx\right|$$

$$\leq \frac{\eta(b,a)}{2(p+1)^{\frac{1}{\mathrm{p}}}}\left(\frac{1}{s+1}\right)^{\frac{1}{q}} |\boldsymbol{f}'(a)| + |\boldsymbol{f}'(b)|.$$

Proof. The above inequality is obtained by using the fact $\sum_{i=1}^n (\alpha_i+\beta_i)^k \leq \sum_{i=1}^n (\alpha_i)^k + \sum_{i=1}^n (\beta_i)^k$for $k \in (0,1)$ with $0 \leq \frac{\mathrm{p}}{\mathrm{p}-1}$, for $\mathrm{p} > 1$.

Theorem 6. Let the assumption of Theorem 2 are satisfied with $\mathrm{p} > 1$,such that $\mathrm{q} = \frac{\mathrm{p}}{\mathrm{p}-1}$ if the mapping $|\boldsymbol{f}'|^{\mathbf{q}}$is s-preconcave on $[a,b]$.then,

$$\left|\frac{f(a)+f\big(a+\eta(b,a)\big)}{2} - \frac{1}{\eta(b,a)}\int_a^{a+\eta(b,a)} f(x)dx\right| \left|\boldsymbol{f}'\,\frac{a+b}{2}\right|^q \leq$$

$$\frac{\eta(b,a)}{2}(p+1)^{\frac{1}{\mathrm{p}}}.\, 2^{\frac{s-1}{q}} \left|\boldsymbol{f}'\,\frac{a+b}{2}\right|^q \quad (2.18)$$

Proof. We proceed similarly as in Theorem 4. By s-preconcavity of $|\boldsymbol{f}'|^q$we obtain

$$\int_0^1 \left|\boldsymbol{f}'\big(a+t\eta(b,a)\big)\right|^q dt = 2^{\frac{s-1}{q}} \left|\boldsymbol{f}'\,\frac{a+b}{2}\right|^q. \quad (2.19)$$

Now (2.18) immediately follows from Theorem 1.

Theorem 7. Let the assumption of Theorem 4 are satisfied, we have another result:

$$\left|\frac{f(a)+f\big(a+\eta(b,a)\big)}{2} - \frac{1}{\eta(b,a)}\int_a^{a+\eta(b,a)} f(x)dx\right|$$

$$\leq \frac{\eta(b,a)}{2^{\frac{p+1}{p}}}\left[\frac{s.2^s+1}{2^s}\right]\left(\frac{|\boldsymbol{f}'(a)|^q + |\boldsymbol{f}'(b)|^q}{(s+1)(s+2)}\right)^{\frac{1}{q}}. \quad (2.20)$$

Proof. By using Lemma 2, , we get

$$\left|\frac{f(a)+f\big(a+\eta(b,a)\big)}{2} - \frac{1}{\eta(b,a)}\int_a^{a+\eta(b,a)} f(x)dx\right|$$

$$\leq \frac{\eta(b,a)}{2}\int_0^1 |1-2t|\, \boldsymbol{f}'\big(a+t\eta(b,a)\big)dt$$

$$= \frac{\eta(b,a)}{2}\int_0^1 |1-2t|^{\frac{1}{p}}$$

$$|1-2t|^{\frac{1}{p}}\left|\boldsymbol{f}'\big(a+t\eta(b,a)\big)\right|dt \qquad (2.21)$$

By applying Hölder's inequality on (2.21), for $q > 1$,we have,

$$\left|\frac{f(a)+f\big(a+\eta(b,a)\big)}{2} - \frac{1}{\eta(b,a)}\int_a^{a+\eta(b,a)} f(x)dx\right|$$

$$\leq \frac{\eta(b,a)}{2}\left(\int_0^1 |1-2t|\, dt\right)^{\frac{1}{\mathrm{p}}}$$

$$\left(\int_0^1 |1-2t|\left|\boldsymbol{f}'\big(a+t\eta(b,a)\big)\right|^q dt\right)^{\frac{1}{\mathrm{q}}} (2.22)$$

since $|\boldsymbol{f}'|$ is s-preinvex on K for everya, b $\in$ Kand t $\in [0,1]$.(2.22) can be written as:

$$\left|\frac{f(a)+f\big(a+\eta(b,a)\big)}{2} - \frac{1}{\eta(b,a)}\int_a^{a+\eta(b,a)} f(x)dx\right|$$

$$\leq \frac{\eta(b,a)}{2}\left(\frac{1}{2}\right)^{\frac{1}{p}}\int_0^1 |1 - 2t|\,[(1-t)^s|\boldsymbol{f}'(a)| + (t)^s|\boldsymbol{f}'(b)|]^{\frac{1}{q}}dt$$

$$\leq \frac{\eta(b,a)}{2^{\frac{p+1}{p}}}\int_0^1 |-2t|\,[(1-t)^s|\boldsymbol{f}'(a)| + (t)^s|\boldsymbol{f}'(b)|]^{\frac{1}{q}}dt \qquad (2.23)$$

Where we use the fact from Muddassar et al [12],

$$\int_0^1 |1-2t|\,(1-t)^s dt = \int_0^1 |1-2t|\, t^s dt = \left[\frac{s.2^s}{(s+1)(s+2)}\right]$$

By(2.23), and (2.24), in(2.21),we get (2.20).

Corollary 8. From Theorem 7 Let the assumption of Theorem 4 be satisfied with $p > 1$,such that $q = \frac{p}{p-1}$ if the mapping $|\boldsymbol{f}'|$ is s-preinvex on $[a,b]$.then,

$$\left|\frac{f(a)+f\big(a+\eta(b,a)\big)}{2} - \frac{1}{\eta(b,a)}\int_a^{a+\eta(b,a)} f(x)dx\right|$$

$$\leq \frac{\eta(b,a)}{2^{\frac{p+1}{p}}}\left[\frac{s.2^s+1}{2^s}\right]^{\frac{1}{q}} |\boldsymbol{f}'(a)| + |\boldsymbol{f}'(b)|$$

Proof. Theproof is similar to that of Corollary 5.

Theorem 9. Let the assumption of Theorem 2 are satisfied with $p > 1$,such that $q = \frac{p}{p-1}$ if the mapping $|\boldsymbol{f}'|$ is s-preconcave on $[a,b]$.then

$$\left|\frac{f(a)+f\big(a+\eta(b,a)\big)}{2} - \frac{1}{\eta(b,a)}\int_a^{a+\eta(b,a)} f(x)dx\right|$$

$$\leq \frac{\eta(b,a)}{2^{\frac{p+1}{p}}}\left[\frac{s.2^s+1}{2^s}\right]^{\frac{1}{q}} \left|\boldsymbol{f}'\,\frac{a+b}{2}\right|^q . (2.25)$$

Proof. We proceed similarly as in theorem 6. By s-concavity of $|\boldsymbol{f}'|^{\mathbf{q}}$we obtain

$$\int_0^1 |1-2t|\left|\boldsymbol{f}'\big(a+t\eta(b,a)\big)\right|^q dt =$$

$$\left[\frac{s.2^s+1}{2^s}\right]^{\frac{1}{q}} \left|\boldsymbol{f}'\,\frac{a+b}{2}\right|^q . (2.26)$$

Now (2.25) immediately follows from Theorem 1.

Theorem 10. Let the assumption of Theorem 2 are satisfied, then

$$\left|\frac{f(a)+f\big(a+\eta(b,a)\big)}{2} - \frac{1}{\eta(b,a)}\int_a^{a+\eta(b,a)} f(x)dx\right|$$

$$\leq \frac{\eta(b,a)}{2}\left(\frac{s^2+3s+4}{(s+1)(s+2)(s+3)}\right)^{\frac{1}{q}} |\boldsymbol{f}'(a)| + |\boldsymbol{f}'(b)|. \quad (2.27)$$

Proof. From Lemma 2

$$\left|\frac{f(a)+f\big(a+\eta(b,a)\big)}{2} - \frac{1}{\eta(b,a)}\int_a^{a+\eta(b,a)} f(x)dx\right|$$

$$\leq \frac{\eta(b,a)}{2}\int_0^1\int_0^1 \begin{pmatrix} \boldsymbol{f}'\big(a+t\eta(b,a)\big) \\ -\boldsymbol{f}'\big(a+u\eta(b,a)\big)\end{pmatrix} |u-t|dtdu$$

$$\leq \frac{\eta(b,a)}{2}\int_0^1\int_0^1 \Big(\boldsymbol{f}'\big(a+t\eta(b,a)\big)\Big)|u-t|dtdu$$

$$+\frac{\eta(b,a)}{2}\int_0^1\int_0^1 \Big(\boldsymbol{f}'\big(a+u\eta(b,a)\big)\Big)|u-t|dtdu$$

$$= \eta(b,a)\int_0^1\int_0^1 \Big(\boldsymbol{f}'\big(a+t\eta(b,a)\big)\Big)|u - t|dtdu. \quad (2.28)$$

since $|\boldsymbol{f}'|$ is s-preinvex on K for everya, b $\in$ Kand t $\in [0,1]$.we have

$$\left|\frac{f(a)+f\big(a+\eta(b,a)\big)}{2} - \frac{1}{\eta(b,a)}\int_a^{a+\eta(b,a)} f(x)dx\right|$$

$$\leq \frac{\eta(b,a)}{2}\int_0^1\int_0^1 [(1-t)^s|\boldsymbol{f}'(a)| + (t)^s|\boldsymbol{f}'(b)|]|u - t|dtdu \quad (2.29)$$

But

$$\int_0^1\int_0^1 t^s|u-t|dtdu =$$

$$\int_0^1\int_0^1 (1-t)^s|u-t|dtdu = \frac{s^2+3s+4}{(s+1)(s+2)(s+3)} \quad (2.30)$$

By (2.29) and (2.30),we get (2.27).

Theorem 11. Let the assumption of Theorem 2 are satisfied. Furthermore, if the mapping $|\boldsymbol{f}'|^{\mathbf{q}}$is s-concave on $[a,b]$. For $q > 1$,then,

$$\left|\frac{f(a)+f\big(a+\eta(b,a)\big)}{2} - \frac{1}{\eta(b,a)}\int_a^{a+\eta(b,a)} f(x)dx\right| \leq$$

$$\eta(b,a)\left(\frac{2}{(p+1)(p+2)}\right)^{\frac{1}{p}} \left|\boldsymbol{f}'\,\frac{a+b}{2}\right|. \quad (2.31)$$

Proof. From Lemma 2

$$\left|\frac{f(a)+f\big(a+\eta(b,a)\big)}{2}-\frac{1}{\eta(b,a)}\int_a^{a+\eta(b,a)}f(x)dx\right|$$

$$\leq\frac{\eta(b,a)}{2}\int_0^1\int_0^1\begin{pmatrix}\boldsymbol{f}'\big(a+t\eta(b,a)\big)\\-\boldsymbol{f}'\big(a+u\eta(b,a)\big)\end{pmatrix}|u-t|dtdu$$

$$\leq\frac{\eta(b,a)}{2}\int_0^1\int_0^1\Big(\boldsymbol{f}'\big(a+t\eta(b,a)\big)\Big)|u-t|dtdu$$

$$+\frac{\eta(b,a)}{2}\int_0^1\int_0^1\Big(\boldsymbol{f}'\big(a+u\eta(b,a)\big)\Big)|u-t|dtdu$$

$$=\eta(b,a)\int_0^1\int_0^1\Big(\boldsymbol{f}'\big(a+t\eta(b,a)\big)\Big)|u-t|dtdu. \quad (2.32)$$

By applying Hölder's inequality in (2.32),we have,

$$\left|\frac{f(a)+f\big(a+\eta(b,a)\big)}{2}-\frac{1}{\eta(b,a)}\int_a^{a+\eta(b,a)}f(x)dx\right|$$

$$\leq\frac{\eta(b,a)}{2}\left(\int_0^1\int_0^1\Big(\big|\boldsymbol{f}'\big(a+t\eta(b,a)\big)\big|^q\Big)^{\frac{1}{q}}dtdu\right)^{\frac{1}{p}}\left(\int_0^1\int_0^1|u-t|^p\,dtdu\right)$$

But

$$\int_0^1\int_0^1|u-t|^p\,dtdu=$$

$$\int_0^1\left\{\int_0^u(u-t)^p dt+\int_u^1(t-u)^p dt\right\}du=$$

$$\frac{2}{(p+1)(p+2)}\ (2.34)$$

Since$|\boldsymbol{f}'|^{\mathbf{q}}$isconcave, by applying Jensen's integral inequality on the first integral in R.H.S we have

$$\int_0^1\int_0^1\big|\boldsymbol{f}'\big(a+t\eta(b,a)\big)\big|^q\,dtdu\leq$$

$$\int_0^1\left[\left(\int_0^1 t^0dt\right)\left|\frac{\int_0^1\big|\boldsymbol{f}'\big(a+t\eta(b,a)\big)\big|^q\,dt}{\int_0^1 t^0dt}\right|\right]du$$

$$=\int_0^1\left|\boldsymbol{f}'\frac{a+b}{2}\right|^q du=\left|\boldsymbol{f}'\frac{a+b}{2}\right|^q\ (2.35)$$

Hence (2.33), (2.34), and (2.35), together imply (2.31).

Theorem 12. Let the assumption of Theorem 2 are satisfied. Futhermore, if the mapping $|\boldsymbol{f}'|^{\mathbf{q}}$is s-preinvex on $[a,b]$. For $q>1$,then,

$$\left|\frac{f(a)+f\big(a+\eta(b,a)\big)}{2}-\frac{1}{\eta(b,a)}\int_a^{a+\eta(b,a)}f(x)dx\right|$$

$$\leq\eta(b,a)\left[\frac{2}{(p+1)(p+2)}\right]^{\frac{1}{p}}\left(\frac{|\boldsymbol{f}'(a)|^q+|\boldsymbol{f}'(b)|^q}{(s+1)}\right)\ (2.36)$$

Proof. From Lemma 2

$$\left|\frac{f(a)+f\big(a+\eta(b,a)\big)}{2}-\frac{1}{\eta(b,a)}\int_a^{a+\eta(b,a)}f(x)dx\right|$$

$$\leq\frac{\eta(b,a)}{2}\int_0^1\int_0^1\begin{pmatrix}\boldsymbol{f}'\big(a+t\eta(b,a)\big)\\-\boldsymbol{f}'\big(a+u\eta(b,a)\big)\end{pmatrix}|u-t|dtdu\leq$$

$$\frac{\eta(b,a)}{2}\int_0^1\int_0^1\Big(\boldsymbol{f}'\big(a+t\eta(b,a)\big)\Big)|u-t|dtdu$$

$$+\frac{\eta(b,a)}{2}\int_0^1\int_0^1\Big(\boldsymbol{f}'\big(a+u\eta(b,a)\big)\Big)|u-t|dtdu$$

$$=\eta(b,a)\int_0^1\int_0^1\Big(\boldsymbol{f}'\big(a+t\eta(b,a)\big)\Big)|u-t|dtdu. \quad (2.37)$$

By applying Hölder's inequality in (2.37), we have,

$$\left|\frac{f(a)+f\big(a+\eta(b,a)\big)}{2}-\frac{1}{\eta(b,a)}\int_a^{a+\eta(b,a)}f(x)dx\right|$$

$$\leq\eta(b,a)\left(\int_0^1\int_0^1\big|\boldsymbol{f}'\big(a+t\eta(b,a)\big)\big|^q\right)^{\frac{1}{q}\frac{1}{p}}dtdu\left(\int_0^1\int_0^1|u-t|^p\,dtdu\right) \quad (2.38)$$

Since $|\boldsymbol{f}'|$ is s-preinvex on K for everya, b $\in$ Kand t $\in[0,1]$.we have

$$\left|\frac{f(a)+f\big(a+\eta(b,a)\big)}{2}-\frac{1}{\eta(b,a)}\int_a^{a+\eta(b,a)}f(x)dx\right|$$
$$\leq \eta(b,a)\int_0^1\int_0^1([(1-t)^s|\boldsymbol{f}'(a)|^{\mathrm{q}}+(t)^s|\boldsymbol{f}'(b)|^{\mathrm{q}}]dtdu)^{\frac{1}{q}} \quad (2.39)$$

But

$$\int_0^1\int_0^1|u-t|^p\,dtdu=\int_0^1\left\{\int_0^u(u-t)^p dt+\int_u^1(t-u)^p dt\right\}du=\frac{2}{(p+1)(p+2)} \quad (2.40)$$

And

$$\int_0^1\int_0^1 t^s dtdu=\int_0^1\int_0^1(1-t)^s dtdu=\frac{1}{(s+1)}. \quad (2.41)$$

By (2.39), (2.40), (2.40), and (2.41),(2.41), we have(2.36).

Corollary 13. From Theorem 12, Let the assumption of Theorem 2 are satisfied. Futhermore, if the mapping $|\boldsymbol{f}'|^{\mathbf{q}}$is s-preinvex on $[a,b]$.For $q>1$,then,

$$\left|\frac{f(a)+f\big(a+\eta(b,a)\big)}{2}-\frac{1}{\eta(b,a)}\int_a^{a+\eta(b,a)}f(x)dx\right|$$
$$\leq \eta(b,a)\left[\frac{2}{(p+1)(p+2)}\right]^{\frac{1}{p}}\left(\frac{1}{(s+1)}\right)^{\frac{1}{q}}(|\boldsymbol{f}'(a)|+|\boldsymbol{f}'(b)|)$$

Proof. The proof is similar to that of Corollary 5.

Theorem 14. Let the assumption of Theorem 2 are satisfied. Futhermore, if the mapping $|\boldsymbol{f}'|^{\mathbf{q}}$is s-preconcave on $[a,b]$.For $q>1$,then,

$$\left|\frac{f(a)+f\big(a+\eta(b,a)\big)}{2}-\frac{1}{\eta(b,a)}\int_a^{a+\eta(b,a)}f(x)dx\right|$$
$$\leq \eta(b,a)\left[\frac{2}{(p+1)(p+2)}\right]^{\frac{1}{p}}.2^{\frac{s-1}{q}}\left|\boldsymbol{f}'\frac{a+b}{2}\right|. \quad (2.42)$$

Proof. We proceed similarly as in theorem 10. By s-preconcavity of $|\boldsymbol{f}'|^{\mathbf{q}}$we obtain

$$\int_0^1\int_0^1\left|\boldsymbol{f}'\big(a+t\eta(b,a)\big)\right|^q dtdu$$
$$\leq 2^{s-1}\left|\boldsymbol{f}'\frac{a+b}{2}\right|^q \quad (2.43)$$

Now (2.42), immediately follows from Theorem 1.

Theorem 15. Let $K\subseteq\mathbb{R}$ be an open invex subset with respect to $\eta: K\times K\to\mathbb{R}$suppose that$f: K\to\mathbb{R}$be differentiable function. If$|\boldsymbol{f}'|^{\mathbf{q}}$ is s-preinvex on K, then the following inequality holds:

$$\left|\frac{f(a)+f\big(a+\eta(b,a)\big)}{2}-\frac{1}{\eta(b,a)}\int_a^{a+\eta(b,a)}f(x)dx\right|$$
$$\leq\frac{\eta(b,a)}{3^{\frac{1}{p}}}\left(\frac{s^2+3s+4}{2(s+1)(s+2)(s+3)}\right)^{\frac{1}{q}}$$

$$(|\boldsymbol{f}'(a)|^q+|\boldsymbol{f}'(b)|^q)^{\frac{1}{q}} \quad (2.44)$$

Proof. From Lemma 2

$$\left|\frac{f(a)+f\big(a+\eta(b,a)\big)}{2}-\frac{1}{\eta(b,a)}\int_a^{a+\eta(b,a)}f(x)dx\right|$$
$$\leq\frac{\eta(b,a)}{2}\int_0^1\int_0^1\begin{pmatrix}\boldsymbol{f}'\big(a+t\eta(b,a)\big)\\-\boldsymbol{f}'\big(a+u\eta(b,a)\big)\end{pmatrix}|u-t|dtdu$$

$$\leq\frac{\eta(b,a)}{2}\int_0^1\int_0^1\Big(\boldsymbol{f}'\big(a+t\eta(b,a)\big)\Big)|u-t|dtdu$$
$$+\frac{\eta(b,a)}{2}\int_0^1\int_0^1\Big(\boldsymbol{f}'\big(a+u\eta(b,a)\big)\Big)|u-t|dtdu$$
$$=\eta(b,a)\int_0^1\int_0^1\Big(\boldsymbol{f}'\big(a+t\eta(b,a)\big)\Big)|u-t|dtdu. \quad (2.45)$$

By applying Holder's inequality in(2.45) we follows as,

$$\left|\frac{f(a)+f\big(a+\eta(b,a)\big)}{2} - \frac{1}{\eta(b,a)}\int_a^{a+\eta(b,a)} f(x)dx\right| \le \eta(b,a)\left(\int_0^1\int_0^1 |u-t|\left|\boldsymbol{f}'\big(a+t\eta(b,a)\big)\right|^q\right)^{\frac{1}{q}} dtdu \left(\int_0^1\int_0^1 |u-t|\, dtdu\right)^{\frac{1}{p}} \quad (2.46)$$

Here

$$\int_0^1\int_0^1 |u-t|\, dtdu = \frac{1}{3} \quad (2.47)$$

And

$$\int_0^1\int_0^1 |u-t|\left|\boldsymbol{f}'\big(a+t\eta(b,a)\big)\right|^q dtdu \le \eta(b,a)\int_0^1\int_0^1 (|u-t|(1-t)^s|\boldsymbol{f}'(a)|^q + |u-t|(t)^s|\boldsymbol{f}'(b)|^q dtdu) \quad (2.48)$$

Since $|\boldsymbol{f}'|$ is s-preinvex on K for every $a, b \in K$ and $t \in [0,1]$.we have

By solving (2.48), we have

$$\int_0^1\int_0^1 |u-t|\left|\boldsymbol{f}'\big(a+t\eta(b,a)\big)\right|^q dtdu \le \left(\frac{s^2+3s+4}{2(s+1)(s+2)(s+3)}\right)^{\frac{1}{q}} (|\boldsymbol{f}'(a)|^q + |\boldsymbol{f}'(b)|^q)^{\frac{1}{q}} \quad (2.49)$$

Relations (2.46), (2.47), and (2.49) together imply (2.44).

Corollary 16. From theorem 15,Let $K \subseteq \mathbb{R}$ be an open invex subset with respect to $\eta: K \times K \to \mathbb{R}$ suppose that $f: K \to \mathbb{R}$ be differentiable function. If $|\boldsymbol{f}'|^{\mathbf{q}}$ is s-preinvex on K, then the following inequality holds:

$$\left|\frac{f(a)+f\big(a+\eta(b,a)\big)}{2} - \frac{1}{\eta(b,a)}\int_a^{a+\eta(b,a)} f(x)dx\right| \le \frac{\eta(b,a)}{3^{\frac{1}{p}}}\left(\frac{s^2+3s+4}{2(s+1)(s+2)(s+3)}\right)^{\frac{1}{q}} (|\boldsymbol{f}'(a)| + |\boldsymbol{f}'(b)|)$$

Proof. Theproof is similar to that of Corollary 5.

Theorem 17. Let $K \subseteq \mathbb{R}$ be an open invex subset with respect to $\eta: K \times K \to \mathbb{R}$ suppose that $f: K \to \mathbb{R}$ be differentiable function. If $|\boldsymbol{f}'|^{\mathbf{q}}$ is s-preconcave on K, then the following inequality holds:

$$\left|\frac{f(a)+f\big(a+\eta(b,a)\big)}{2} - \frac{1}{\eta(b,a)}\int_a^{a+\eta(b,a)} f(x)dx\right| \le \frac{\eta(b,a)}{3^{\frac{1}{p}}}\left[\frac{s^2+3s+4}{(s+2)(s+3)}\right]^q . 2^{\frac{s-2}{q}}\left|\boldsymbol{f}'\frac{a+b}{2}\right|. \quad (2.50)$$

Proof. We proceed similarly as in theorem 12. By s-preconcavity of $|\boldsymbol{f}'|^{\mathbf{q}}$ we obtain

$$\int_0^1\int_0^1 |u-t|\left|\boldsymbol{f}'\big(a+t\eta(b,a)\big)\right|^q dtdu \le \left[\frac{s^2+3s+4}{(s+2)(s+3)}\right]^q \left|\boldsymbol{f}'\frac{a+b}{2}\right| \quad (2.51)$$

Now (2.50) immediately follows from Theorem 1.

3. APPLICATION TO SOME SPECIAL MEANS

We now consider the applications of our theorem to the special means.

(a) The arithmetic mean;

$$A = A(a,b) := \frac{a+b}{2}, \qquad a,b > 0,$$

(b) The geometric mean;

$$G = G(a,b) := \sqrt{ab}, \qquad a,b > 0,$$

(c) The Harmonic mean:

$$H = H(a,b) := \frac{2ab}{a+b}, \qquad a,b > 0,$$

(d) The logarithmic mean:

$$L = L(a,b) := \begin{cases} a, & if a = b \\ \frac{b-a}{lnb-lna}, & if a \neq b \end{cases}, \quad a,b > 0,$$

(e) The identric mean:

$$I = I(a,b) := \begin{cases} a, & if a = b \\ \frac{1}{e}\left(\frac{b^b}{a^a}\right)^{1/_{b-a}}, & if a \neq b \end{cases} a,b > 0,$$

(f) The p- logarithmic mean:

$$I = I(a,b) := \begin{cases} a, & if a = b \\ \sqrt[p]{\dfrac{b^{p+1} - a^{p+1}}{(p+1)(b-a)}}, & if a \neq b \end{cases} \quad a, b > 0,$$

The following inequality is well known in the literature in [9]:

$$\boldsymbol{H \leq G \leq L \leq I \leq A}.$$

It is also known that L_P is monotonically increasing over $p \in \mathbb{R}$,denoting $L_0 = I$ and $L_{-1} = L$.

Proposition 1. Let$p > 1, 0 < a < b$ and $\frac{p}{p-1}$.then one has the inequality.

$$|A(a,b) - L(a,b)| \leq \frac{(lnb - lna)}{3} A(|a|, |b|). \quad (3.52)$$

Proof. By Theorem 10 applied for the mapping $f(x) = e^x$ for $s = 1$. .we have the above inequality (3.52)

Proposition 2. Let $p > 1$, , $0 < a < b$ and $q = \frac{p}{p-1}$.then one has the inequality.

$$\left|\frac{I(1-a, 1-b)}{G(1-a, 1-b)}\right| \leq exp\left(\left(\frac{b-a}{3}\right) H^{-1}(|1-a|, |1-b|)\right)$$

Proof. By Theorem 12 applied for the mapping $f(x) = -ln(1-x)$ for $s = 1$.

Another result which is connected with p-logarithmic mean$L_P(a,b)$ is following one :

Proposition 3. Let $p > 1, 0 < a < b$ and $q = \frac{p}{p-1}$.

$$\left|A[(1-a)^n, (1-b)^n] - L_n^p[(1-a)^n, (1-b)^n]\right| \leq |n|(b-a)\left[\frac{2}{(p+1)(p+2)}\right]^{\frac{1}{p}} \left[A\left(|1-a|^{\frac{q}{n-1}}, |1-b|^{\frac{q}{n-1}}\right)\right]^{\frac{1}{q}}.$$

Proof . Following by Theorem 15, setting$f(x) = (1-x)^n, |n| \geq 2$ and $n \in \mathbb{R}$ for $s = 1$.

4. APPLICATION TO QUADRATURE FORMULA

Let D be the division or the partition of the interval $[a,b]$,i.e., $d: a = x_0 < x_1 < \cdots < n - 1 < x_n = b$, and consider the quadrature formula

$$\int_a^b f(x)\,dx = S(f,D) + R(f,D) \quad (4.53)$$

Where

$S(f,D) = \sum_{k=0}^{n-1} \frac{f(x_k)+f(x_{k+1})}{2}(x_{k+1} - x_k)$For the trapezoidal version and $R(f,D)$ denotes the related approximation error.

Proposition 4. . Let $K \subseteq \mathbb{R}$ be an open invex subset with respect to $\eta: K \times K \to \mathbb{R}$suppose that $f: K \to \mathbb{R}$be differentiable function. If$|\boldsymbol{f}'|^{\mathbf{p}/(\mathbf{p-1})}$ is s-preinvex on $K, p > 1$,for every division D of $[a,b]$, then the following inequality holds:

$$|R(f,D)| \leq \frac{1}{2^{\frac{p+1}{p}}}\left(\frac{s.2^s + 1}{(s+1)(s+2)}\right)^{\frac{1}{q}} \sum_{k=0}^{n-1}(x_{k+1} - x_k)^2\,[|\boldsymbol{f}'(x_k)| + |\boldsymbol{f}'(x_{k+1})|] \quad (4.54)$$

Proof. Applying Corollary 8 on the subintervals $[x_k, x_{k+1}], (k = 0,1, \ldots \ldots . n-1)$ of the division D and using the fact :

$\sum_{m-1}^{n-1}(\emptyset_m + \mu_m)^r \leq \sum_{m-1}^{n-1}(\emptyset_m)^r + \sum_{m-1}^{n-1}(\mu_m)^r$ for $(0 < r < 1)$ and for each m both $\emptyset_m, \mu_m \geq 0$,we have

$$\left|\frac{1}{x_{k+1} - x_k}\int_{x_k}^{x_{k+1}} \boldsymbol{f}(x) - \boldsymbol{f}\left(\frac{x_{k+1} - x_k}{2}\right)\right| \leq \frac{x_{k+1} - x_k}{2^{\frac{p+1}{p}}}\left(\frac{s.2^s + 1}{(s+1)(s+2)}\right)^{\frac{1}{q}} [|\boldsymbol{f}'(x_k)| + |\boldsymbol{f}'(x_{k+1})|] \quad (4.55),$$

Summing over k from 0 to $n-1$ and taking into account that $|f'|$ is s-preinvex ,

By triangle inequality ,we have

$$\left|\int_a^b f(x)\,dx - S(f,D)\right| =$$

$$\left|\sum_{k=0}^{n-1}\left\{\int_{x_k}^{x_{k+1}} f(x) - (x_{k+1}-x_k) f\left(\frac{x_{k+1}+x_k}{2}\right)\right\}\right| \leq$$

$$\sum_{k=0}^{n-1}\left|\left\{\int_{x_k}^{x_{k+1}} f(x) - (x_{k+1}-x_k) f\left(\frac{x_{k+1}-x_k}{2}\right)\right\}\right|$$

$$|R(f,D)| \leq \sum_{k=0}^{n-1}(x_{k+1}-x_k)\left|f\left(\frac{x_{k+1}+x_k}{2}\right) - \frac{1}{x_{k+1}-x_k}\int_{x_k}^{x_{k+1}} f(x)\right| \quad (4.56),$$

By combining(4.55), (4.56),we get (4.54).

Proposition 5. Let $K \subseteq \mathbb{R}$ be an open invex subset with respect to $\eta: K \times K \to \mathbb{R}$suppose that $f: K \to \mathbb{R}$be differentiable function. If$|f'|^{p/(p-1)}$ is s-preinvex on K, $p > 1$,for every division$D$ of $[a,b]$, then the following inequality holds:

$$|R(f,D)| \leq \frac{1}{3^{\frac{1}{p}}}\left(\frac{s^2+3s+4}{2(s+1)(s+2)(s+3)}\right)^{\frac{1}{q}}$$

$$\sum_{k=0}^{n-1}(x_{k+1}-x_k)^2\,[|f'(x_k)| + |f'(x_{k+1})|]$$

Proof. The proof is similar to that of Proposition 4 and using Corollary 16.

5. CONCLUSIONS

Convexity has been playing a key role in mathematical programming, engineering, and optimization theory. The generalization of convexity is one of the most important aspects in mathematical programming and optimization theory. There have been many attempts to weaken the convexity assumptions in the literature. A significant generalization of convex functions is that of invex functions introduced by Hanson [9]. Ben-Israel and Mond [4] introduced the concept of preinvex functions, which is a special case of invexity. Pini [17] introduced the concept of prequasiinvex functions as a generalization of invex functions. Noor [13, 14] has established some Hermite-Hadamardtype inequalities for preinvex and log-preinvex functions. In this paper we developed more results on hermite-Hadamard's type inequalities by weaken the condition of convexity and found some new results which are related with some special mean; we also applied these results on quadrature rules that gave better estimates than previously presented. We can further find some new relations in the same way as above associating with some special means by taking some other convex functions. For example, choosing different convex functions like $f(x) = -ln\,x, f(x) = \frac{1}{x}$ and $f(x) = -ln(1-x)$ for different values of $s$in s-invexity (concavity), we get new relations relating to some special means.

6. REFERENCES

1. Antczak, T. Mean value in invexity analysis. *Nonlinear Analysis* 60: 1471-1484 (2005).
2. Barani, A., A.G. Ghazanfari & S.S. Dragomir, Hermite-Hadamard inequality through prequsi-invex functions. Article 48, In: *RGMIA Research Report Collection*, p. 14 (2011).
3. Barani, A., A.G. Ghazanfari & S.S. Dragomir, Hermite-Hadamard inequality for functions whose derivatives absolute values are preinvex, Article 64, In: *RGMIA Research Report Coll*ection, 14 (2011).
4. Ben-Israel, A. & B. Mond, What is invexity. *The Journal of the Australian Mathematical Society, Series B. Applied Mathematics* 28(1): 1-9 (1986).
5. Dragomir, S.S. Two mappings in connection to Hadamard's inequalities. *Journal of Mathematical Analysis and Applications* 167: 49–56 (1992).
6. Dragomir, S.S. & C.E. M. Pierce, *Selected Topics on Hermite-Hadamard Inequalities and Applications*. RGMIA, Monographs Victoria University (2000). (online:http://ajmaa.org/ RGMIA/monographs.php/).
7. Dragomir , S.S. & R.P. Agarwal, Two inequalities for differentiable mappings and applications tospecial means of real numbers and to trapezoidal formula. *Applied Mathematics Letters* 11: 91–95 (1998).
8. Dragomir, S.S., Y.J. Cho & S.S. Kim, Inequalities of Hadamard's type for Lipschitzian mappings andtheir applicaitions, *Journal of Mathematical Analysis and Applications* 245: 489–501 (2000).
9. Hanson, M.A. On su¢ ciency of the Kuhn-Tucker conditions, *Journal of Mathematical Analysis and Applications* 80: 545-550 (1981).

10. Hudzik, H. & L. Maligrada, Some remarks on s-convex functions. *Equations Math*. 48: 100-111, (1994).
11. Ion, D.A. Some estimates on the Hermite-Hadamard inequality through quasi-convex functions, Annals of University of Craiova Math. *Comp. Sci. Se*r. 34: 82-87 (2007).
12. Muddassar, M., M. I. Bhatti & M. Iqbal, Some new s-Hermite-Hadamard type inequalities for differentiable functions and their Applications, Proceedings of the Pakistan Academy of Sciences 49(1): 9-17 (2012).
13. Noor, M.A. Some new classes of nonconvex functions. *Nonlinear Functions Anal. Appl.* 11: 165-171 (2006).
14. Noor, M.A. On Hadamard integral inequalities involving two log-preinvex functions, *J. Inequal. Pure Appl. Math.,* 8 (3): 1-14 (2007).
15. Pearce, C.E. M. & J. Pečarić. Inequalities for differentiable mappings with application to special means and quadrature formula. *Applied Mathematics Letters* 13: 51–55 (2000).
16. Pečarić, J., F. Proschan & Y.L. Tong. *Convex Functions, Partial Ordering and Statistical Applications*, Academic Press, New York (1991).
17. Pini, R. Invexity and generalized convexity. *Optimization* 22: 513-525 (1991).
18. Weir, T. & B. Mond. Preinvex functions in multiple objective optimization. *Journal of Mathematical Analysis and Applications* 136: 29-38 (1988a).
19. Yang, G. S., D. Y. Hwang and K. L. Tseng, Some inequalities for differentiable convex and concavemappings, *Applied Mathematics Letters* 47: 207–216 (2004).
20. Yang, X.M., X.Q. Yang & K.L. Teo. Characterizations and applications of prequasi-invex functions, properties of preinvex functions. *Journal of Optimization Theory and Applications* 110: 645-688 (2001).
21. Yang, X.M. & D. Li. On properties of preinvex functions. *Journal of Mathematical Analysis and Applications* 256: 229-241 (2001).

Proceedings of the Pakistan Academy of Sciences 51 (2): 157–165 (2014)

ISSN: 0377 - 2969 (print), 2306 - 1448 (online)

Pakistan Academy of Sciences

Research Article

A Non-Polynomial Spline Method for Solving Linear Twelfth Order Boundary Value Problem

A. Pervaiz[1*], Z . Zafar[2] and M. O. Ahmad[1]

[1]Department of Mathematics, University of Engineering & Technology, Lahore, Pakistan
[2]Faculty of Engineering, University of Central Punjab, Lahore, Pakistan

Abstract: In this work, a numerical technique based on non-polynomial cubic spline was developed for solving linear twelfth order BVP. We first reduce the problem to a system of second order boundary value problems. Then the related scheme was constructed by using the developed numerical technique. The effectiveness of the method is demonstrated with two numerical examples which show that the method converges with sufficient accuracy to the exact solution.

Keywords: Boundary value problems, Non-polynomial spline, finite differences, system of algebraic equations

1. INTRODUCTION

In this paper we developed a numerical technique with non-polynomial cubic spline for obtaining an approximate solution of a twelfth order linear BVP, which is in the form

$$u^{(12)}(x) + a_1(x)u^{(11)}(x) + a_2(x)u^{(10)}(x) + a_3(x)u^{(9)}(x) + a_4(x)u^{(8)}(x) + a_5(x)u^{(7)}(x) + a_6(x)u^{(6)}(x) + a_7(x)u^{(5)}(x) + a_8(x)u^{(4)}(x) + a_9(x)u^{(3)}(x) + a_{10}(x)u^{(2)}(x) + a_{11}(x)u^{(1)}(x) + a_{12}(x)u(x) = f(x) \ ; x \in [a,b] \quad (1)$$

Subject to the boundary conditions

$$u(a) = \alpha_0 \quad , \quad u(b) = \beta_0$$
$$u^{(2)}(a) = \alpha_1 \quad , \quad u^{(2)}(b) = \beta_1$$
$$u^{(4)}(a) = \alpha_2 \quad , \quad u^{(4)}(b) = \beta_2$$
$$u^{(6)}(a) = \alpha_3 \quad , \quad u^{(6)}(b) = \beta_3$$
$$u^{(8)}(a) = \alpha_4 \quad , \quad u^{(8)}(b) = \beta_4$$
$$u^{(10)}(a) = \alpha_5 \quad , \quad u^{(10)}(b) = \beta_5 \quad (2)$$

where $(\alpha_i, \beta_i ; i = 0,1,\cdots,5)$ are arbitrary fixed real constants, and $(a_i(x); i = 1,2,\cdots,12)$ and $f(x)$ are continuous functions defined on the interval $[a,b]$. In literature the numerical solutions of twelfth order BVPs and the linked characteristic value problem is rare. When an infinite horizontal film of fluid is heated from below, with the supposition that a consistent magnetic field is also functional from corner to corner the fluid in the same course as gravity and the fluid is subjected to the feat of rotational, unsteadiness begins. When unsteadiness sets in as usual convection, it is modeled by tenth order BVP. When instability begins as over stability, it can be modeled by twelfth order BVP. Chandrasekhar [1]. Numerical methods for eighth, tenth and twelfth order characteristic value problems arising in thermal unsteadiness were developed by Twizell et al [2]. Siddiqui and Twizell [3, 4] presented the solutions of tenth and twelfth order BVPs using tenth and twelfth degree splines respectively. In 1975 the solution of second order boundary value problems was presented by Alberg and Ito [5]. Usmani [6] in 1980 developed cubic, quartic and sextic spline methods for solving non-linear second order BVP. Siraj-ul-Islam et al [7] (2006) presented a quadratic non-polynomial spine method for solving second order obstacle problems. Caglar [8] used non-polynomial spline technique to solve a

Received, December 2013; Accepted, May 2014
*Corresponding Author: anjumpervaiz1@hotmail.com

time-dependent heat-like Lame-Emden equation. In [9] Papamichael et al successively developed the cubic spline scheme for the solution of two-point BVPs. Omotayo et al [10] solved fourth order BVPs by reducing it to a system of second order BVPs using a non-polynomial spline method and obtained a convergence of order four.

In this paper, we solve equation (1) along with the associated boundary conditions (2) by reducing equation (1) to a system of second order differential equations of the form:

$$p^{(2)}(x) + a_1(x)p^{(1)}(x) + a_2(x)p(x) + a_3(x)t^{(1)}(x) + a_4(x)t(x) + a_5(x)r^{(1)}(x) + a_6(x)r(x) + a_7(x)w^{(1)}(x) + a_8(x)w(x) + a_9(x)v^{(1)}(x) + a_{10}(x)v(x) + a_{11}(x)u^{(1)}(x) + a_{12}(x)u(x) = f(x) \;;\quad a \le x \le b \tag{3}$$

$$u^{(2)}(x) - v(x) = 0$$

$$v^{(2)}(x) - w(x) = 0$$

$$w^{(2)}(x) - r(x) = 0$$

$$r^{(2)}(x) - t(x) = 0$$

$$t^{(2)}(x) - p(x) = 0 \tag{4}$$

Subject to the boundary conditions

$$\begin{aligned} u(a) &= \alpha_0 \quad , \quad u(b) = \beta_0 \\ v(a) &= \alpha_1 \quad , \quad v(b) = \beta_1 \\ w(a) &= \alpha_2 \quad , \quad w(b) = \beta_2 \\ r(a) &= \alpha_3 \quad , \quad r(b) = \beta_3 \\ t(a) &= \alpha_4 \quad , \quad t(b) = \beta_4 \\ p(a) &= \alpha_5 \quad , \quad p(b) = \beta_5 \end{aligned} \tag{5}$$

2. DESCRIPTION OF NON-POLYNOMIAL SPLINE METHOD

In order to derive non-polynomial spline approximation S to (4) along with the boundary conditions (5), we divide the interval $[a, b]$ into n equal subintervals using the grid points:

$x_i = a + ih,\ i = 0,1,\cdots,n$ where $a = x_0$, $b = x_n$, $h = \frac{b-a}{n}$, and n is any arbitrary positive integer.

Let $u(x)$ be the exact solution and u_i be an approximation to $u(x_i)$ obtained by the non-polynomial cubic spline $S_i(x)$ passing through the points $(x_i, u_i)$and (x_{i+1}, u_{i+1}). $S_i(x)$is required to satisfy the interpolating conditions at x_i and x_{i+1}, the boundary conditions (5) and also the continuity of first derivative at the common nodes (x_i, u_i). For each segment (x_i, x_{i+1}); $i = 0,1,\cdots,n-1$, we write the non-polynomial spline $S_i(x)$ in the form

$$S_i(x) = a_i + b_i(x - x_i) + c_i \sin\tau(x - x_i) + d_i \cos\tau(x - x_i) \;;i = 0,1,\cdots,n-1 \tag{6}$$

Where a_i, b_i, $c_i$and d_i are constants and τ is a free parameter. A non-polynomial function $S(x)$ of class $C^2[a, b]$ which interpolates $u(x)$ at the grid points x_i; $i = 0,1,\cdots,n$ depends on a parameter τ and reduces to an ordinary cubic spline $S(x)$ in $[a, b]$ as $\tau \to 0$.

For the derivation of the expression for coefficients of equation (6) in terms of u_i, u_{i+1}, L_i and L_{i+1}, we first define

$$\begin{aligned} S_i(x_i) &= u_i \quad , \quad S_i(x_{i+1}) = u_{i+1} \\ S_i''(x_i) &= L_i \quad , \quad S_i''(x_{i+1}) = L_{i+1} \end{aligned} \tag{7}$$

By using the simple algebraic manipulation we obtain the following expressions for the coefficients of (6) as

$$a_i = u_i + \frac{L_i}{\tau^2} \quad , \quad b_i = \frac{u_{i+1} - u_i}{h} + \frac{L_{i+1} - L_i}{\tau\theta} \quad , \quad c_i = \frac{L_i \cos\theta - L_{i+1}}{\tau^2 \sin\theta} \quad , \quad d_i = -\frac{L_i}{\tau^2}$$

Where $\theta = \tau h$, $i = 0,1,\cdots,n-1$.

Using the continuity condition of first derivative at the grid point (x_i, u_i) $i.e.$, $S_{i-1}'(x_i) = S_i'(x_i)$ we get the following consistency relation for $i = 1,\cdots,n-1$.

$$\alpha L_{i+1} + 2\beta L_i + \alpha L_{i-1} = \frac{1}{h^2}(u_{i+1} - 2u_i + u_{i-1}) \tag{8}$$

Where $\alpha = \frac{1}{\theta \sin\theta} - \frac{1}{\theta^2}$, $\beta = -\frac{1}{\theta^2} - \frac{\cos\theta}{\theta}$ and $\theta = \tau h$

On similar lines we obtain relations for $v(x)$, $w(x)$, $r(x)$, $t(x)$ and $p(x)$ respectively as;

$$\alpha M_{i+1} + 2\beta M_i + \alpha M_{i-1} = \frac{1}{h^2}(v_{i+1} - 2v_i + v_{i-1}) \tag{9}$$

$$\alpha N_{i+1} + 2\beta N_i + \alpha N_{i-1} = \frac{1}{h^2}(w_{i+1} - 2w_i + w_{i-1}) \tag{10}$$

$$\alpha Q_{i+1} + 2\beta Q_i + \alpha Q_{i-1} = \frac{1}{h^2}(r_{i+1} - 2r_i + r_{i-1}) \quad (11)$$

$$\alpha R_{i+1} + 2\beta R_i + \alpha R_{i-1} = \frac{1}{h^2}(t_{i+1} - 2t_i + t_{i-1}) \quad (12)$$

$$\alpha W_{i+1} + 2\beta W_i + \alpha W_{i-1} = \frac{1}{h^2}(p_{i+1} - 2p_i + p_{i-1}) \quad (13)$$

Where we have substituted

$v^{(2)}(x) = M$, $w^{(2)}(x) = N$, $r^{(2)}(x) = Q$, $t^{(2)}(x) = R$, $p^{(2)}(x) = W$

The described method is fourth order convergent if $1 - 2\alpha - 2\beta = 0$ and $\alpha = \frac{1}{12}$ [10].

3. NON-POLYNOMIAL SPLINE APPLICATIONS

To illustrate the applications of the method developed in the previous section, we discretize (4) at the grid points (x_i, u_i) , (x_i, v_i) , (x_i, w_i) , (x_i, r_i) , (x_i, t_i) and (x_i, p_i) , so we have

$$p_i^{(2)} + a_1(x_i)p_i^{(1)} + a_2(x_i)p_i(x) + a_3(x_i)\, t_i^{(1)} + a_4(x_i)t_i$$

$$+a_5(x_i)r_i^{(1)} + a_6(x_i)r_i + a_7(x_i)w_i^{(1)} + a_8(x_i)w_i$$

$$+a_9(x_i)v_i^{(1)} + a_{10}(x_i)v_i + a_{11}(x_i)u_i^{(1)} + a_{12}(x_i)u_i = f(x_i)$$

$$u_i^{(2)} = v_i$$

$$v_i^{(2)} = w_i$$

$$w_i^{(2)} = r_i$$

$$r_i^{(2)} = t_i$$

$$t_i^{(2)} = p_i \quad (14)$$

Substituting $u_i^{(2)} = L_i$, $v_i^{(2)} = M_i$, $w_i^{(2)} = N_i$, $r_i^{(2)} = Q_i$, $t_i^{(2)} = R_i$, $p_i^{(2)} = W_i$ in (14) and rewriting, we get

$$W_i = f(x_i) - a_1(x_i)p_i^{(1)} - a_2(x_i)p_i(x)$$

$$-a_3(x_i)\, t_i^{(1)} - a_4(x_i)t_i - a_5(x_i)r_i^{(1)} - a_6(x_i)r_i$$

$$-a_7(x_i)w_i^{(1)} - a_8(x_i)w_i - a_9(x_i)v_i^{(1)} - a_{10}(x_i)v_i$$

$$-a_{11}(x_i)u_i^{(1)} - a_{12}(x_i)u_i$$

$$L_i = v_i$$

$$M_i = w_i$$

$$N_i = r_i$$

$$Q_i = t_i$$

$$R_i = p_i \quad (15)$$

The following approximations of $O(h^2)$ for the first order derivative of u, v, w, r, t and p in (15) can be used;

$$u_i' \cong \frac{u_{i+1} - u_{i-1}}{2h} \quad , \quad v_i' \cong \frac{v_{i+1} - v_{i-1}}{2h}$$

$$u_{i+1}' \cong \frac{3u_{i+1} - 4u_i + u_{i-1}}{2h} \quad , \quad v_{i+1}' \cong \frac{3v_{i+1} - 4v_i + v_{i-1}}{2h}$$

$$u_{i-1}' \cong \frac{-u_{i+1} + 4u_i - 3u_{i-1}}{2h} \quad , \quad v_{i-1}' \cong \frac{-v_{i+1} + 4v_i - 3v_{i-1}}{2h}$$

$$w_i' \cong \frac{w_{i+1} - w_{i-1}}{2h} \quad , \quad r_i' \cong \frac{r_{i+1} - r_{i-1}}{2h}$$

$$w_{i+1}' \cong \frac{3w_{i+1} - 4w_i + w_{i-1}}{2h} \quad , \quad r_{i+1}' \cong \frac{3r_{i+1} - 4r_i + r_{i-1}}{2h}$$

$$w_{i-1}' \cong \frac{-w_{i+1} + 4w_i - 3w_{i-1}}{2h} \quad , \quad r_{i-1}' \cong \frac{-r_{i+1} + 4r_i - 3r_{i-1}}{2h}$$

$$t_i' \cong \frac{t_{i+1} - t_{i-1}}{2h} \quad , \quad p_i' \cong \frac{p_{i+1} - p_{i-1}}{2h}$$

$$t_{i+1}' \cong \frac{3t_{i+1} - 4t_i + t_{i-1}}{2h} \quad , \quad p_{i+1}' \cong \frac{3p_{i+1} - 4p_i + p_{i-1}}{2h}$$

$$t_{i-1}' \cong \frac{-t_{i+1} + 4t_i - 3t_{i-1}}{2h} \quad , \quad p_{i-1}' \cong \frac{-p_{i+1} + 4p_i - 3p_{i-1}}{2h} \quad (16)$$

By using (16) the results in (15) become

$$W_i = f(x_i) - a_1(x_i)\frac{p_{i+1} - p_{i-1}}{2h} - a_2(x_i)p_i(x)$$

$$-a_3(x_i)\frac{t_{i+1} - t_{i-1}}{2h} - a_4(x_i)t_i - a_5(x_i)\frac{r_{i+1} - r_{i-1}}{2h} - a_6(x_i)r_i$$

$$-a_7(x_i)\frac{w_{i+1} - w_{i-1}}{2h} - a_8(x_i)w_i - a_9(x_i)\frac{v_{i+1} - v_{i-1}}{2h}$$

$$-a_{10}(x_i)v_i - a_{11}(x_i)\frac{u_{i+1}-u_{i-1}}{2h} - a_{12}(x_i)u_i$$

$$W_{i+1} = f(x_{i+1}) - a_1(x_{i+1})\frac{3p_{i+1}-4p_i+p_{i-1}}{2h} - a_2(x_{i+1})p_i(x)$$

$$-a_3(x_{i+1})\frac{3t_{i+1}-4t_i+t_{i-1}}{2h} - a_4(x_{i+1})t_i - a_5(x_{i+1})\frac{3r_{i+1}-4r_i+r_{i-1}}{2h}$$

$$-a_6(x_{i+1})r_i - a_7(x_{i+1})\frac{3w_{i+1}-4w_i+w_{i-1}}{2h} - a_8(x_{i+1})w_i$$

$$-a_9(x_{i+1})\frac{3v_{i+1}-4v_i+v_{i-1}}{2h} - a_{10}(x_{i+1})v_i$$

$$-a_{11}(x_{i+1})\frac{3u_{i+1}-4u_i+u_{i-1}}{2h} - a_{12}(x_{i+1})u_i$$

$$W_{i-1} = f(x_{i-1}) - a_1(x_{i-1})\frac{-p_{i+1}+4p_i-3p_{i-1}}{2h}$$

$$-a_2(x_{i-1})p_i(x) - a_3(x_{i-1})\frac{-t_{i+1}+4t_i-3t_{i-1}}{2h}$$

$$-a_4(x_{i-1})t_i - a_5(x_{i-1})\frac{-r_{i+1}+4r_i-3r_{i-1}}{2h} -$$

$$a_6(x_{i-1})r_i - a_7(x_{i-1})\frac{-w_{i+1}+4w_i-3w_{i-1}}{2h}$$

$$-a_8(x_{i-1})w_i - a_9(x_{i-1})\frac{-v_{i+1}+4v_i-3v_{i-1}}{2h}$$

$$-a_{10}(x_{i-1})v_i - a_{11}(x_{i-1})\frac{-u_{i+1}+4u_i-3u_{i-1}}{2h} - a_{12}(x_{i-1})u_i$$

$L_i = v_i$, $M_i = w_i$, $N_i = r_i$, $Q_i = t_i$, $R_i = p_i$

$L_{i+1} = v_{i+1}$, $M_{i+1} = w_{i+1}$, $N_{i+1} = r_{i+1}$, $Q_{i+1} = t_{i+1}$, $R_{i+1} = p_{i+1}$

$L_{i-1} = v_{i-1}$, $M_{i-1} = w_{i-1}$, $N_{i-1} = r_{i-1}$, $Q_{i-1} = t_{i-1}$,$R_{i-1} = p_{i-1}$ (17)

Substituting (17) in equations from (8) to (13) and simplifying we obtain

$$\left(-\frac{1}{h^2} + \frac{3\,\alpha a_1(x_{i-1})}{2h} + \frac{\beta a_1(x_i)}{h} - \frac{\alpha\, a_1(x_{i+1})}{2h} - \alpha a_2(x_{i-1})\right)p_{i-1}$$
$$+\left(\frac{2}{h^2} - \frac{2\,\alpha a_1(x_{i-1})}{h} + \frac{2\,\alpha\, a_1(x_{i+1})}{h} - 2\,\beta a_2(x_i)\right)p_i$$
$$+\left(-\frac{1}{h^2} + \frac{\alpha a_1(x_{i-1})}{2h} - \frac{\beta a_1(x_i)}{h} - \frac{3\,\alpha\, a_1(x_{i+1})}{2h} - \alpha a_2(x_{i+1})\right)p_{i+1}$$
$$+\left(\frac{3\,\alpha a_3(x_{i-1})}{2h} + \frac{\beta a_3(x_i)}{h} - \frac{\alpha\, a_3(x_{i+1})}{2h} - \alpha a_4(x_{i-1})\right)t_{i-1}$$
$$+\left(-\frac{2\,\alpha a_3(x_{i-1})}{h} + \frac{2\,\alpha\, a_3(x_{i+1})}{h} - 2\,\beta a_4(x_i)\right)t_i$$
$$+\left(\frac{\alpha a_3(x_{i-1})}{2h} - \frac{\beta a_3(x_i)}{h} - \frac{3\,\alpha\, a_3(x_{i+1})}{2h} - \alpha a_4(x_{i+1})\right)t_{i+1}$$
$$+\left(\frac{3\,\alpha a_5(x_{i-1})}{2h} + \frac{\beta a_5(x_i)}{h} - \frac{\alpha\, a_5(x_{i+1})}{2h} - \alpha a_6(x_{i-1})\right)r_{i-1}$$
$$+\left(-\frac{2\,\alpha a_5(x_{i-1})}{h} + \frac{2\,\alpha\, a_5(x_{i+1})}{h} - 2\,\beta a_6(x_i)\right)r_i$$
$$+\left(\frac{\alpha a_5(x_{i-1})}{2h} - \frac{\beta a_5(x_i)}{h} - \frac{3\,\alpha\, a_5(x_{i+1})}{2h} - \alpha a_6(x_{i+1})\right)r_{i+1}$$
$$+\left(\frac{3\,\alpha a_7(x_{i-1})}{2h} + \frac{\beta a_7(x_i)}{h} - \frac{\alpha\, a_7(x_{i+1})}{2h} - \alpha a_8(x_{i-1})\right)w_{i-1}$$

$$+\left(-\frac{2\,\alpha a_7(x_{i-1})}{h}+\frac{2\,\alpha\,a_7(x_{i+1})}{h}-2\,\beta a_8(x_i)\right)w_i$$
$$+\left(\frac{\alpha a_7(x_{i-1})}{2h}-\frac{\beta a_7(x_i)}{h}-\frac{3\,\alpha\,a_7(x_{i+1})}{2h}-\alpha a_8(x_{i+1})\right)w_{i+1}$$
$$+\left(\frac{3\,\alpha a_9(x_{i-1})}{2h}+\frac{\beta a_9(x_i)}{h}-\frac{\alpha\,a_9(x_{i+1})}{2h}-\alpha a_{10}(x_{i-1})\right)v_{i-1}$$
$$+\left(-\frac{2\,\alpha a_9(x_{i-1})}{h}+\frac{2\,\alpha\,a_9(x_{i+1})}{h}-2\,\beta a_{10}(x_i)\right)v_i$$
$$+\left(\frac{\alpha a_9(x_{i-1})}{2h}-\frac{\beta a_9(x_i)}{h}-\frac{3\,\alpha\,a_9(x_{i+1})}{2h}-\alpha a_{10}(x_{i+1})\right)v_{i+1}$$
$$+\left(\frac{3\,\alpha a_{11}(x_{i-1})}{2h}+\frac{\beta a_{11}(x_i)}{h}-\frac{\alpha\,a_{11}(x_{i+1})}{2h}-\alpha a_{12}(x_{i-1})\right)u_{i-1}$$
$$+\left(-\frac{2\,\alpha a_{11}(x_{i-1})}{h}+\frac{2\,\alpha\,a_{11}(x_{i+1})}{h}-2\,\beta a_{12}(x_i)\right)u_i$$
$$+\left(\frac{\alpha a_{11}(x_{i-1})}{2h}-\frac{\beta a_{11}(x_i)}{h}-\frac{3\,\alpha\,a_{11}(x_{i+1})}{2h}-\alpha a_{12}(x_{i+1})\right)u_{i+1}$$
$$=-\alpha f(x_{i-1})-2\beta f(x_i)-\alpha f(x_{i+1}) \qquad (18)$$

$$\frac{1}{h^2}(u_{i+1}-2u_i+u_{i-1})=\alpha v_{i+1}+2\beta v_i+\alpha v_{i-1} \qquad (19)$$

$$\frac{1}{h^2}(v_{i+1}-2v_i+v_{i-1})=\alpha w_{i+1}+2\beta w_i+\alpha w_{i-1} \qquad (20)$$

$$\frac{1}{h^2}(w_{i+1}-2w_i+w_{i-1})=\alpha r_{i+1}+2\beta r_i+\alpha r_{i-1} \qquad (21)$$

$$\frac{1}{h^2}(r_{i+1}-2r_i+r_{i-1})=\alpha t_{i+1}+2\beta t_i+\alpha t_{i-1} \qquad (22)$$

$$\frac{1}{h^2}(t_{i+1}-2t_i+t_{i-1})=\alpha p_{i+1}+2\beta p_i+\alpha p_{i-1} \qquad (23)$$

Equations (18) to (23) along with the boundary conditions (5) give a complete system of $6(n+1)$ linear equations in $6(n+1)$ unknowns, which can be obtained by applying simple numerical techniques.

4. NUMERICAL APPLICATIONS

In this section we test the performance of the method developed by solving two boundary value problems with step size $h=\frac{1}{5}$ and $h=\frac{1}{10}$. The numerical results have been presented in tables and the graphical results have been shown in fig.

Example 1

$$u^{(12)}(x)+xu(x)=-(120+23x+x^3)e^x\ ;\quad 0\le x\le 1$$

Subject to

$u(0)=0$, $u(1)=0$

$u^{(2)}(0)=0$, $u^{(2)}(1)=-4e$

$u^{(4)}(0)=-8$, $u^{(4)}(1)=-16e$

$u^{(6)}(0)=-24$, $u^{(6)}(1)=-36e$

$u^{(8)}(0)=-48$, $u^{(8)}(1)=-64e$

$u^{(10)}(0)=-80$, $u^{(10)}(1)=-100e$

Exact solution:

$u(x)=x(1-x)e^x;\quad 0\le x\le 1$

Example 2

$$u^{(12)}(x)-u(x)=-12(2x\,Cos\,x+11\,Sin\,x)\ ;\quad -1\le x\le 1$$

Subject to

$u(-1)=0$, $u(1)=0$

$u^{(2)}(-1)=-4\,Cos\,1-2\,Sin\,1$,

$u^{(2)}(1)=4\,Cos\,1+2\,Sin\,1$

$u^{(4)}(-1)=8\,Cos\,1+12\,Sin\,1$,

$u^{(4)}(1)=-8\,Cos\,1-12\,Sin\,1$

Graphical representation of absolute error in u_i in Fig. 1, in $u_i^{(2)}$ in Fig. 2, in $u_i^{(4)}$ in Fig. 3, in $u_i^{(6)}$ in Fig. 4, in $u_i^{(8)}$ in Fig. 5, in $u_i^{(10)}$ in Fig. 6, for Example 1.

Fig. 1.

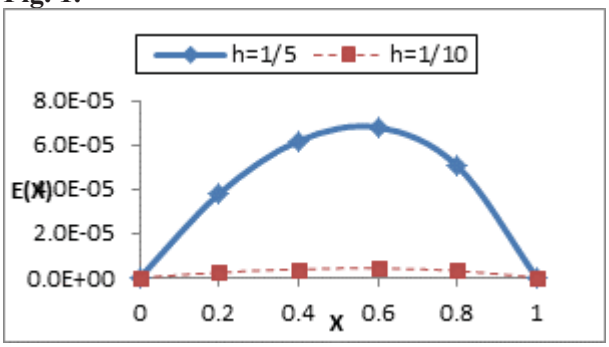

Fig. 2.

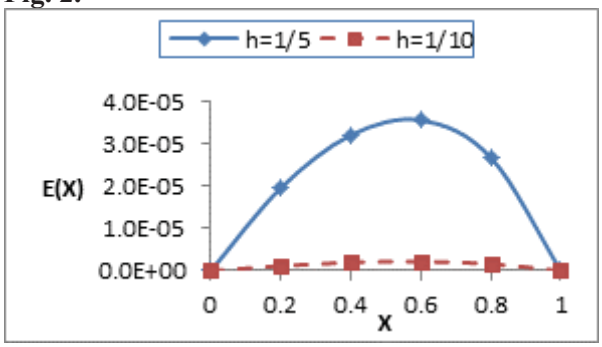

Fig. 3.

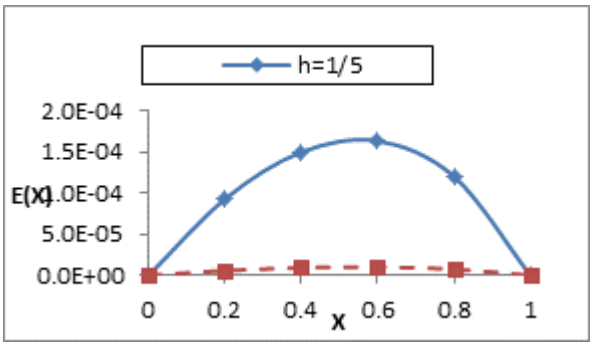

Fig. 4.

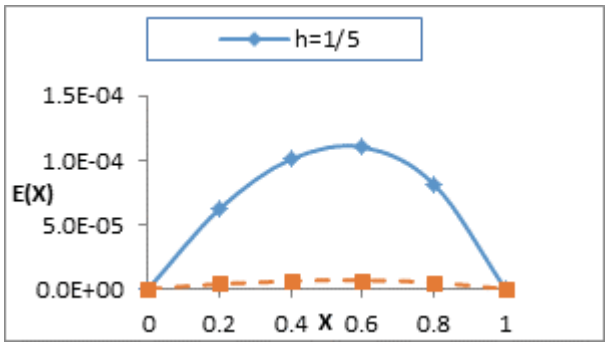

Fig. 5.

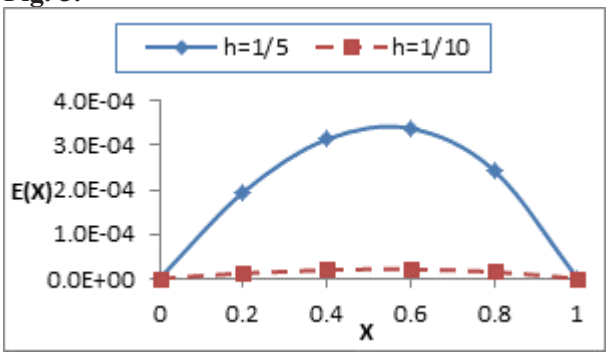

Fig. 6.

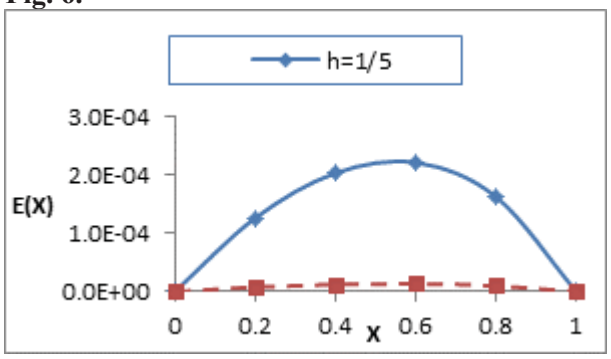

Graphical representation of absolute error in u_i in Fig. 7, in $u_i^{(2)}$ in Fig. 8, in $u_i^{(4)}$ in Fig. 9, in $u_i^{(6)}$ in Fig. 10, in $u_i^{(8)}$ in Fig. 11, in $u_i^{(10)}$ in Fig. 12, for Example 2.

Fig. 7.

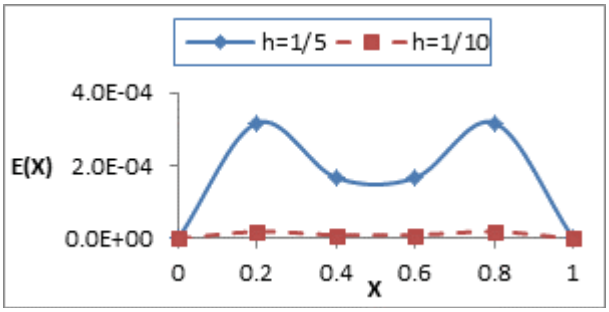

Fig. 8.

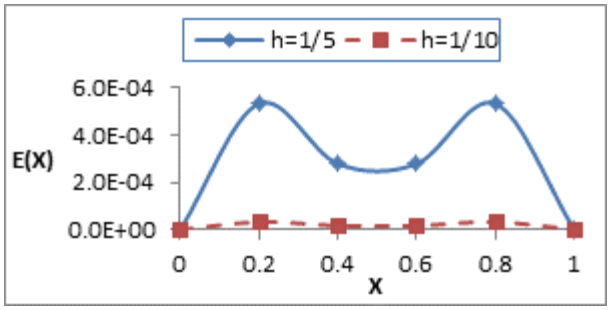

Fig. 9.

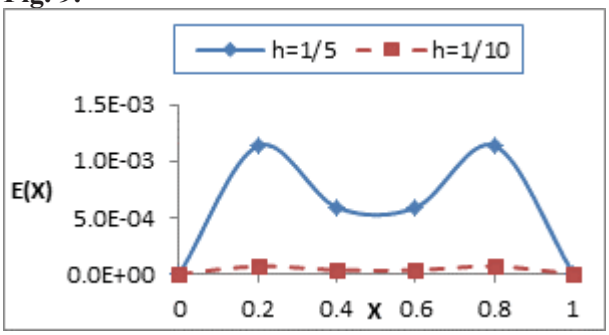

Fig. 10.

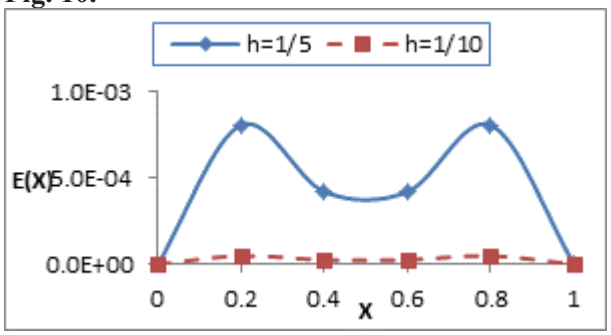

Fig. 11.

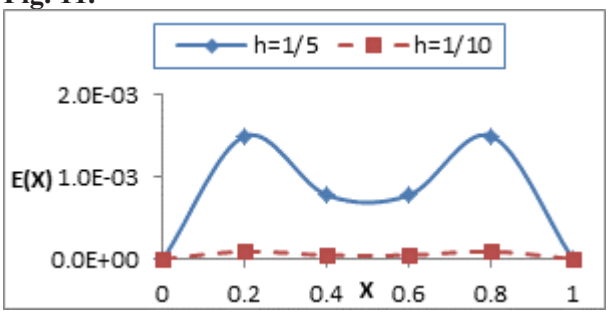

Fig. 12.

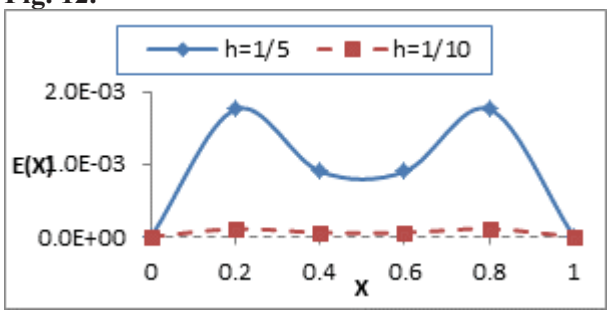

$u^{(6)}(-1) = -12\,Cos\,1 - 30\,Sin\,1,$

$u^{(6)}(1) = 12\,Cos\,1 + 30\,Sin\,1$

$u^{(8)}(-1) = 16\,Cos\,1 + 56\,Sin\,1,$

$u^{(8)}(1) = -16\,Cos\,1 - 56\,Sin\,1$

$u^{(10)}(-1) = -20\,Cos\,1 - 90\,Sin\,1,$
$u^{(10)}(1) = 20\,Cos\,1 + 90\,Sin\,1$

Exact solution:

$u(x) = (x^2 - 1)\,Sin\,x\ ; \qquad -1 \le x \le 1$

Numerical results are shown in the table 1 to 4 for the two test problems. An improvement in the results has seen as reflected in the reduction in the absolute error for $h = \frac{1}{5}$ and $h = \frac{1}{10}$.

Table 1. Absolute error comparison in Example 1.

x_i	u_i		$u_i^{(2)}$	
	$h = 1/5$	$h = 1/10$	$h = 1/5$	$h = 1/10$
0.0	0	0	0	0
0.2	1.9649E-05	1.2309E-06	3.8072E-05	2.3841E-06
0.4	3.2198E-05	2.0169E-06	6.1887E-05	3.8753E-06
0.6	3.5765E-05	2.2403E-06	6.8035E-05	4.2603E-06
0.8	2.6881E-05	1.6838E-06	5.0521E-05	3.1635E-06
1.0	0	0	0	0

Table 2. Absolute error comparison in Example 1.

x_i	$u_i^{(4)}$		$u_i^{(6)}$	
	$h = 1/5$	$h = 1/10$	$h = 1/5$	$h = 1/10$
0.0	0	0	0	0
0.2	6.2358E-05	3.9042E-06	9.2847E-05	5.8124E-06
0.4	1.0093E-04	6.3193E-06	1.4988E-04	9.3830E-06
0.6	1.1035E-04	6.9091E-06	1.6327E-04	1.0221E-05
0.8	8.1418E-05	5.0974E-06	1.1991E-04	7.5068E-06
1.0	0	0	0	0

Table 3. Absolute error comparison in Example 1.

x_i	$u_i^{(8)}$		$u_i^{(10)}$	
	$h = 1/5$	$h = 1/10$	$h = 1/5$	$h = 1/10$
0.0	0	0	0	0
0.2	1.2622E-04	7.9009E-06	1.9465E-04	1.2185E-05
0.4	2.0335E-04	1.2729E-05	3.1398E-04	1.9654E-05
0.6	2.2136E-04	1.3857E-05	3.3847E-04	2.1186E-05
0.8	1.6263E-04	1.0180E-05	2.4381E-04	1.5261E-05
1.0	0	0	0	0

Table 4. Absolute error comparison in Example 2.

x_i	u_i		$u_i^{(2)}$	
	$h = 1/5$	$h = 1/10$	$h = 1/5$	$h = 1/10$
0.0	0	0	0	0
0.2	3.1687E-04	1.9635E-05	5.3323E-04	3.3071E-05
0.4	1.6698E-04	1.0347E-05	2.7953E-04	1.7337E-05
0.6	1.6698E-04	1.0347E-05	2.7953E-04	1.7337E-05
0.8	3.1687E-04	1.9635E-05	5.3323E-04	3.3071E-05
1.0	0	0	0	0

Table 5. Absolute error comparison in Example 2.

x_i	$u_i^{(4)}$		$u_i^{(6)}$	
	$h = 1/5$	$h = 1/10$	$h = 1/5$	$h = 1/10$
0.0	0	0	0	0
0.2	8.0637E-04	5.0039E-05	1.1347E-03	7.0442E-05
0.4	4.2137E-04	2.6148E-05	5.9151E-04	3.6721E-05
0.6	4.2137E-04	2.6148E-05	5.9151E-04	3.6721E-05
0.8	8.0637E-04	5.0039E-05	1.1347E-03	7.0442E-05
1.0	0	0	0	0

Table 6. Absolute error comparison in Example 2.

x_i	$u_i^{(8)}$		$u_i^{(10)}$	
	$h = 1/5$	$h = 1/10$	$h = 1/5$	$h = 1/10$
0.0	0	0	0	0
0.2	1.5025E-03	9.3312E-05	1.7548E-03	1.0900E-04
0.4	7.8043E-04	4.8468E-05	8.9833E-04	5.5803E-05
0.6	7.8043E-04	4.8468E-05	8.9833E-04	5.5803E-05
0.8	1.5025E-03	9.3312E-05	1.7548E-03	1.0900E-04
1.0	0	0	0	0

5. CONCLUSIONS

The twelfth order boundary value problems have rare numerical solution in literature, so it is important to find reliable numerical technique for solving these problems. Approximate solutions of the twelfth order BVPs have been obtained by using the non-polynomial spline method. The method is applied on two test problems and the results obtained are sufficiently accurate and encouraging, reflecting the validity of the developed method. Richardson's extrapolation can be employed along with the proposed method to further enhance its validity.

6. REFERENCES

1. Chandrasekhar. *Hydrodynamic and Hydromagnetic Stability*. Clarendon Press, Oxford, England (1961).
2. Twizell, E.H. & A. Boutayeb. Numerical methods for eighth, tenth and twelfth-order eigenvalue problems arising in thermal instability. *Advances in Computational Mathematics* 2: 407-436 (1994).
3. Siddiqi, S.S. & E.H. Twizell. Spline solutions of linear twelfth-order boundary value problems. *Journal of Computational* & *Applied Mathematics* 78: 371-390 (1997).
4. Siddiqi, S.S. & E.H. Twizell. Spline solutions of linear tenth-order boundary value problems. *Journal of Computational* & *Applied Mathematics* 68: 345-362 (1998).
5. Alberg J.H. & T. ItO. A collocation method for two-point boundary value problems. *Mathematics of Computation* 29: 761-776 (1975).
6. Usmani, R.A. The use of quartic splines in the numerical solution of a fourth order boundary value problem. *Journal of Computational* & *Applied Mathematics* 44: 187-199 (1992).
7. Siraj-ul-Islam, M.A. Noor, I.A. Tirmizi & M.A. Khan. Quadratic non-polynomial spline approach to the solution of a system of second order boundary value problems. *Applied Mathematics* & *Computation* 179: 153-160 (2006).
8. Caglar, S.H & M.F. Ucar. Non-polynomial spline method for a time-dependent heat-lime Lane-Emden equation. *Acta Physica Polonica A*. 121: 262-264 (2012).
9. Papamichael, N. & A.J. Worsey. A cubic spline method for the solution of a linear fourth-order boundary value problems. *Journal of Computational* &. *Applied Mathematics* 7: 187-189 (1981).
10. Omotayo, A.T. & O.M. Oguniaran. A non-polynomial spline method for solving linear fourth-order boundary value problems. *International Journal of the Physical Sciences* 6: 3246-3254 (2011).

Proceedings of the Pakistan Academy of Sciences 51 (2): 167–176 (2014)

ISSN: 0377 - 2969 (print), 2306 - 1448 (online)

Pakistan Academy of Sciences

Research Article

Assessment of Spectral, Electrical and Physical Properties of Polyaniline-dodecylbenzenesulfonic Acid Salts

Salma Gul[1], Anwar-ul-Haq Ali Shah[2] and Salma Bilal[1*]

[1]National Centre of Excellence in Physical Chemistry, University of Peshawar, Peshawar, Pakistan

[2]Institue of Chemical Sciences, University of Peshawar, Peshawar, Pakistan

Abstract: In the present study some results related to various properties polyaniline salt synthesized via inverse emulsion polymerization pathway [1] has been discussed. The synthesized PANI salt was found to be completely soluble in tetrahydrofuran (THF), dimethyl sulfoxide (DMSO), dimethylformamide (DMF), chloroform and in a mixture of toluene and 2-propanol. The synthesized polymer salt was also further characterized with cyclic voltammetry (CV), scanning electron microscope (SEM), X-ray diffraction (XRD), UV-vis spectroscopy and viscosity measurements. Thermogravimetric analysis (TGA) was used to analyze the thermal properties of synthesized polymer. The extent of doping of the PANI salt was determined from UV-vis spectra and TGA analysis. The activation energy for the degradation of the polymer was calculated with the help of TGA.

Keywords: Polyaniline (PANI), Intrinsically conducting polymers, PANI-DBSA salt, common organic solvents, CV, SEM, XRD, UV-Vis spectroscopy

1. INTRODUCTION

Intrinsically conducting polymers (ICPs) have generated a tremendous interest due to interesting electrical and optical properties [2]. Among often studied ICPs like polyacetylene, polyaniline (PANI), polythiphene, polypyrrole, poly(paraphenylene vinylene), polyaniline is particularly attractive because of its ease of synthesis with high yield, the good environmental stability and the ability to reversibly tune its conductivity to any value from the insulating to metallic regime [3]. There are four principal oxidation states of PANI. Among them leucoemeraldine (fully reduced), emeraldine (half reduced and half oxidized), pernigraniline (fully reduced) are insulating while emeraldine salt is the only conducting state of PANI [4, 5]. This polymer can be applied to batteries [6, 7], anion exchanger [8, 9], tissue engineering [10], inhibition of steel corrosion [11], sensors [12, 13] and so on.

PANI can be synthesized through either electrochemical or chemical polymerization [14]. The latter one is of particular importance since this process is the most feasible route for the production of PANI on large scale [15]. However, like other ICPs, PANI also exhibit poor thermal stability and poor processability in common organic solvents which limit its various technological applications. Numerous methods have been developed to overcome these shortcomings. These include the use of substituted aniline as monomer, synthesis of co-polymers and synthesis of PANI by emulsions/ inverse emulsions polymerization [16]. Cao et a.[17] used dodecylbenzene sulfonic acid (DBSA) and dinonylnaphthalinic acid (DNNSA) as dopant for improvement of processability. However, the PANI salts produced were partially soluble in organic solvents [18].

In order to fulfill this goal, we started a systematic

Received, April 2012; Accepted, May 2014
* Corresponding author: Salma Bilal; Email: anw_sk@yahoo.com

study aimed at establishing effective polymerization pathway for the synthesis of processable polyaniline. Recently, we developed a novel method for synthesis of completely soluble and highly thermally stable polyaniline- dodecylbenzene sulfonic acid (PANI-DBSA) salts [1]. The purpose of present study was to analyze these polymers by various testing techniques to further assess its spectral, electrical and physical properties.

2. MATERIALS AND METHODS

Reagent grade Aniline (Acros, USA) was distilled under vacuum, the resulting colorless liquid was stored under nitrogen. Chloroform (Scharlau, Spain), Benzoyl Peroxide (Merck, Germany), 2-Butanol (Aldrich, Italy), DBSA (Acros, USA), 2-Propanol (Merck, Germany), Toluene (Scharalau, Spain), Tetrahydrofuran (Scharalau, Spain) were used as received.

The polyaniline-dodecylbenzenesulfonic acid salts were synthesized via pathway reported elsewhere [1]. In a typical experiment desired amount of chloroform was taken in a 100 mL round bottom flask. Then benzoyl peroxide was added to it under mechanical stirring. To this solution 2-butanol, DBSA, and aniline were added. The resulting mixture of deionized water (Millipore) was added to form a milky white emulsion. The mixture turned green in 5 hours and polymerization reaction was allowed to proceed for 24 hours. In the end the organic phase containing polyaniline salt was separated and washed four times with 50 mL of acetone. After thorough washing, a dark green highly concentrated polyaniline salt was obtained. Then it was dried at room temperature for 24 hours in a Petri dish. On addition of small amount of acetone to the Petri dish the film broke into flakes. Then PANI-DBSA salt was separated by filtration and dried in a desiccator. Prior to this the experimental conditions were optimized by stepwise changing concentration of oxidants, monomer and surfactant. The polymers obtained with the varying amount of aniline were labeled as sample 1, sample 2, sample 3 and sample 4 where the aniline concentrations were 5.36×10^{-4}, 6.52×10^{-4}, and 7.66×10^{-4} and 8.18×10^{-3} mol, respectively. Similarly, the samples with different concentrations of benzoyl peroxide were named as sample 5, sample 6, and sample 7 when the concentrations of benzoyl peroxide were 4.17×10^{-4}, 1.25×10^{-3} and 2.08×10^{-3} mol, respectively. Sample 8, 9 and 10 represent polymers with 3.73×10^{-3}, 4.35×10^{-3} and 4.97×10^{-3} mol of DBSA respectively.

2.1 Characterization

Percent yield of PANI-DBSA was calculated by using following formula [19].

$$\text{Percent yield} = \frac{\text{weight of PANI} - \text{DBSA}}{\text{weight of xM aniline} + \text{weight of xM DBSA}} \text{ X } 100$$

Viscosities of PANI-DBSA were determined using capillary viscometer. Intrinsic viscosity [η] was obtained by linearly extrapolating the line of specific viscosity divided by the c (η_{sp}/c) vs c and the line of the natural logarithm of relative viscosity divided by c (ln η_{rel}/ c) vs c to the same intercept at zero concentration [20].

CV was recorded in 0.5 M H_2SO_4 in a three electrode cell, using bipotentiostat Model 2323. In this system gold disk electrode was used as working electrode. PANI dissolved in tetrahydrofuran (THF) was dip-coated onto this electrode. Saturated calomel electrode and a platinum coiled wire were used as reference and as counter electrode, respectively. UV-vis spectra were obtained using Perkin Elmer 650 (UK) spectrophotometer. A quartz cell of 1cm path length was used for recording spectra of different samples of PANI-DBSA dissolved in different solvents. The morphology of PANI-DBSA was done by using a JSM5910 (JEOL Japan) scanning electron microscope (SEM). Powder material was deposited on adhesive tape fixed to stub and then coated with gold by sputter coater prior to SEM measurements. X ray diffraction patterns were recorded by using Rigaku (Japan) X-ray diffractometer using Cu Kα radiations of wavelength 1.5405 A°) with a continuous scan speed of 0.05°/s. The diffraction patterns were collected between 2 - 65°.

Thermal analysis of the polymer was carried out by using Perkin Elmer Diamond series TG/ DTA 1300 °C (USA) at a heating rate 10°/min in the presence of N_2 atmosphere.

3. RESULTS

3.1. Yield of PANI-DBSA

The inverse emulsion polymerization reaction of aniline was carried out by varying the amount of

benzoyl peroxide, aniline and surfactant. At first for low concentration of aniline no product was obtained, attained a maximum value at 5.36 x 10^{-4} mol and then decreased with further increasing the monomer concentration. Similar observations were obtained with benzoyl peroxide and surfactant concentration. The results are represented in Table 1.

Table 1. Percent yield of PANI-DBSA.

S. No.	Sample Code	% Yield
1	1	21.2
2	2	9.8
3	3	9.7
4	4	8.6
5	5	0
6	6	21.2
7	7	0
8	8	21.2
9	9	16.3
10	10	17.1

3.2. Solubility

The synthesized PANI-DBSA was completely soluble in mixture of toluene and 2-propanol and chloroform. The polymers were also found to be soluble in THF, DMSO and DMF [1].

3.3. Intrinsic Viscosity

The viscosity plots of polyaniline salts are given in Fig.1. It was observed that intrinsic viscosity of PANI-DBSA decreased with increasing monomer concentration in the order of 33.13 > 23.86 > 22.74 > 20 for sample 1, 2, 3 and 4, respectively.

3.4 Cyclic Voltammetry (CV)

The redox property of the synthesized PANI-DBSA was investigated by cyclic voltammetry. Fig. 2. shows the representative CV of sample 1 showing two redox peaks. The first redox peak around E_{SCE} = 0.2 V was assigned to the transition of leucoemeraldine to emeraldine state and the second peak around E_{SCE} 0.6V was due to the emeraldine to pernigraniline transition. These peaks confirmed the electroactivity of the synthesized polymer [21].

3.5 UV-Vis Spectrum

UV-vis spectrum of PANI-salt was recorded by diluting the sample in tetrahydrofuran. The

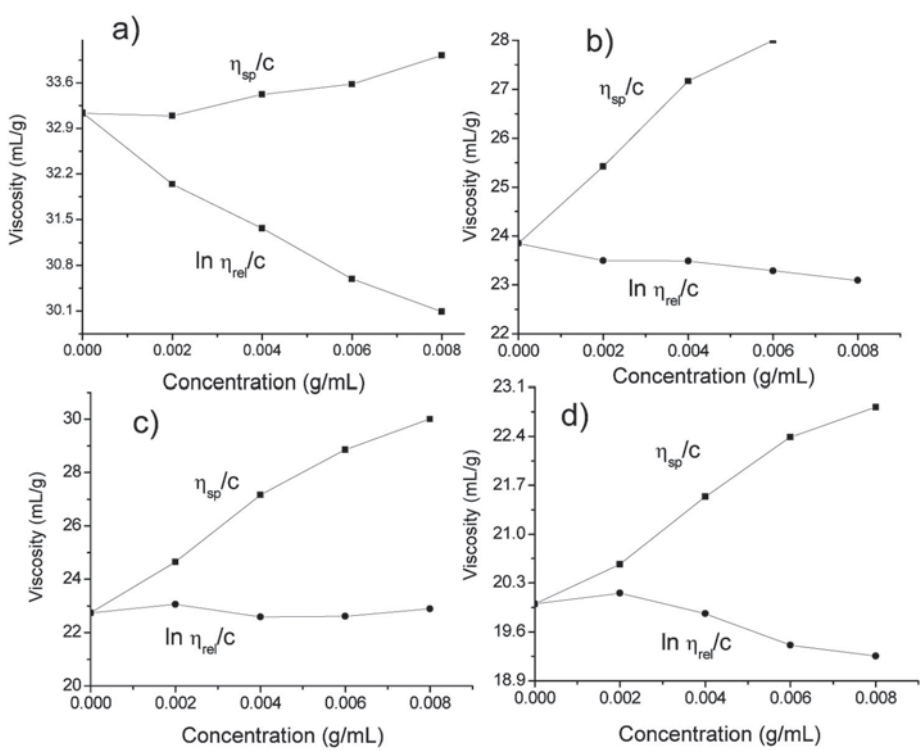

Fig. 1. Viscosity vs concentration plots for determination of intrinsic viscosity of polyaniline salt for a) Sample 1, b) Sample 2, c) Sample, 3 d) Sample 4.

spectrum given in Fig.3 showed three characteristic peaks. The first band was observed at around 338 nm, the second at 428 nm and third peak was observed at 801 nm.

3.5.1 Extent of Doping

The extent of doping can be estimated from the absorption spectra of PANI in which the exiton (π-polaron transition)/ benzenoid (π-π* transition) ratio indicates the doping level [22]. It is seen from the Table 2 that sample 1 has the biggest ratio among all sample which means that doping level of sample 1 is higher than the others.

Table 2. Absorption ratio exiton/benzenoid (E/B) for different concentrations of aniline.

S. No.	Sample Code	E/B
1	1	2.47
2	2	2.36
3	3	2.28
4	4	2.26

3.6 X-ray Diffraction of PANI-DBSA

XRD is extensively used in material identification. It is a non destructive, very simple and rapid technique for powder and other microcrystalline samples. The XRD patterns of PANI-DBSA are shown in Fig. 4 which demonstrates the characteristic peaks at 2θ = 2.5°, 19°, 20° and 25°.

3.7. Thermogravimetry of PANI-DBSA

The results of the TGA of PANI-DBSA are given in Fig.5. The DBSA doped polyaniline salts synthesized at room temperature showed three main weight loss stages. The first step weight loss was of about 5-12%. The second step weight loss being in the range 48-66 %. A slow and somewhat gradual weight loss was observed for these polymers at around 500°C.

3.7.1 Activation Energy for the Degradation of PANI-DBSA

According to Chan et al. [23] a plot of (ln k/w) versus 1/T gives a straight line with the slope equal to –Ea / R

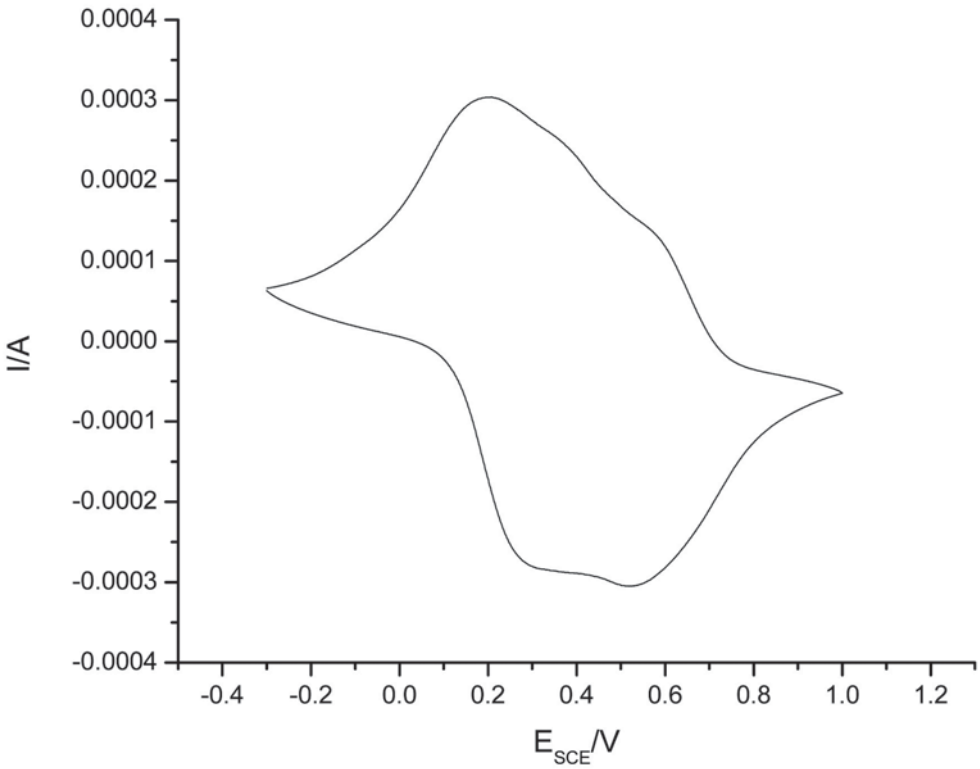

Fig. 2. Cyclic voltammogram of sample 1 on a gold disc electrode (vs SCE) in solution of 0.5 **M** H_2SO_4.

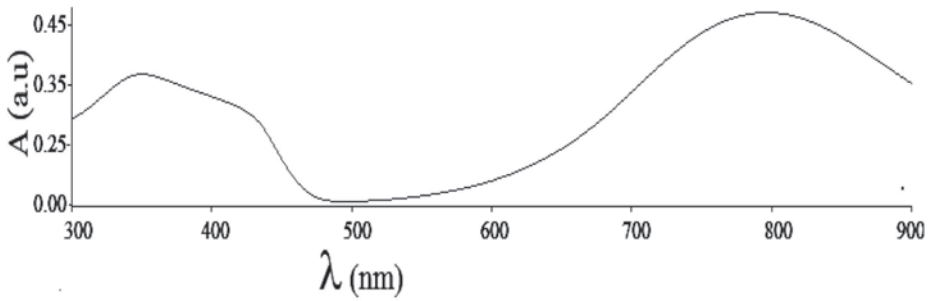

Fig. 3. UV-Vis spectrum of polyaniline salt recorded in tetrahydrofuran.

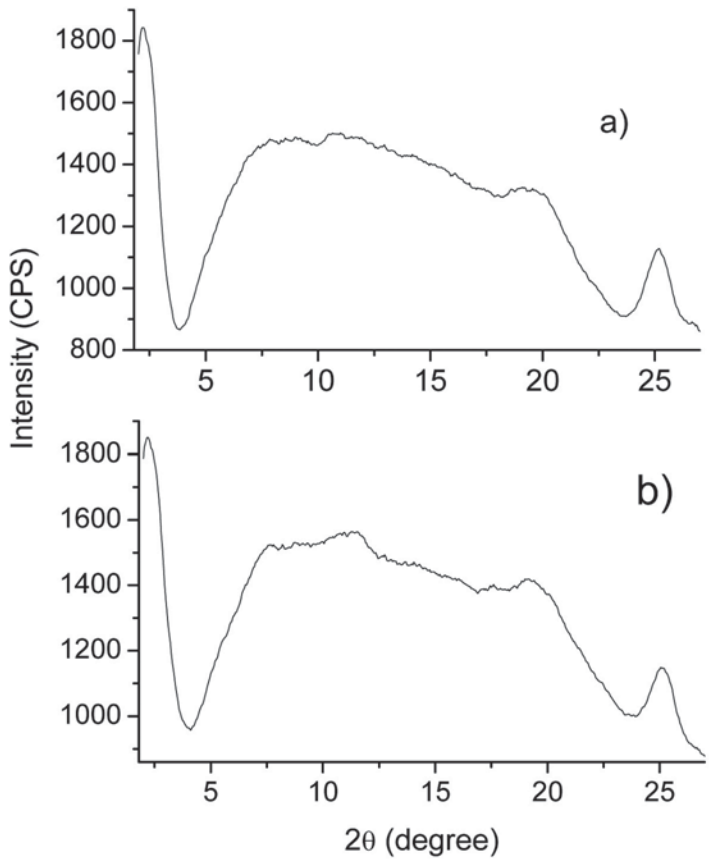

Fig. 4. X-ray diffraction patterns of polyaniline salts (a) Sample 1, (b) Sample 4.

Where

k = rate of weight loss [ln%(orginal wt) min^{-1}) at temperature T

w = corresponding weight [ln% (original wt) of the polymer remaining.

From the slope (-Ea/R) of this plot activation energy for the degradation of polymer can be calculated. Fig. 6 shows the plots obtained from kinetic analysis of TGA data of PANI doped with DBSA and activation energy calculated from these plots is 55.39kJ/mol, 81.67kJ/mol, 92.43kJ/mol and 76.75kJ/mol for sample 1, 2, 3 and 4, respectively.

3.8 Morphology of PANI-DBSA

The morphology of PANI-DBSA was obtained from scanning electron microscope. The result is presented in Fig. 7 showing aggregated granular morphology.

4. DISCUSSION

There have been several reports on the polymerization mechanism of polyaniline [24,

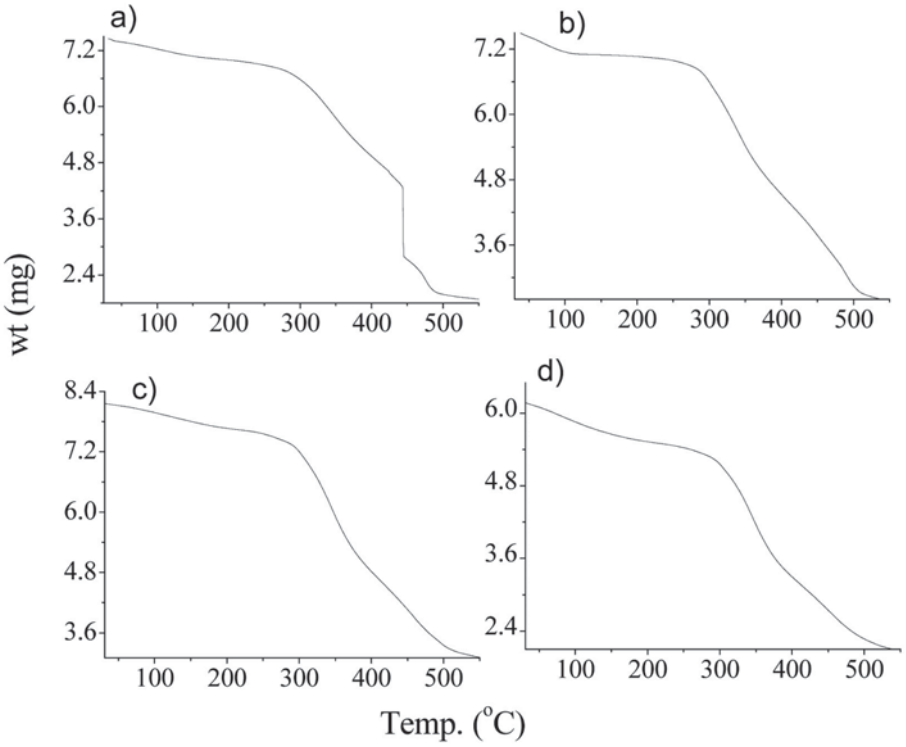

Fig. 5. Thermogravimetric curves for polyaniline salts a) Sample 1, b) Sample 2, c) Sample, 3 d) Sample 4.

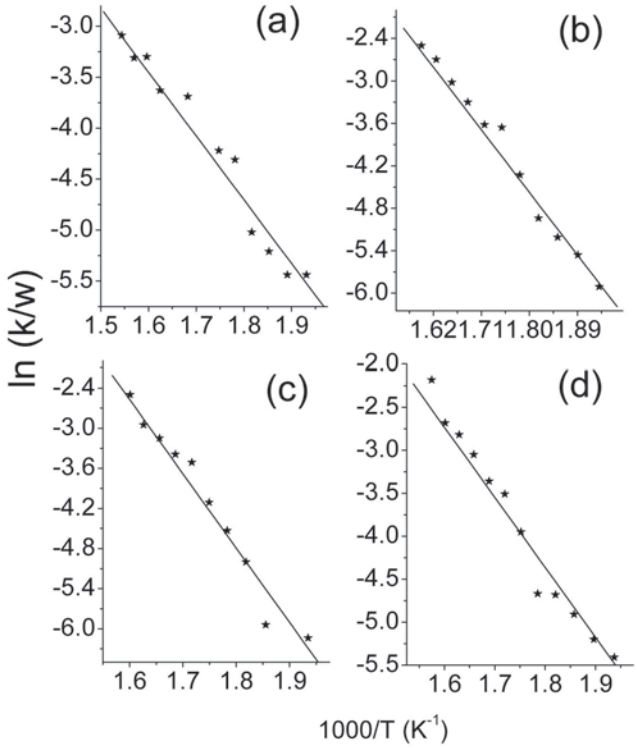

Fig. 6. Calculation of activation energy for polyaniline salts a) Sample 1, b) Sample 2, c) Sample, 3 d) Sample 4.

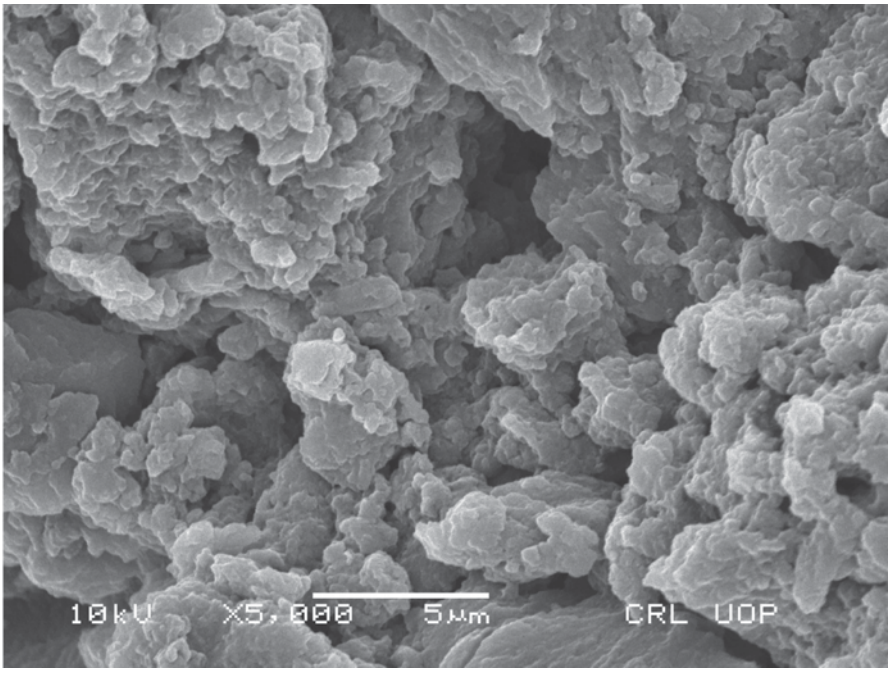

Fig. 7. Scanning electron micrograph of polyaniline salt.

25, 26]. In the first step oxidation of aniline into a radical cation takes place by an oxidant. The second step involves the formation of the intermediately oxidized nitrenium cation by losing one proton. Continuous combination of these intermediates leads to the formation of PANI. In this study aniline is oxidized by benzoyl peroxide which further makes PANI chain as shown in scheme 1.

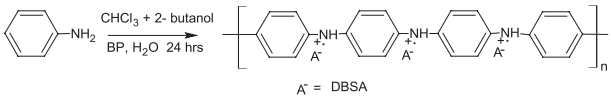

Scheme 1. PANI-DBSA

After successful synthesis, the reaction parameters were optimized by changing the reactant concentrations in the feed. The observed change in the yield of the product with different parameters may be due to over oxidation process or may be that the kinetic effects were favored in the oxidation of aniline [27]. Generally, soluble PANI exhibits low % yield. Dan and Sengupta [28] prepared soluble polyaniline in formic acid media but they obtained very low yield i.e. 7.8% and 6.9 %. The high % yield results in the present case reveal that the soluble polymers were successfully prepared with quite high yield [1].

All these PANI salts are highly soluble in common organic solvent due to proper incorporation of DBSA moieties in its backbone. Indeed, the large sized organic sulfonic acids (DBSA) have a good solubility and processability in common organic solvents. It is due to enlarge interchain distance, which means weaker interchain reaction and strong interaction between dopant and solvent [29].

These PANI salts were systematically characterized by various techniques to investigate their properties. It is seen that with increasing concentration in the feed the intrinsic viscosity decreases. The results are in accordance with Dan and Sengupta [28]. They concluded that the dropping trend in the intrinsic viscosity is due to the direct consequence of rapid lowering in initiator efficiency.

UV-vis spectrum showed three characteristic peaks. The results are similar to Han et al [22]. They assigned the first absorption band at 338 nm to π-π* electron transition within benzoid (B) ring. The second and third at around 428 and 801 nm, respectively, is attributed to the polaron-transitin and bipolaron transition respectively. The last two bands relates to the doping level and formation of polaron lattice. The results support the formation of

PANI-DBSA salt. The calculation of doping level demonstrates that the concentration of aniline plays an important role in the synthesis of PANI-DBSA.

The XRD patterns of PANI-DBSA observed in Fig. 4 show the characteristic peaks of PANI-DBSA. The peaks from 20° to 27° are ascribed to the momentum transfer and periodicity and perpendicular to the chain direction [30, 31]. The peaks at 2Θ ≈ 19° and another one at 2Θ ≈ 25° are characteristics of van der waals distances between aliphatic chain and between stakes of phenylene rings respectively [32, 33]. The peak at 2.5° observed in both sample 1 and 4, showed the well organized layered structure in which stacks of charged aniline backbone are uniformly spaced by the alkyl tails of DBSA [34]. All peaks are observed at lower value of 2Θ indicating the better crystallinity [1, 35]. SEM study revealed the typical granular morphology of these PANI salts [36, 37]. It is seen in the TGA study that the DBSA doped polyaniline salts showed three main weight loss stages. The first step weight loss of about 6-13% is associated with the loss of moisture. PANI always shows high moisture loss because it is highly hygroscopic in nature and some moisture still remains even after vaccume drying [38]. The second step weight loss being in the range 47-65%, is attributed to destroy of the NH^{+}…..SO^{-}_{3} interaction between the PANI chain and the DBSA dopant with degradation of DBSA [39]. A slow and gradual weight loss was observed for these polymers at around 500°C, is due to the structure decomposition of PANI backbone. This is quite high temperature for its degradation compared to the reported literature. Chen [40] found that the degradation temperature of ES form of PANI was lower (around 360-410 °C) than that of the EB form (around 420-450°C). Svelko et al [41] prepared PANI in the presence of non-ionic surfactants which was stable upto 400°C. Jayakkannan et al [42] synthesized azobenzenesulfonic acids doped PANI which was stable upto 300°C. In present study high thermal stability up to about 500°C was achieved which presents effectiveness of polymerization pathway [1]. The PANI-DBSA salts were not completely destroyed because in nitrogen atmosphere carbonization of polymer takes place leaving a marked residue [43]. It was found that among all samples, Ea is highest for sample 3. Therefore it is thermally more stable. These results show that DBSA doped PANI material is highly stable and can be used for various high temperature applications.

5. CONCLUSIONS

In this study, PANI- DBSA salts were successfully prepared from DBSA reversed micelle solution. High yield of PANI was obtained by optimizing reaction conditions. The characterizations of PANI-DBSA revealed comparable or preferable properties i.e. percent yield, solubility, crystallinity, electrochemical activity, thermal stability and intrinsic viscosity with the products obtained from other approaches. Thus this inverse emulsion polymerization is a feasible and attractive approach to prepare processable PANI- DBSA salts with a number of valuable chemical properties which may be used for various technological applications.

6. ACKNOWLEDGEMENTS

Financial support of the Higher Education Commission, Islamabad, Pakistan is acknowledged gratefully.

7. REFERENCES

1. Bilal, S, S. Gul, K. Ali & A.A. Shah. Synthesis and characterization of completely soluble and highly thermally stable PANI-DBSA salts. *Synthetic Metals* 162: 2259-2266 (2012).
2. Nabid, M.R., Z. Zamiraei, R. Sedghi & N. Safari. Cationic metaloporphyrins for synthesis of conducting, water-soluble polyaniline. *Reactive and Functional Polymers* 69: 319-324 (2009).
3. Yang, J., Y. Ding, G. Chen, & C. Li. Synthesis of conducting polyaniline using novel anionic gemini surfactant as micellar stabilizer. *European Polymer Journal* 43: 3337-3343 (2007).
4. Gettinger, C.L., A.J. Heeger, D.J. Pin, & Y. Cao. Solution characterization of surfactant solubilized polyaniline. *Synthetic Metals* 74: 81-88 (1995).
5. Hassan, P.A., S.N. Sawant, N.C. Bagkar & J.V. Yakhmi. Polyaniline nanoparticles prepared in rodlike micelles. *Langmuir* 20: 4874-4880 (2004).
6. Xiao, L., Y. Cao, J. Xiao, B. Schwenzer, M.H. Engelhard, L.V. Saraf, Z. Nie, G.J. Exarhos & J. Liu. A Soft Approach to encapsulate sulfur: polyaniline nanotubes for lithium-sulfur batteries with long cycle life. *Advanced Materials* 24: 117-1181 (2012).

7. Ghenaatiana, H.R., M.F. Mousavia, & M.S. Rahmanifar. High performance battery supercapacitor hybrid energy storage system based on self-doped polyaniline nanofibers. *Synthetic Metals* 161: 2017-2023 (2011).
8. Ansari, R. Application of polyaniline and its composites for adsorption/recovery of chromium (VI) from aqueous solutions. *Acta Chimica Slovenica* 53: 88-94 (2006).
9. Ghorbani, M., H. Esfandian, N. Taghipour, & R. Katal. Application of polyaniline and polypyr role composites for paper mill wastewater treatment. *Desalination* 263: 279-284 (2010).
10. Li, M., Y. Guo, Y. Wei, A.G. MacDiarmid, & P.I. Lelkes.Electrospinning polyaniline-contained gelatin nanofibers for tissue engineering applications. *Biomaterials* 27: 2705-2715 (2006).
11. El-Shazly, A.H. & H.A. Al-Turaif. Improving the corrosion resistance of buried steel by using polyaniline coating. *International Journal of Electrochemical Science* 7: 211-221 (2012).
12. Liu, C., K. Hayashi & K. Toko. Au nanoparticles decorated polyaniline nanofiber sensor for detecting volatile sulfur compounds in expired breath. *Sensors and Actuators B: Chemical* 161: 504-509 (2012).
13. Srivastavaa, S., S.S. Sharma, S. Agrawala, S. Kumara, M. Singha & Y.K. Vijay. Study of chemiresistor type CNT doped polyaniline gas sensor. *Synthetic Metals* 160: 529-534 (2010).
14. Palaniappan, S. Benzoyl peroxide oxidation route to polyaniline salts-Part I. *Polymers of Advanced Technologies* 15: 111-117 (2004).
15. Cao, Y., A. Andreatta, A. J. Heeger, & P. Smith. Influence of chemical polymerization conditions on the properties of polyaniline. *Polymer* 30: 2305-2311 (1989).
16. Palaniappan, S. & A. John. Polyaniline materials by emulsion polymerization pathway. *Progress in Polymer Science* 33: 732-758 (2008).
17. Cao, Y., P. Smith & A.J. Heeger. Counter-ion induced processsibility of conducting polyaniline and of conducting polyblends of polyaniline in bulk polymers. *Synthetic Metals* 48: 91-97 (1992).
18. Kinlen, P.J., J. Liu, Y. Ding, C.R. Graham & E.E. Remsen. Emulsion polymerization process for organically soluble and electrically conducting polyaniline. *Macromolecules* 31: 1735-1744 (1998).
19. Shreepathi, S. & R. Holze. Spectroelectro-chemistry and preresonance raman spectroscopy of polyaniline-dodecylbenzenesulfonic acid colloidal dispersions. *Langmuir* 22: 5196-5204 (2006).
20. Yang, J, & B. Weng. Inverse emulsion polymerization for high molecular weight and electrical ly conducting polyanilines. *Synthetic Metals* 159: 22249-2252 (2009).
21. Shreepathi, S. & R. Holze. Spectroelectrochemical investigations of soluble polyaniline synthesized via new inverse emulsion pathway. *Chemistry of Materials* 17: 4078-4085 (2005).
22. Han, Y-G., T. Kusunose & T. Sekino. One-step reverse micelle polymerization of organic dis persible polyaniline nanoparticles *Synthetic Metals* 159: 123-131 (2009).
23. Chan, H.S.O., P.K. H. Ho, E. Khor & M.M. Tan. Preparation of polyaniline doped in mixed protonic acids: their characterization by X-ray photoelectron spectroscopy and thermogravimetry. *Synthetic Metals* 31: 95-108 (1989).
24. Wei, Y., X. Tang, Y. Sun, & W. W. Focke. A study of the mechanism of aniline polymerization. *Journal of Polymer Science Part A: Polymer Chemistry* 27: 138-2396 (1989).
25. Ding, Y., A.B. Padias, H.K. Hall & Jr. Chemical trapping experiments support a cation-radical mechanism for the oxidative polymerization of aniline. *Journal of Polymer Science Part A: Polymer Chemistry* 37: 2569- 2579 (1999).
26. 29. Kim, J., S. Kwon & D.W. Ihm. Synthesis and characterization of organic soluble polyaniline prepared by one-step emulsion polymerization. *Current Applied Physics 7:* 205-210 (2007).
27. Palaniappan, S. & C.A. Amarnath. A novel polyaniline– maleicacid–dodecylhydrogensulfatesalt: Soluble polyaniline powder. *Reactive and Functional Polymers* 66: 1741-1748 (2006).
28. Dan, A. & P.K. Sengupta. Synthesis and characterization of polyaniline prepared in formic acid medium. *Journal of Applied Polymer Science* 91: 991-999 (2004).
29. Huang, J. & M. Wan. Polyaniline doped with different sulfonic acids by in situ doping polymerrization. *Journal of Polymer Science Part A: Polymer Chemistry* 37: 1277-1284 (1999).
30. Chen, J., Y. Xu, Y. Zheng, L. Dai, & H. Wu. The design, synthesis and characterization of po lyaniline nanophase materials. *Comptes. Rendus Chimie* 11: 84-89 (2008).
31. Palaniappan, S. & S. L. Devi. Thermal stability and structure of electroactive polyaniline fluoroboric acid dodecylhydrogensulfate salt. *Polymer Degradation and Stability* 91: 2415- 2422 (2006).
32. Sarvanan, C., S. Palaniappan, & F. Chandezon. Synthesis of nanoporous conducting polyaniline using ternary surfactant. *Materials Letters* 62: 882-885 (2008).
33. Duffour, B., P. Rannon, P. Fedorko, D. Djurado, J.P. Travers & A. Pron. Effect of plasticizing dopants on spectroscopic properties, supramolecular structure, and electrical transport in metallic polyaniline. *Chemistry of Materials* 13**:** 4032-4040 (2001).
34. Han, M.G., S.K. Cho, G.S. Oh, & S.S. Im. Preparation and characterization of polyaniline nanoparticles

synthesis from DBSA micellar solution. *Synthetic Metals* 126: 53-60 (2002).

35. Vijayan, M, & D. C. Trivedi. Studies on polyaniline in methane sulphonic acid (MeSA). *Synthetic Metals* 107: 57-64 (1999).
36. Konyushenko, E.N., M. Trchova, J. Stejskal, & I. Sapurina. The role of acidity profile in the nanotubular growth of polyaniline. *Chemical Papers* 64: 56-64 (2010).
37. Stejskal, J., I. Sapurina, M. Trchova, & E.N. Konyushenko, Oxidation of aniline: polyaniline granules, Nanotubes, and oligoaniline microspheres, *Macromolecules* 41: 3530-3536 (2008).
38. Bhadra, S., S. Chattpadhyay, N.K. Singa, & D. Khastgir. Improvement of conductivity of elec trochemically synthesized polyaniline. *Journal of Applied Polymer Science* 108: 57-64 (2008).
39. Babazadeh, M. Aqueous dispersions of DBSA-doped polyaniline: one-pot preparation, character rization and properties study. *Journal of Applied Polymer Science* 113: 3980-3984 (2009).
40. C. -H. Chen. Thermal and morphological studies of chemically prepared emeraldine-base-form polyaniline powder. *Journal of Applied Polymer Science* 89: 2142-2148 (2003).
41. N. K. Svelko, S. Reynaud. J. Francois, Synthesis and characterization of polyaniline prepared in the presence of nonionic surfactants in an aqueous dispersion, Synth. Met. 150 (2005) 107-114. .
42. M. Jayakannan, P. Anilkumar, A. Sanju, Synthesis and characterization of new azobenzenesulfonic acids doped conducting polyaniline. *European Polymer Journal* 42: 2623-2631 (2006).
43. Brozova, L., P. Holler, J. Kovarova, J. Stejskal, & M. Trchova. The stability of polyaniline in strongly alkaline or acidic aqueous media. *Polymer Degradation and Stability* 93: 592-600 (2008).

Proceedings of the Pakistan Academy of Sciences 51 (2): 177–184 (2014)

ISSN: 0377 - 2969 (print), 2306 - 1448 (online)

Pakistan Academy of Sciences

Research Article

Impact of Zonal Movement of Indian Ocean High Pressure on Winter Precipitation over South East Australia

Shahnilla H. Rizvi [1*] and Muhammad J. Iqbal [2]

[1]Department of Mathematical Sciences, University of Karachi, Karachi, Pakistan
[2] Institute of Space and Planetary Astrophysics, University of Karachi, Karachi, Pakistan

Abstract: Southeastern Australia (SEA) has suffered from 10 years of low rainfall from 1997 to 2006. A protracted dry spell of this severity has been recorded once before during the 20th century, but current drought conditions are exacerbated by increasing temperatures. Impacts of this dry decade are wide-ranging, so a major research effort is being directed to better understand the region's recent climate, its variability and climate change. Large-scale factors that influence the climate of southeastern part of Australia include the El Niño – Southern Oscillation (ENSO), the Indian Ocean Dipole (IOD) and the Southern Annular Mode (SAM). This paper explores rainfall variability and trends within the State of South East Australia over the past century. For much of the State experiences large variations in rainfall over space as well as over time. We use the centre of action approach for the study of wintertime rainfall variability over the mentioned region, taking into account variations in Indian Ocean High pressure system. It is also found that east-west shifts in the position of this subtropical Indian Ocean high significantly influence winter rainfall in South East Australia. The negative correlation implies that when the Indian High shifted to the east there is less rainfall over south east Australia. Similarly when the Indian Ocean High Pressure maximum there is less rainfall observed and vice versa. It indicates that the Indian High pressure in the winter has steadily increased and expanded since the 1950s which is the most direct explanation of the drying trend over the South East Australia. (IOHP and IOHLN) explain 22% variability of rainfall over SEA. Our calculations suggest the variability of winter precipitation over South East Australia is not only influenced by the intensity of Indian Ocean High pressure system but it also depends on its zonal movement.

Keywords: Indian Ocean High Pressure, Precipitation, Teleconnection

1. INTRODUCTION

Australia is the driest inhabited continent on earth; its climate is harsh and extreme. Its interior has one of the lowest rainfalls in the world, and about three-quarters of the land are arid or semi-arid. Rainfall records reveal regular drought cycles, sometimes persisting for a decade and beyond, interspersed with years of above-average rain. Rainfall trends are important from an environmental and an economic perspective. For thousands of years, Australia has experienced strong year-to-year variations in rainfall. These natural variations and any more extreme variations or changes in the normal scope of variation that may result from anthropogenic climate change are important indicators for the condition of the atmosphere.

Particularly, in south-east Australia, since 1950, rainfall has decreased and droughts have become hotter and the number of extremely hot days has risen [1]. Climate change projections indicate that the south-east is likely to become hotter and drier in future. Most of South-Eastern Australia (SEA) has seen reduced rainfall since the late 1990s (National Climate Centre – NCC-, 2008). Rainfall across south-eastern Australia is highly variable on inter-annual and decadal time-scales (Fig. 1).

The first half of the 20th century was markedly drier than the second half, with a significant increase

Received, April 2014; Accepted, May 2014
*Corresponding Author: Shahnilla H. Rizvi; Email: rshahnilla@hotmail.com

in the late 1940s [2]. In the late 1990s, most of the region entered an extended dry spell. From 1997 to 2009, virtually the entire area experienced rainfall below the long-term average, with some places recording the lowest totals on record. Most of the rainfall decline up to 2006 occurred in autumn, with 2006 through 2008 also experiencing relatively poor rainfall in winter and spring. The rainfall decline affected the southern area of the Murray-Darling Basin and the whole of Victoria, with impacts on the environment, irrigation industries and the cities of Adelaide, Melbourne and Canberra. It has been shown that a 13% reduction in rainfall in the southern Murray-Darling Basin from 1997-2006 led to a stream flow decrease of 44% [3].

Large-scale factors that influence the climate of southeastern part of Australia include the El Niño – Southern Oscillation (ENSO), the Indian Ocean Dipole (IOD) and the Southern Annular Mode (SAM). The ENSO represents the effects of the Pacific Ocean, the IOD represents the Indian Ocean impacts, and the SAM represents the effects of the atmospheric circulation at high latitudes. These factors have been shown to have varying influences on seasonal rainfall patterns.

This study aimed at investigating the variability of rainfall over South East Australia (south of 33.5ºS and east of 135.5ºE) using the Center of Action (COA) approach. In the scheme used in this paper a COA is characterized by three indices representing its area-averaged longitude, latitude and pressure. The atmospheric centers of action are the large scale semi-permanent features of high and low pressure that are prominent in seasonal maps of global sea level pressure. Several recent studies have illustrated these advantages of the COA approach, such as the variations of zooplankton in the Gulf of Maine [4], the position of the Gulf stream north wall [5], the inter annual variability of Saharan mineral dust transport over the Atlantic [6], and the variability of wintertime Greenland tip jet [7]. These studies have demonstrated that not only changes in pressure but also changes in the latitude and longitude positions of the COA are in impact regional climates.

A recent study demonstrates the impact of the Indian Ocean high pressure system on winter precipitation over western and southwestern Australia [8]. In fact, the Indian Ocean High and South Pacific High are the centers of action that dominates atmospheric circulations that bring moisture to regions of SEA. Thus, this study proposes to investigate the impact of changes in pressures and positions of the Indian Ocean High on seasonal rainfall.

2. DATA

This study employed the Australian Bureau of Meteorology (BOM) gridded monthly rainfall datasets from 1950 to 2008. The datasets were developed using topography-resolving analysis methods applied to all available rainfall station data passed by a series of internal quality tests (see, http://www.bom.gov.au) It is the best available dataset for the analysis of variability in Australian rainfall.

Monthly averaged gridded mean sea-level pressure (MSLP) data from the National Center for Environmental Prediction (NCEP) reanalysis [9] for 1950–2008 were used for calculating objective COA indices for the monthly averaged pressure, latitude and longitude of the Indian Ocean High and the South Pacific High systems, as described by Hameed and Piontkovski [5]. The NCEP reanalysis was also used for constructing composite maps to understand meteorological changes that accompany different extreme conditions.

Southern Oscillation Index (SOI) is available at the Climate Data Centre, National Centers for Environmental Prediction. Indices for SAM prior to 1979 are based on very limited observations because there are only a small number of stations over the high latitudes of the southern hemisphere. The data of Indian Ocean Dipole (IOD) was used from 1958 to 2008, provided by Japan Agency for Marine-Earth Science and Technology (JAMSTEC). All calculations in this paper are for the season from June to August (JJA).

3. METHODOLOGY

The relationship between the atmospheric pressure fluctuation and rainfall variability over Australia,

can be obtained through a quantitative assessment of the fluctuation in the pressure and location of the Indian Ocean High and South Pacific High, the two atmospheric centers of action that flank Australia. The pressure index I_P of a High pressure system can be defined as an area-weighted pressure departure from a threshold value over the domain (*I, J*) as suggested by Hameed et al [10] and Santer [11].

$$I_{p,\Delta t} = \frac{\sum_{i=1}^{I}\sum_{j=1}^{J}(P_{ij,\Delta t}-P_t)\ \cos\emptyset_{ij}\ \delta_{ij,\Delta t}}{\sum_{i=1}^{I}\sum_{j=1}^{J} cos\emptyset_{ij}\ \delta_{ij,\Delta t}}$$

Where $P_{ij,\Delta t}$ is the MSLP value at grid point (*i , j*) averaged over a time interval Δt, in this case monthly MSLP values are taken from NCEP reanalysis, P_t is the threshold MSLP value (P_t = 1016 hPa for both the Indian Ocean High and the South Pacific High), φ_{ij} is the latitude of the grid point *(i, j)*. δ = 1 if $(P_{ij,\Delta t} - P_t) > 0$ and δ = 0 if $\left(P_{ij,\Delta t} - P_t\right) < 0$. This ensures that the pressure difference is due to the High pressure system. The intensity is thus a measure of the anomaly of the atmospheric mass over the section *(I, J)*. The domain of the Indian Ocean High was chosen as 10°S to 45°S and 40°E to 120°E and that of the South Pacific High as 10°S to 45°S and 160°E to 70°W.The domains of the two Highs and their threshold values were chosen by examining their geographical ranges in NCEP reanalysis data over the period 1948–2006. Similarly, the latitudinal index is defined as:

$$I_{\varphi,\Delta t} = \frac{\sum_{i=1}^{I}\sum_{j=1}^{J}\left(P_{ij,\Delta t} - P_t\right)\varphi_{ij}\ \cos\emptyset_{ij}\ \delta_{ij,\Delta t}}{\sum_{i=1}^{I}\sum_{j=1}^{J}\left(P_{ij,\Delta t} - P_t\right)cos\,\emptyset_{ij}\ \delta_{ij,\Delta t}}$$

and the longitudinal index $I_{\lambda,\Delta t}$ is defined in an analogous manner.

4. RESULTS AND DISSCUSSION

We first assessed the dominance of the key drivers (COA indices, including pressure, latitude and longitude of the Indian Ocean High (IOH), of rainfall variability in south east Australia (SEA) by computing the correlation of these indices with the rainfall at each grid point across SEA. We do this in a moving 3 month window and then find the driver that accounts for the most variability (strongest correlation) in each 3 month season. The results are shown in Table1.

Table 1. Correlation Matrix of JJA Precipitation for South East Australia and Center of Action Variables, SOI, SAM and IOD during 1951– 2008. Values significant at the 0.05 statistical level are shown in bold.

COA Variables	SEA Rainfall
Indian Ocean High Pressure (IOHPS)	**-0.263**
Indian Ocean High Longitude (IOHLN)	**-0.409**
Indian Ocean High Latitude (IOHLT)	0.075
SOI	**0.584**
Southern Annular Mode (SAM)	**-0.295**
Indian Ocean Dipole (IOD)	**-0.397**

The two variables Indian Ocean High Pressure and Indian Ocean High Longitude are significantly correlated with South-East Australia (SEA)

Table 2. Correlation Matrix for Indian Ocean High Pressure, Indian Ocean High Longitude, SOI, SAM and IOD for JJA Season during 1951–2008. Values significant at 0.05 statistical level are shown in bold.

	Indian Ocean High Pressure (IOHPS)	Indian Ocean High Longitude (IOHLN)	SOI	SAM	IOD
Indian Ocean High Pressure(IOHPS)	1.00	0.086	**-0.365**	**0.714**	0.139
Indian Ocean High Longitude(IOHLN)	0.086	1.00	**-0.327**	**0.315**	**0.374**
Southern Oscillation index (SOI)	**-0.365**	**-0.327**	1.00	-0.187	**-0.547**
Southern Annual Mode(SAM)	**0.714**	**0.315**	-0.187	1.00	0.267
Indian Ocean Dipole (IOD)	0.139	**0.374**	**-0.547**	0.267	1.00

precipitation. In order to evaluate interdependencies among these variables we calculated their correlation matrix shown in Table 2. The Indian Ocean High Pressure is not correlated with the other variable i.e. Indian Ocean High Longitude. As Indian Ocean High longitude and Indian Ocean High Pressure are mutually independent; we construct a linear model of winter rainfall over SEA which yields:

$$SEAprecip = 5673.230 - 2.031(IOHLN) - 5.360(IOHPS)$$

R^2 for this regression is 0.220. It reveals that the variability of winter precipitation over South East Australia is influenced by the intensity of Indian Ocean High pressure system but it also depends on its zonal movement.

A drying trend in South East Australian rainfall since 1990 is apparent in Fig. 1. However, the intensity of Indian Ocean High pressure has been increasing trend. The negative correlation between rainfall over SEA and IOHP shows that the Indian High pressure in the winter has steadily increased and expanded since the 1950s which is the most direct explanation of the drying trend over the South East Australia. This result is consistent with that of Mitas and Clement [12] who showed a statistically significant intensification of their Hadley circulation indices throughout the second part of the 20th century.

4.1. Physical Mechanism for the Relationship between Indian Ocean High and Rainfall

The data in Table 1 revealed that the rainfall is negatively correlated with the Indian Ocean high pressure consequently there is more rainfall in winter when Indian ocean high pressure was the lowest is constructed and compared with composites obtained for the 10 winters in which Indian ocean high pressure was highest .Using NCEP/NCAR reanalysis monthly averaged fields, the composite mean of vector wind at 500 mb between the winters in which the Indian Ocean High was low is plotted in Fig. 2.

We can see the wind flow from the Indian Ocean brings moisture eastwards and its influence reaches in the region of South east Australia. Also, Fig. 3 shows that relative humidity was high when Indian ocean high was minimum and the weather is less humid when Indian ocean high is maximum so that the composite difference is positive i.e. 6% in SEA.

Fig. 4 shows composite difference of 500 mb vector wind velocities between the ten winters when the IOH was located most to the west (more rain in SEA) and the ten winters when the High was located most to the east (less rain in SEA). It shows

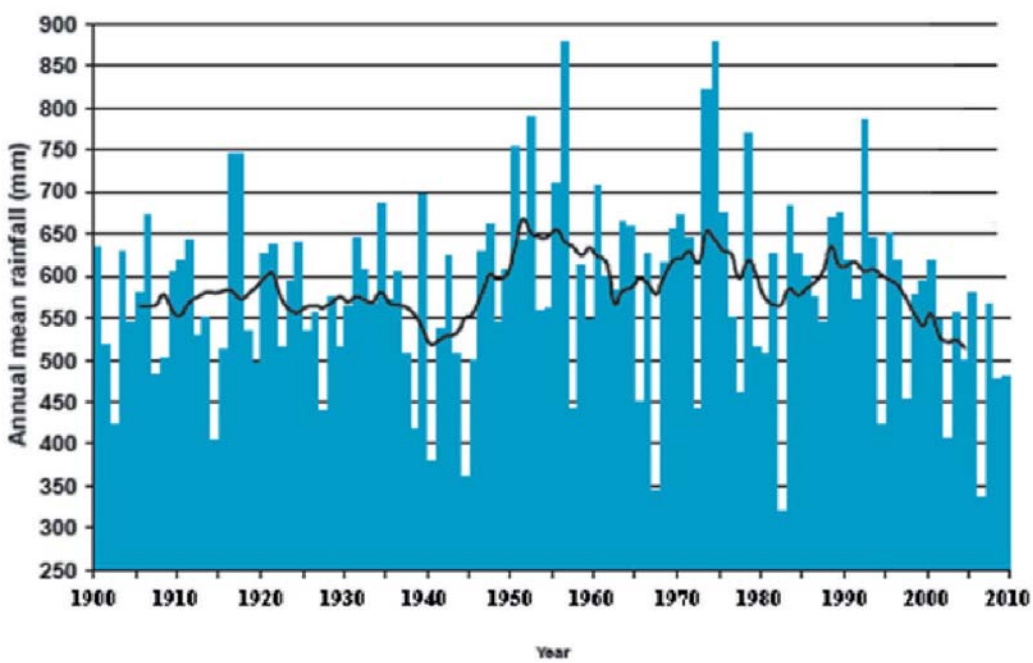

Fig. 1. Mean annual **rainfall** over mainland southeast australia from 1990 to 2009.Also shown is the 11th year running mean (solid black).

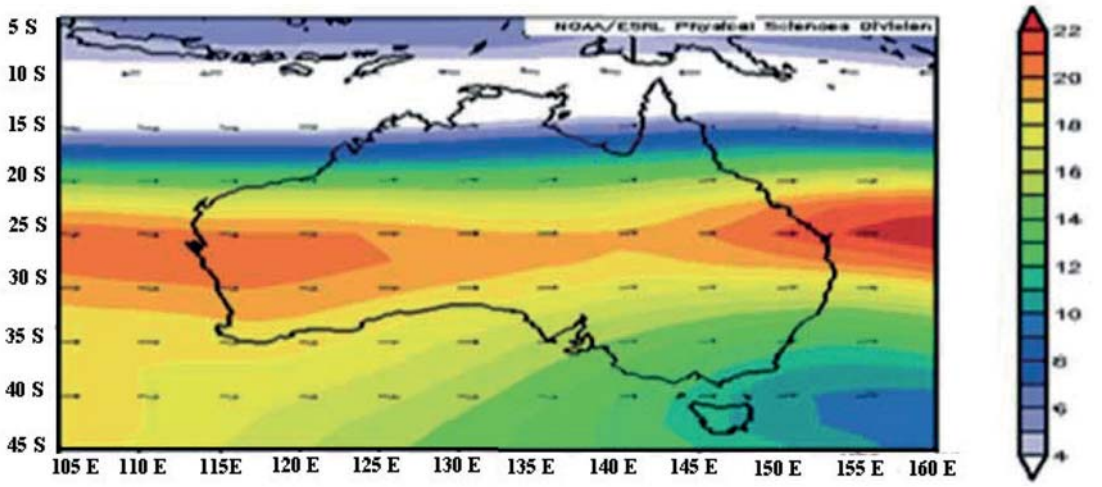

Fig. 2: Composite mean of **vector wind (500mb)** over the 10 winters when Indian Ocean High pressure was minimum.

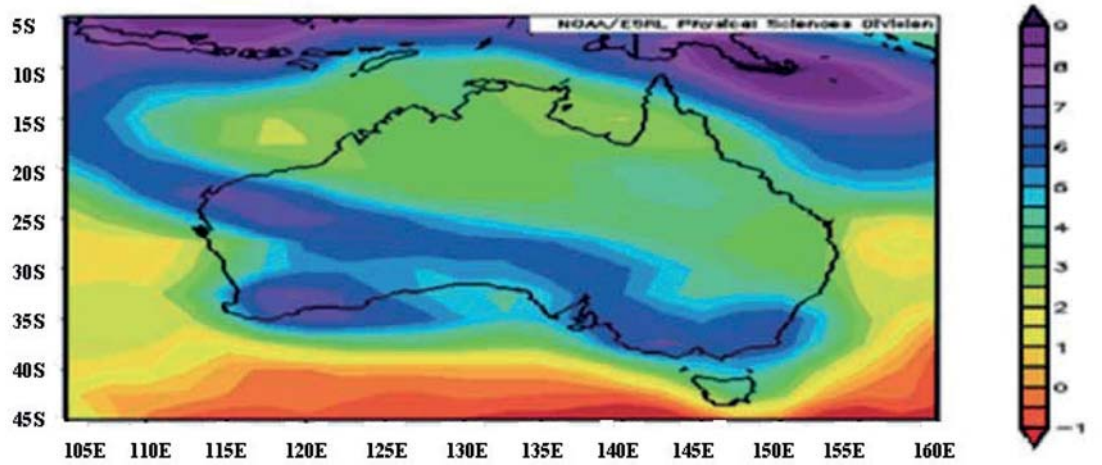

Fig. 3: Composite difference of **Relative Humidity (850mb)** during 1951–2008, between the ten winters when Indian High Pressure was minimum (more rain in SEA) and the ten winter when the Indian High Pressure was maximum (less rain in SEA).

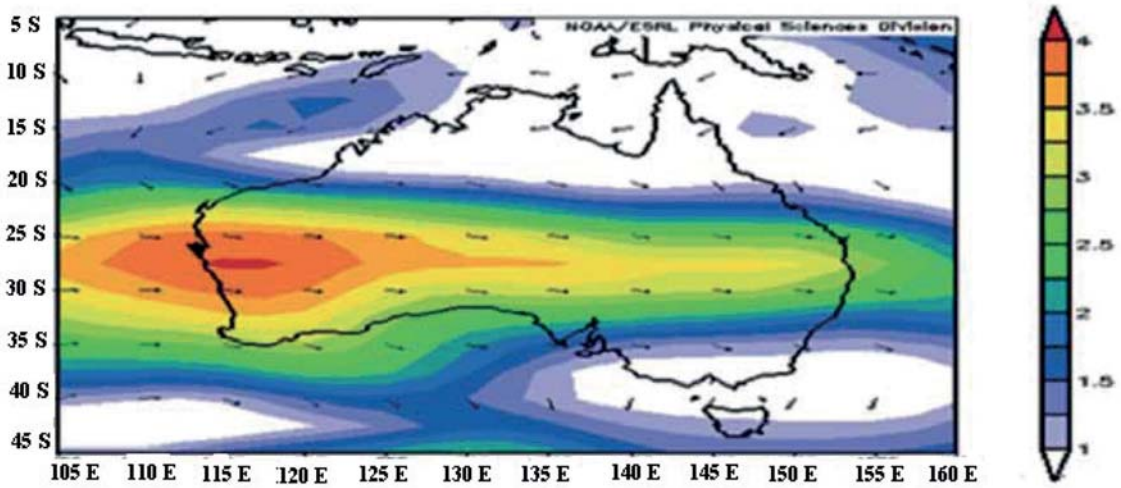

Fig. 4: Composite difference of **Vector Wind (500mb)** during 1951–2008, between the ten winters when Indian High Longitude was minimum (more rain in SEA) and the ten winters when the Indian High Longitude was maximum (less rain in SEA).

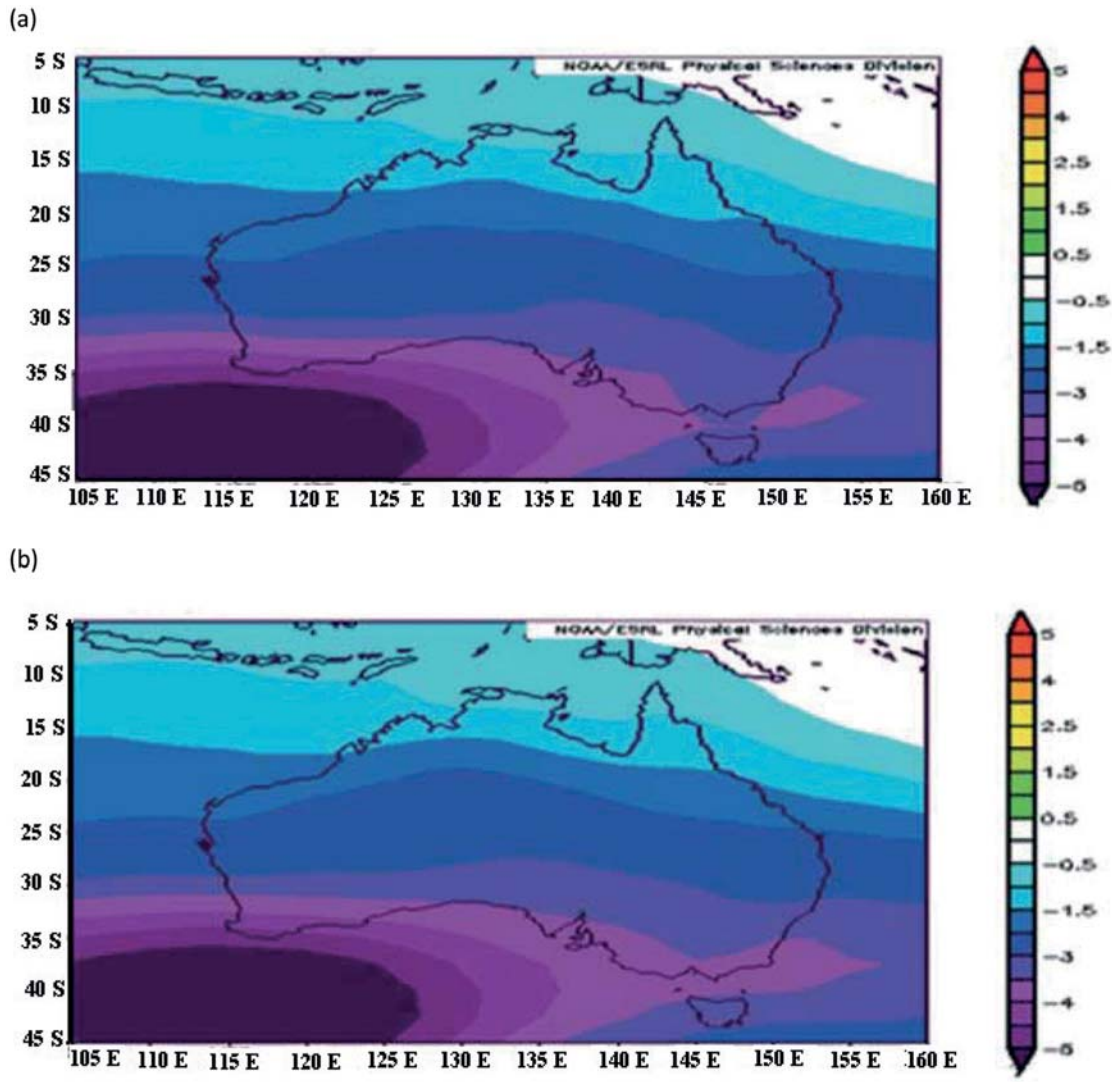

Fig. 5: Composite difference during 1951–2008, between the ten winters when Indian High Longitude was minimum (more rain in SEA) and the ten winters when the Indian High Longitude was maximum (less rain in SEA) (a) **Pressure (surface) (b) Sea level pressure(surface).**

anomalous flow from the ocean into west Australia with magnitude 4 m/s and in south east Australia it was reduced to 1 m/s to 1.5 m/s. Also we can see in Figs. 5 (a-b), which are the composite differences of Surface Pressure and Sea level pressure during 1951–2008, between the ten winters when Indian High Longitude was minimum (more rain in SEA) and the ten winters when the Indian High Longitude was maximum (less rain in SEA), these figures reveal that the low pressure was developed which was extended to the region of SEA.

Fig. 6 shows that weather was more humid when the IOH was located most to the west (more rain in SEA) as was located most to the east (less rain in SEA). Finally, it is noted that the impacts of Zonal Movement of Indian Ocean High Pressure on SEA rainfall exhibit important seasonal variations. NCEP reanalysis data show that atmospheric circulation is consistent with our empirical results.

5. CONCLUSIONS

Previous studies have identified large-scale factors that influence the climate of southeastern Australia includes the El Niño – Southern Oscillation (ENSO), the Indian Ocean Dipole (IOD) and the

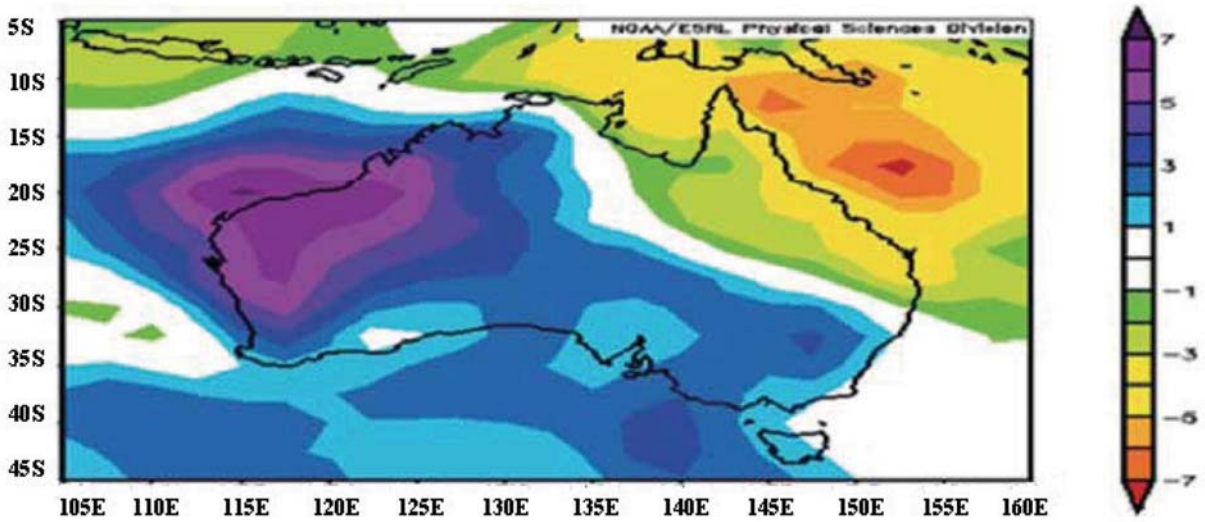

Fig. 6: Composite difference of **Relative Humidity (850mb)** during 1951–2008, between the ten winters when Indian High Longitude was minimum (more rain in SEA) and the ten winters when the Indian High Longitude was maximum (less rain in SEA).

Southern Annular Mode (SAM).These factors have been shown to have varying influences on seasonal rainfall patterns. The present paper has examined this relationship in terms of the dynamics of the Indian Ocean High pressure system which dominates atmospheric circulations that bring moistures to regions of South East Australia. Specifically, it was found that east-west shifts in the position of this subtropical Indian Ocean high significantly influence winter rainfall in South East Australia. The negative correlation implies that when the Indian High shifted to the east there is less rainfall over south east Australia. Similarly when the Indian Ocean High Pressure maximum there is less rainfall observed and vice versa. It shows that the Indian High pressure in the winter has steadily increased and expanded since the 1950s which is the most direct explanation of the drying trend over the South East Australia. The pressure and the longitude position of the IOH are not significantly correlated with each other. A statistical model of JJA rainfall in South East Australia using the IOH pressure and longitude as independent variables is presented. It explains 22 per cent of the observed rainfall variance. Our calculations suggest that the variability of winter precipitation over South East Australia is not only influenced by the intensity of Indian Ocean High pressure system but it also depends on its zonal movement.

6. REFERENCES

1. Nicholls, N. Continued anomalous warming in Australia. *Geophysical Research Letters* 30: 1370, dio:10.1029/2003GL017037 (2003).
2. Murphy, B. & B. Timbal. A review of recent climate variability and climate change in south-eastern Australia. *International Journal of Climatology* 28(7): 859-879 (2008).
3. N.J. Potter, F.H.S. Chiew & A.J. Frost. An assessment of the severity of recent reductions in rainfall and runoff in the Murray–Darling Basin, *Journal of Hydrology* 381(1–2): 52-64 (2010).
4. Piontkovski, S.A. & S.Hameed. Precursors of copepod abundance in the Gulf of Maine in atmospheric centers of action and sea surface temperature. *The Global Atmosphere and Ocean System* 8: 283-291 (2002).
5. Hameed, S. & S.A. Piontkovski. The dominant influence of the Icelandic Low on the position of the Gulf Stream north wall". Geophysical. Research Letters.,31, L09303, doi:10.1029/2004GL019561 (2004).
6. Riemer, N. O.M. Doherty & S. Hameed. On the variability of African dust transport across the Atlantic. *Geophysical Research Letters* 33, L13814, doi:10.1029/2006GL026163 (2006).
7. Bakalian, F.M., S. Hameed, & R. Pickart. Influence of the Icelandic Low Latitude on the frequency of Greenland Tip Jet Events: Implications for Irminger Sea convection. *Journal of Geophysical Research* 112: C04020 (2007).
8. Hameed, S., M.J. Iqbal, S. Rehaman & D. Collins. Impact of the Indian Ocean high pressure system

on winter precipitation over Western Australia and Southwest Western Australia. *Australian Meteorological and Oceanographic Journal* 61: 159-170 (2011).

9. Kalnay, E. & coauthors. The NCEP/NCAR 40-year reanalysis project, Bull. *American Meteorological Society* 77: 437–471 (1996).
10. Hameed, S., W. Shi, J. Boyle & B. Santer. *Investigation of the Centers of Action in the Northern Atlantic and North Pacific in the ECHAM AMIP Simulation*. Proceedings of the First International AMIP Scientific Conference, WCRP 92, Monterey, California, p. 221-226 (1995).
11. Santer, B.D. & T.M.L. Wigley. Regional validation of means, variances and spatial patterns in GCM control runs. *Journal of Geophysical Research* 95: 829-850 (1990).
12. Mitas, C. M. & A. Clement. Recent behavior of the Hadley cell and tropical thermodynamics in climate models and reanalysis. *Geophysical Research Letter* 33, L01810, doi:10.1029/2005GL024406 (2006).

Proceedings of the Pakistan Academy of Sciences

Instructions for Authors

Aims and Scope: *Proceedings of the Pakistan Academy of Sciences* is official journal of the Academy, published quarterly, in English. This open access journal publishes research papers in *Engineering Sciences & Technology, Life Sciences, Medical Sciences, and Physical Sciences*. State-of-the-art reviews (~20 pages, supported by recent references) summarizing R&D in a particular area of science, especially in the context of Pakistan, and suggesting further R&D are also considered. Manuscripts undergo double-blind review. Authors are not required to be Fellows or Members of the *Pakistan Academy of Sciences* or citizens of Pakistan.

Manuscript Format
Manuscript may contain **Abstract, Keywords, INTRODUCTION, MATERIALS AND METHODS, RESULTS, DISCUSSION (or RESULTS AND DISCUSSION), CONCLUSIONS, ACKNOWLEDGEMENTS and REFERENCES** *and any other information that the author(s) may consider necessary.* The Manuscript sections must be numbered, i.e., **1. INTRODUCTION, 2. MATERIALS AND METHODS,** and so on.

Manuscripts, in *Times New Roman*, 1.5-spaced (but single-space the Tables), with line numbering and one-inch margins on all sides on A-4 size paper, should not exceed 20 pages including Tables and Figures. Number manuscript pages throughout. The text (in **Font Size 11,** except for the sections mentioned in **Font Size 10)** must be typed in a single column across the paper width. All Tables and Figures must be placed after the text, i.e., after REFERENCES section.

Title Page: For Online submission of the manuscript, Title Page should not be included. However, for submitting as an email attachment, the title page must be as under:
(a) **Title** of the article **(**Capitalize initial letter of each main word; font size 16; **bold**), max 160 characters (no abbreviations or acronyms), depicting article's contents; (b) Author' first name, middle initial and last name (font size 12, **bold**), and professional affiliation (i.e., each author's Department, Institution, Mailing address and Email; but no position titles) (font size 12); (c) Indicate the corresponding author with *; (d) **Short running title**, max 50 characters (font size 10).

The **next Page** should start with **Title** of the Article, followed by entire manuscript.

Headings and Subheadings (font size 11): All flush left

LEVEL-1: **ALL CAPITAL LETTERS; bold**
Level-2: **Capitalize each main word; bold**
Level-3: Capitalize each main word; Bold, Italic
Level-4: *Run-in head*; *Italics*, *in the normal paragraph position. Capitalize the initial word only and end in a colon (i.e.,* ***:)***

Abstract (font size 10; max 250 words)**:** Must be self-explanatory**,** stating rationale, objective(s), methodology, main results and conclusions of the study. Abbreviations, if used, must be defined on first mention in the Abstract as well as in the main text. Abstract of review articles may have variable format.
Keywords (font size 10)**:** Three to eight keywords**,** depicting the article.

For Online Submission:

- **Separate submission of Abstract along with Title is required**
- **Author(s)' names and affiliations should not be included in the manuscript or in the Abstract**

INTRODUCTION: Provide a clear and concise statement of the problem, citing relevant recent literature, and objectives of the investigation.

MATERIALS AND METHODS: Provide an adequate account of the procedures or experimental details, including statistical tests (if any), in a concise manner but sufficient enough to replicate the study.

RESULTS: Be clear and concise with the help of appropriate Tables, Figures and other illustrations. Data should not be repeated in Tables and Figures, but must be supported with statistics.

DISCUSSION: Provide interpretation of the RESULTS in the light of previous relevant studies, citing published references.

ACKNOWLEDGEMENTS (font size 10)**:** In a brief statement, acknowledge financial support and other assistance.

REFERENCES (font size 10)**:** Cite references in the text **by number only** in **square brackets**, e.g. "Brown et al [2] reported ..." or "... as previously described [3, 6–8]", and list them in REFERENCES section, in the order of citation in the text, Tables and Figures (not alphabetically). Only published (and accepted for publication) journal articles, books, and book chapters qualify for REFERENCES.

List of REFERENCES must be prepared as under:

a. **Journal Articles** *(Name of journals must be stated in full)*

1. Golding, I. Real time kinetics of gene activity in individual bacteria. *Cell* 123**:** 1025–1036 (2005).
2. Bialek, W. & S. Setayeshgar. Cooperative sensitivity and noise in biochemical signaling. *Physical Review Letters* 100**:** 258–263 (2008).
3. Kay, R.R. & C.R.L. Thompson. Forming patterns in development without morphogen gradients: differentiation and sorting. *Cold Spring Harbor Perspectives in Biology* 1: doi: 10.1101/cshperspect.a001503 (2009).

b. **Books**

4. Luellen, W.R. *Fine-Tuning Your Writing*. Wise Owl Publishing Company, Madison, WI, USA (2001).
5. Alon, U. & D.N. Wegner (Ed.). *An Introduction to Systems Biology: Design Principles of Biological Circuits*. Chapman & Hall/CRC, Boca Raton, FL, USA (2006).

c. **Book Chapters**

6. Sarnthein, M.S. & J.D. Stanford. Basal sauropodomorpha: historical and recent phylogenetic developments. In: *The Northern North Atlantic: A Changing Environment.* Schafer, P.R. & W. Schluter (Ed.), Springer, Berlin, Germany, p. 365–410 (2000).
7. Smolen, J.E. & L.A. Boxer. Functions of Europhiles. In: *Hematology, 4th ed*. Williams, W.J., E. Butler & M.A. Litchman (Ed.), McGraw Hill, New York, USA, p. 103–101 (1991).

Tables, with concise but self-explanatory headings must be numbered according to the order of citation (like **Table 1**, **Table 2**). Round off data to the nearest three significant digits. Provide essential explanatory footnotes, with superscript letters or symbols keyed to the data. Do not use vertical or horizontal lines, except for separating column heads from the data and at end of the Table.

Figures may be printed in two sizes: column width of 8.0 cm or page width of 16.5 cm; number them as **Fig. 1**, **Fig. 2**, … in the order of citation in the text. Captions to Figures must be concise but self-explanatory. Laser printed line drawings are acceptable. Do not use lettering smaller than 9 points or unnecessarily large. Photographs must be of high quality. A scale bar should be provided on all photomicrographs.

Declaration: Provide a declaration that: (i) the results are original; (ii) the same material is neither published nor under consideration elsewhere; (iii) approval of all authors has been obtained; and, (iv) in case the article is accepted for publication, its copyright will be assigned to *Pakistan Academy of Sciences*. Authors must obtain permission to reproduce copyrighted material from other sources.

Reviewers: Authors may suggest four relevant reviewers, two local and two from scientifically advanced countries.

Online Manuscript Submission:
Proceedings of the Pakistan Academy of Sciences is using a web-enabled online manuscript submission and review system, which offers authors the option to track the progress of manuscripts in real time.
For online submission, authors are required to register at website of the Academy (www.paspk.org) by clicking the "Journal and Publications" tab.

Manuscripts must be submitted in Microsoft Word (.doc or .docx format; **pdf** files not acceptable). Figures can be submitted in Word format, TIFF, GIF, JPEG, EPS, PPT.

NOTE: In case of online submission, authors are not required to submit the manuscript as email attachment.
In case of any difficulty while submitting your manuscript, please get in touch with:

Editor-in-Chief
Pakistan Academy of Sciences
3-Constitution Avenue, G-5/2, Islamabad, Pakistan
Email: pas.editor@gmail.com
Tel: +92-51-920 7140
Website: www.paspk.org

Proceedings
OF THE PAKISTAN ACADEMY OF SCIENCES

CONTENTS

Volume 51, No. 2, June 2014 Page

PAKISTAN ACADEMY OF SCIENCES, ISLAMABAD, PAKISTAN
HEC Recognized, Category X; PM&DC Recognized